Title
Charging of Proteins and Protein Complexes in Native Mass Spectrometry

Author
Susa, Anna Christine

Publication Date
2017

Peer reviewed|Thesis/dissertation

Charging of Proteins and Protein Complexes in Native Mass Spectrometry

by

Anna Christine Susa

A dissertation submitted in partial satisfaction

of the requirements for the degree of

Doctor of Philosophy

in

Chemistry

in the

Graduate Division

of the

University of California, Berkeley

Committee in charge:

Professor Evan R. Williams, Chair
Professor Kristie A. Boering
Professor Robert M. Glaeser

Spring 2017

Charging of Proteins and Protein Complexes in Native Mass Spectrometry

by

Anna Christine Susa

Abstract

Charging of Proteins and Protein Complexes in Native Mass Spectrometry

by

Anna Christine Susa

Doctor of Philosophy in Chemistry

University of California, Berkeley

Professor Evan R. Williams, Chair

Electrospray ionization (ESI) mass spectrometry is a powerful analytical tool for investigating the identities, structures, functions, and energetics of biomolecules. ESI transfers intact molecules from buffered aqueous solutions in which they are folded or in native conformations into the gas phase for mass spectral analysis. ESI is widely used for the analysis of proteins in mass spectrometry, but the factors that influence charging of protein ions formed by ESI are not well understood. Higher charge states of protein ions are desirable because they fragment more easily in tandem mass spectrometry methods, leading to more sequence coverage than lower charge protein ions. Lower charge protein ions are advantageous in native mass spectrometry when preservation of native protein conformation is desirable. The work described in this dissertation explores factors that control charging of macromolecular ions in native mass spectrometry. This work provides evidence that the charging of macromolecular ions is not significantly limited by ion evaporation of cations, such as alkylammonium or alkali metal ions, or proton transfer to salts that are commonly added to aqueous buffered ESI solutions. In addition, a novel and simple method for ESI of proteins directly from buffers commonly used in biochemistry laboratories is demonstrated. In native mass spectrometry, protein solutions are typically desalted and buffer exchanged into volatile ammonium salt buffers to prevent salt adduction to the protein ions because salt adduction significantly hinders detection and sensitivity of mass spectral analysis. However, some salts are essential for protein structure and function, and this new method of ion desalting allows formation of protein and protein complex ions directly from buffers that contain high ionic strengths of nonvolatile salts to mimic the intracellular and extracellular environments. This technique greatly impacts the way native mass spectrometry is performed because it eliminates the need to reinvestigate properties of the proteins and protein complexes in traditional ammonium salt buffers used in mass spectrometry. Therefore, biochemists will no longer need to adapt their protein solutions to make them suitable for mass spectrometry.

Table of Contents

Acknowledgments

This work would not have been possible without the love and endless support of my parents and sister, Marie, John and Katherine Susa. I also thank my advisor Professor Evan R. Williams who taught me to think critically about science. Evan supports and encourages of all his graduate students. He truly tries to teach us how to think scientifically, which is a rare and valuable quality in an advisor. I would like to thank my best friend Dr. Janine Tom for inspiring me to take Chem 1A while at UC Santa Barbara. The chance to pursue undergraduate research at UC Santa Barbara sparked my interest in research, and I owe this opportunity to Professor Michael T. Bowers. His undying loyalty to his lab and lifelong pursuit of high quality scientific research is admirable. Many people during my time here at UC Berkeley influenced my graduate career. I would like to thank the current and former members of the Williams lab for their help in my research as well as companionship. Thank you Dr. Harry Sterling and Dr. Tawnya Flick for guiding me as a first year graduate student, and Dr. Catherine Going for wisdom and friendship. Thank you Dr. Terrence Chang, Beryl Xia, and Chrissy Stachl for cheerful attitudes and Dr. Richard Cooper, Dr. Daniel Mortensen, Matthew DiTucci, Andrew Elliot and Conner Harper for remarkable level-headedness and willingness to help around the lab. My friends here in the chemistry program were also essential for my happiness and well being. The time we spent together made graduate school experience brighter.

Chapter 1

Introduction

1.1 Overview

A major analytical challenge that arose at end of the 20th century and continued into the 21st century is determining components of complex mixtures from biological or environmental sources. Complex biological mixtures such as the human genome,[1,2] proteome,[3-5] metabolome,[6] and glycome[7] require distinguishing anywhere from ten to hundreds of thousands of individual components.[8] Other complex mixtures such as petroleum can contain over twenty thousand components with distinct elemental compositions.[9,10] New instrumentation and techniques are constantly being developed to probe these biological and environmental complex mixtures reliably, rapidly and accurately.[11-13]

Mass spectrometry has been a leading technique for the analysis of complex mixtures because analytes can be detected and identified at concentrations as low as parts-per-trillion based on the mass-to-charge ratio (m/z) of the analyte. Mass spectrometry (MS) was limited to the study of atoms and small molecules with moderate to high vapor pressures until the ionization of relatively large molecules such as tetrodotoxin (319 Da), bleomycin (1512 Da), and palytoxin (2680 Da) with Californium-252 plasma desorption in the 1970s.[14,15] In the late 1980s and early 1990s, electrospray ionization (ESI) and matrix-assisted laser desorption ionization (MALDI) were developed.[16-19] With these new ionization methods, intact biomolecules such as proteins, virus capsids, and ribosomes could now be detected and analyzed in the gas phase.[20-23] In the years since the development of ESI and MALDI, the majority of research in the field of mass spectrometry has been focused on the development of applications and instrumentation as well as understanding fundamentals of these two ionization techniques.

Native mass spectrometry is the study of biomolecular ions formed from buffered aqueous solutions and detected and analyzed with mass spectrometry. A key advantage of studying biomolecules in the gas phase is that separating biomolecules from solvent or other components of buffers can simplify analysis, yet information about structures, functions, and reactivities of the biomolecules can be retained into the gas phase.[24-26] Even weakly-bound protein complexes can be ionized with ESI and detected while maintaining memory of native structures and functions.[27-29] However, factors that affect the charging of proteins and protein complexes formed by ESI from solutions in which they have native forms and functions are not fully understood.[30-33] In Chapters 2 and 3, new insights for factors that affect charging of proteins and protein complexes in the final stages of the ESI droplet as the ion goes from solution to the gas phase are explored. A method for manipulating protein ion charge from buffered aqueous solutions is demonstrated. In Chapters 4 and 5, a simple and fast method for counteracting the adverse effects of salts on the ionization and detection of proteins and protein complexes from buffered solutions that contain high ionic strengths of nonvolatile salts to mimic the intracellular and extracellular environments is presented. This is the first technique for native mass spectrometry of protein and protein complex ions formed directly from buffers containing greater than 150 mM nonvolatile salts without any salt removal before ESI. The work described in this dissertation was conducted with the goal of understanding what factors control charging of proteins and protein complexes as well as new advances for detection and analysis of biomolecules in native mass spectrometry. In this chapter, electrospray ionization mechanisms and factors that affect protein ion charging and methods to manipulate protein ion charging are discussed

in depth in sections 1.2 and 1.3, respectively, and techniques to counteract the adverse effects of salts in native mass spectrometry are explored in section 1.4.

1.2 Electrospray Ionization (ESI) of Proteins and Protein Complexes

ESI is initiated by applying a potential difference of 0.5 to 3.0 kV between the solution of interest, which is inside a capillary, and the orifice of the instrument. The potential difference between the capillary and the instrument orifice creates an electric field that pulls the solution out of the capillary as charged droplets which undergo solvent evaporation and fission until just the charged analyte remains. The work in this dissertation describes nano-electrospray ionization (nano-ESI), in which a few microliters of analyte solution are inserted into a borosilicate glass capillary that is pulled to a tip with an opening that is a few micrometers in diameter or smaller. The main benefit of nano-ESI compared to conventional (macrospray) ESI is that the flow rates of nano-ESI are nanoliters per minute compared to microliters per minute; therefore much lower volumes (only a few microliters) of sample solutions are required.[34] In addition, the ionization efficiency of nano-ESI is much higher compared to macrospray.[34]

ESI droplet dynamics and mechanisms are extensively studied,[35-42] but the ion formation mechanism is debated and the factors that control charging of biomolecules from aqueous solutions are not fully understood. [30-32,43-50] It is of interest to understand the factors that control charging of proteins and protein complexes because the charging can affect their structures,[51] and reactivities,[52] as as well as efficiencies of dissociation and detection.[53,54] Droplet fission occurs when the number of charges on an evaporating droplet reaches or is very close to the Rayleigh limit.[40] The droplet surface tension is overcome by Coulombic repulsion and the droplet produces many small progeny droplets. From one fission event, about 100 progeny droplets are produced that have 33 % of the charge and 0.3 % of the mass of the original droplet.[40] Several ion formation mechanisms have been proposed to account for the charging of ions. There are two main ESI mechanisms, the ion evaporation mechanism (IEM) which describes ion formation as ion evaporation of analyte from charged droplets and the charged residue mechanism (CRM) which describes ion formation from solvent evaporation and fission. In addition to these two main ESI mechanisms, several others have been proposed that will also be described in detail.

Charged Residue Mechanism

In the charged residue mechanism (CRM) for ion formation, gas-phase ions are produced by solvent evaporation and Rayleigh fission in the late stages of droplet lifetime.[55] Globular protein and polymer charging is related to the Rayleigh limit charge, Z_R, of spherical droplets roughly the same size as the analyte molecule.[43,56-58] The charge at which the Rayleigh limit is reached for a spherical droplet is given by the equation:

$$Z_R e = 8\pi(\varepsilon_0 \gamma R^3)^{1/2}$$

where Z_R is the integer unit of the Rayleigh charge, e is the elementary charge, ε_0 is the permittivity of the medium, γ is the surface tension of the droplet, and *R* is the radius of the droplet.[59] Some evidence for the CRM is that the charge of globular protein and dendrimer ions of molecular weights 6 to 1400 kDa formed from aqueous solutions is close to the maximum number of charges predicted for spherical water droplets of similar sizes to the globular ions.[56] It has been shown that protein ions formed from aqueous solutions are typically charged close to the number of charges predicted with

the Rayleigh limit for water droplets of similar sizes to the protein ion, and the number of charges on a protein ion increases with the square root of the mass of the ion.[32,56,58] This trend is useful for predicting the charge of globular protein ions for which individual charge states are not resolved due to heterogeneity of the sample. The extent of charging of denatured protein ions often exceeds Z_R and can be limited by the proton-transfer reactivity of the protein ion relative to that of the electrospray solvent or other molecules in solution.[43,60,61]

Ion Evaporation Mechanism

In the ion evaporation mechanism (IEM), gas-phase ions are produced from the surface of the ESI droplet when the electrostatic energy at the surface of the droplet overcomes the Gibbs free energy barrier for the process

$$X^+(aq) \rightarrow X^+(H_2O)_n(g)$$

where X^+ is the ion of interest and n is the number of water molecules.[17,62] This mechanism has been proposed primarily for the formation of salts (such as alkali metal ions) and small molecules,[17] but has also been suggested for the formation of peptide ions.[63]

The experimental evidence for ion evaporation is primarily from the investigation of ESI of alkali metal ions.[17,64,65] Some have shown that relative abundances of monatomic alkali metal ions detected trends with the solvation energy values of the ions,[65,66] but this trend with solvation energy values is not consistent for alkali metal cluster ions or mixtures of alkali metal cluster ions.[64,65] This suggests that solvation free energies of alkali metal ions influence ionization, but other factors also play a role. One of the challenges of correlating the relative abundances of alkali metal ions detected with solvation free energy values is that the efficiency of detection for each metal ion species can be different and therefore needs to be taken into account.

Recently, McLuckey and coworker showed that exposure of aqueous ESI droplets containing proteins to organic vapors can decrease the adduction of alkali metal ions to protein ions,[67] and suggested that this occurs from organic solvent molecules forming clusters with alkali metal ions at the surface of the ESI droplet which evaporate from the droplet at a faster rate than aqueous solvated alkali cluster ions. However, this was only investigated with sodium ions, and it would be interesting to determine if this also occurred with other cations with a range of solvation energy values.

Combined Charged Residue-Field Emission Model

The combined charged residue-field emission model (CCRFEM) for ionization of proteins formed from buffered aqueous solutions combines aspects of both the CRM and IEM. In the CCRFEM, macromolecules, such as protein molecules, are located in the center of the ESI droplet and follow the CRM. "Charge carrier" ions such as salts or buffer ions in ESI solution are emitted from the surface of the droplet at critical electric field strengths.[68,69] The emission of these charge carriers from the surface of the ESI droplet decreases the total charge of the droplet, resulting in fewer charges on the macromolecule after solvent evaporation and fission occurs. The critical electric field strength at which emission of the charge carriers occurs depends on the solvation energy of the charge carrier ion. Ions with lower solvation free energies will undergo ion evaporation at lower electric field strengths, therefore carrying away more charge from the droplet, which will result in lower charged protein ions.

Hogan et al. reported that some evidence for the CCRFEM is that protein ions formed from aqueous solutions with cations of lower solvation energies are less charged than protein ions formed

from solutions containing cations with higher solvation energies.[69] They reported that the average charge of protein ions formed from aqueous ammonium acetate is higher than the average charge of these ions formed from aqueous triethylammonium bicarbonate, and concluded that this is because triethylammonium evaporates from the droplet at a lower critical electric field strength than ammonium because triethylammonium has a lower solvation free energy value.[69] However, an alternative reason for why protein ions formed from triethylammonium bicarbonate solutions are less charged than those from ammonium acetate solutions is that the protein ions undergo proton transfer with triethylammonium/triethylamine, which reduces the protein ion charge. Triethylammonium bicarbonate is a common solution additive to ESI solutions for protein charge reduction because triethylamine is basic.[70-72] In addition, Hogan et al. did not use the same counter ion or pH for all solutions,[69] which could also affect the protein conformation in solution and ion charging.[73,74]

Recently, Bush and coworkers[32] observed that the charging of protein ions formed from aqueous solutions has a molecular weight dependence with the number of charges predicted by the Rayleigh limit for water droplets of similar sizes to the proteins. Protein ions with molecular weights greater than 130 kDa are charged closer to the the number of charges predicted with the Rayleigh limit than protein ions with lower molecular weights.[32] The authors suggested this is consistent with charge-carrier emission of buffer ions from ESI droplets limiting the charging of protein ions (with molecular weights less than 130 kDa).[32] The effects of cations on the charging of proteins formed from aqueous solutions are discussed in Chapters 2 and 3.

Proton Transfer between Ammonia/Ammonium and Protein Ions

Another cation that is sometimes thought to influence the charging of protein ions and protein complex ions formed from aqueous solutions is ammonium. Ammonium salts are commonly used as buffers in native mass spectrometry because ammonium is nonvolatile and does not adduct to protein ions, but the effects of proton-transfer reactivities between ammonium/ammonia and protein ions has been debated. Kebarle and coworkers proposed that charging of protein ions formed by ESI from aqueous ammonium salt solutions is limited by proton-transfer between the protein ion and ammonium or ammonia.[44,75,76] This is suggested to occur at the surface of the ESI droplet in the final stages of solvent evaporation such that NH_3 formed in the last stages of the ESI process can accept a proton from the protein ion resulting in less highly charged protein ions.[75] The effects of proton-transfer between protein ions and ammonia/ammonium are discussed in Chapter 3.

Chain Ejection Model

Another model for ion formation of protein ions is the the chain ejection model (CEM). In this model, unfolded proteins in aqueous ESI droplets are ejected from the droplet as highly charged elongated structures due to a combination of electrostatic repulsion and hydrophobicity.[46,47,49,50,77-79] Coulombic equilibration between the polypeptide chain and the droplet accounts for highly charged unfolded protein ions. It is suggested unfolded proteins ionize by the CEM during the early stages of the ESI droplet, but folded proteins in the droplet ionize by the CRM during late stages of the ESI droplet.

Evidence for CEM is primarily computational,[46,47,49,50,77-79] but recently some experimental evidence has been reported.[80] Protein ion charge states corresponding to unfolded ions typically have fewer sodium ions adducted than those of folded or lower charge protein ions, and Konermann and coworkers[80] suggested this difference in number of sodium ions adducted to folded and unfolded protein ions is due to ejection of unfolded protein ions early in the desolvation of the ESI droplet but folded protein ions remain in the droplet for longer times and therefore adduct more sodium ions.[80]

However, it has also been shown that high charge protein ions formed from solutions containing trivalent metal ions are more adducted with trivalent metal ions than lower charge protein ions.[81] This could be due to either the trivalent metal ions preferentially adducting to the high charge protein ions or adducting to lower charge protein ions and increasing the overall protein ion charge.[81]

1.3 Factors that Influence Protein Ion Charging and Methods to Manipulate Protein Ion Charging

Why Protein Ion Charge is Important

Many factors affect the extent of charging of protein ions in ESI, including the surface tension of the ESI droplet,[43,82] instrumental parameters,[51,83-85] supercharging methods,[43,86-90] and gaseous reactions with acids or bases,[60,61,91,92] but the conformation of a molecule in solution is one of the most significant.[51,83,84] Protein ions formed from solutions in which they are denatured, such as water/organic solvent/acidic, will result in broad high charge-state distributions of ions. In contrast, protein ions formed from solutions in which they are in native or native-like conformations will result in narrow, low charge-state distributions.[51] Multiple conformations of a protein in solution at one time can result in multi-modal charge-state distributions.[51,83]

The number of charges on protein ions affects the types of information obtained in the gas phase. High charge-state protein ions are advantageous for fragmentation techniques such as electron capture dissociation and electron transfer dissociation because higher charge states have larger capture cross sections and therefore fragment more efficiently than lower charge ions.[13,54,93-96] Several types of mass spectrometers are m/z range limited to m/z 4000, which makes it impossible to detect high molecular weight ions with low charge. Increasing the charge of an ion can decrease the m/z value of the ion so it is detectable by most mass spectrometers. Higher charge states are also detected more efficiently in mass spectrometers that use charge sensitive detection.[97,98] In contrast, lower charge ions are desirable because the gas-phase collisional cross sections of lower charge protein ions are often similar to cross sections calculated from protein crystal structures, indicating that lower charge ions retain more native conformations in the gas phase.[25,99] Lower charge protein and protein complex ions are often more compact and more stable against induced conformation changes.[27,72,100] In addition, lower charge-state protein complex ions can also dissociate along the weakest solution-phase interface, which provides information about solution-phase protein complex stability,[28,72] and is useful for determining complex assembly patterns.[27,71,72,100] Because the information obtained by mass spectrometry is affected by the charge of proteins and protein complexes, it is essential to understand what affects protein ion charging and how to manipulate charge.

Ways to Influence Ion Charging

Several methods can be used to manipulate protein ion charge in order to obtain either lower or higher charged ions. One way to increase protein ion charge is with techniques called "supercharging". Supercharging methods typically involve adding reagents to the ESI solution or changing instrumental parameters,[43,81,86,88,101-103] which results in higher charged protein ions formed during ESI. The most common method of supercharging is adding reagents that typically have boiling points and surface tensions higher than that of a typical denaturing solution (water/methanol/acid) to the ESI solution.[86,90,103,104] These reagents concentrate in the ESI droplet such that they constitute most of the droplet in the late stages of ESI and the droplet can hold more charge, resulting in more

highly charged desolvated protein ions.[43,82] Supercharging reagents are effective for both solutions in which proteins are denatured, such as water/methanol/acid, and solutions in which proteins are folded, such as buffered aqueous solutions.[43,82,86,90,102-104] The exact mechanism of supercharging with these reagents in aqueous solutions is debated,[43,86,101,104-110] but is thought to be due to chemical or thermal protein unfolding in the ESI droplet.[107] Another method of supercharging is adding millimolar concentrations of trivalent metal ions to the ESI solution.[81] Trivalent metal ions either preferentially adduct to high charge-state protein ions or adduct to low charge ions and therefore increase the charge of protein ions.[81] A third method of supercharging was discovered, called "electrothermal supercharging".[87,88] In this method, highly charged protein ions are formed from aqueous buffered solutions (typically ammonium bicarbonate) simply by applying a high voltage to the ESI capillary.[87,88] It is thought that the mechanism of electrothermal supercharging is thermal protein unfolding in the ESI droplet due to collisional heating of the droplet at higher ESI voltages.[87] One main benefit of electrothermal supercharging compared to adding supercharging reagents to ESI solutions is that electrothermal supercharging eliminates the need to investigate how supercharging reagents will affect the stability of the protein in solution.[88]

The charge of protein ions formed from solutions in which they are denatured or native can be significantly increased or decreased by reacting the protein ions with bases or acids either in solution or in the gas phase.[52,76,91,92,111-114] A decrease in protein ion charging can occur from adding very basic molecules to aqueous ESI solutions[111,114] as a result of proton-transfer reactions or competition for protons in the ionization process. Proton-transfer reactivities of protein ions with volatile bases, formed by ESI from solutions in which the proteins are denatured, have been investigated extensively both experimentally[52,60,100,113,115-118] and computationally.[45,52,61,75,76,113] The apparent gas-phase basicities of high charge state ions are lower than that of lower charge-state ions.[52,60,113,116] Conformation also affects the apparent gas-phase basicities of protein ions,[52,113,116] such that the apparent gas-phase basicity of compact protein ions is lower than that of denatured protein ions of the same charge state.[52] Even exposing ESI droplets to acidic or basic vapors between the atmospheric and vacuum interfaces of the mass spectrometer[91,92] can increase or decrease protein ion charging from pH induced unfolding of proteins in the ESI droplets.

Another way to reduce protein ion charge is reacting protein ions with anions in the gas phase.[119-121] Recently, Lermyte et al. reduced the charge of large protein complexes (up to 336 kDa) by up to 40 charges to form 2+ protein complex ions by reacting the protein complex ions with dicyanobenzene anions.[121] McLuckey and coworkers showed that the 23+ through 9+ charge states of myoglobin were formed from solutions in which myoglobin was denatured, and upon reaction of these myoglobin ion with perfluorodimethyl-1,3-cyclohexane anions, the charge of myoglobin ion was reduced to only the 1+ and 2+ charge states.[120] These ion/ion reactions are very effective for reducing protein ion charge, and can be useful for distinguishing components in heterogeneous samples. Reducing protein ion or protein complex ion charge simplifies the mass spectra by increasing separation between m/z values of the charge states.

A simple method for decreasing protein ion charge is to form the ions from aqueous solutions containing cations that weakly adduct to the protein ions, then collisionally activate the adducted protein ion to remove the adduct and charge.[122] Tetramethylammonium and tetraethylammonium adduct to protein ions weakly, and can carry away charge without fragmenting the protein ion with collisional activation.[122] This is discussed in detail in Chapter 2.

1.4 Salts in Solution: Essential and Problematic in Native Mass Spectrometry

Adverse Effects of Nonvolatile Salts in Protein Solutions on ESI

Interactions between ions and proteins can significantly influence protein structure and function, and high ionic strengths of salts are often necessary to maintain the native structures and functions of proteins and protein complexes.[123-128] Buffers that mimic the intracellular environment typically contain 150-200 mM ionic strengths of nonvolatile salts.[129] However, salts in solutions can adversely affect the ionization and detection of proteins and protein complexes. Salts can adduct to protein and protein complex ions which distributes the analyte ion signal over multiple peaks. This reduces the detection limit for large ions and the ability to detect and identify post-translational modifications or proteins with similar masses. Salts can form clusters which increase baseline noise and cause ion suppression which significantly lowers sensitivity.[130-133] Individual charge states of protein complex ions can be difficult to resolve by native MS if buffers such as Tris-HCl or HEPES are present in protein solutions in concentrations as low as 10 mM.[130] Although most biochemical laboratories typically use buffers that contain high (>100 mM) ionic strengths of nonvolatile salts for protein solutions, analysis of these protein samples by native mass spectrometry requires the removal of these salts. To prevent these adverse effects of nonvolatile salts in native mass spectrometry, salts are typically removed from solutions with methods such as dialysis,[134] diafiltration,[135] or ion chromatography.[130] Protein and protein complex solutions are buffer exchanged into volatile ammonium salt solutions because ammonium does not adduct to the proteins and protein complexes. Ammonium acetate is most commonly used as a buffer in native mass spectrometry, but ammonium bicarbonate is another popular choice.[88,130] However, ammonium salt buffers can be problematic if specific salts are needed to maintain the native structures and functions of the protein or protein complex.[108] This also requires reinvestigation of the properties of the protein or protein complex in the ammonium salt buffer using traditional biochemical techniques.

Techniques for Desalting Protein Ions

Several techniques for the removal or prevention of salt adducts to protein ions during ESI have been developed. These techniques for desalting protein ions are useful for forming ions from solution that contain low ionic strengths (<25 mM) of nonvolatile salts, and are beneficial if low ionic strengths of nonvolatile salts in solution are necessary to maintain structures and functions of the proteins or protein complexes.[136-138] One technique for decreasing salt adduction to protein ions in ESI is adding reagents to the solution that desalt protein ions,[130,133,139-141] such as high concentrations of ammonium acetate,[108,130,133] or compounds with high affinities for sodium (or other cations) such as anions with low proton affinity values,[140] supercharging reagents,[141] or amino acids.[139] These additives to the ESI solution are useful for decreasing sodium ion adduction to protein and protein complex ions, but they can disrupt protein or protein complex structures or activities.[108] In addition, these solution additives are only useful for desalting protein ions formed from aqueous solutions containing less than 25 mM NaCl.[108,139,141,142]

Another technique for desalting protein ions is reacting ESI droplets with organic vapors.[67] McLuckey and coworkers demonstrated that protein ions formed from aqueous solutions containing 10 mM ammonium acetate and up to 1 mM sodium chloride are less sodium ion adducted after reaction with organic vapors such as acetonitrile during ESI.[67] This method decreases the sodium ion adduction to protein ions by up to 47%.[67] Reaction of positively charged protein ions with organic vapors is useful for solutions containing up to 1 mM sodium chloride, but it is ineffective for negatively charged protein ions.[67] This technique is only useful if a protein solution contains very low concentrations of salts (<1 mM), but most biologically relevant buffers contain two orders of magnitude more salt. A potential complication of this technique is that reacting ESI droplets with organic vapors could disrupt the native conformation of the protein ions. McLuckey and coworkers

showed results indicating that holo-myoglobin ions were not denatured upon reaction with organic vapors, but other protein or protein complex ions were not investigated.[67]

The diameters of ESI emitter tips can affect the extent of salt adduction to protein and peptide ions.[143-145] Schmidt et al.[144] showed that insulin ions formed water/methanol/acid with 1 mM sodium chloride with ~1 μm diameter emitter tips have fewer sodium ions adducted than ions formed with ~12 μm tips, and suggested this is due to solvent evaporation and concentration of salts in the ESI droplets or oxidation of the solvent.[144] Similarly, Hu et al.[143] reported that peptide ions formed from aqueous solutions of 0.1 to 25 mM sodium chloride with 0.6 μm or smaller ESI emitter tips are less sodium ion adducted than those from 1.2 μm emitter tips, and they proposed that the droplets from the smaller emitter tips undergo more solvent acidification and less solvent evaporation and fission events than larger droplets.[143]

These techniques for desalting protein or protein complex ions have only been shown to be effective for ions formed from solutions with sodium chloride concentrations up to 25 mM,[67,130,133,139-141,143,144] but most buffers that mimic the cellular environment contain 150 to 200 mM salt. In addition, these methods for desalting protein and protein complex ions have only been investigated for ions formed from either pure water or aqueous ammonium salt solutions with NaCl, but other ions that adduct to proteins such as potassium or Tris are commonly present in buffers. Currently, methods for desalting protein and protein complex ions from aqueous solutions containing salts other than ammonium and low concentrations of sodium are very limited. A method for desalting proteins and protein complex ions from buffers containing physiologically relevant ionic strengths of nonvolatile salts (150-200 mM) with submicrometer ESI emitter tips is discussed in Chapters 4 and 5. This is the first technique for desalting protein/protein complex ions directly from buffers commonly used in protein chemistry that does not require removal of the salts prior to ESI, and is the only method for ESI of proteins/protein complexes from buffers containing physiologically relevant ionic strengths of nonvolatile salts.

1.5 References

(1) International Human Genome Sequencing Consortium. Finishing the euchromatic sequence of the human genome. *Nature* **2004**, *431* (7011), 931–945.

(2) Lander, E. S.; Linton, L. M.; Birren, B.; Nusbaum, C.; Zody, M. C.; Baldwin, J.; Devon, K.; Dewar, K.; Doyle, M.; FitzHugh, W.; et al. Initial sequencing and analysis of the human genome. *Nature* **2001**, *409* (6822), 860–921.

(3) Wilhelm, M.; Schlegl, J.; Hahne, H.; Gholami, A. M.; Lieberenz, M.; Savitski, M. M.; Ziegler, E.; Butzmann, L.; Gessulat, S.; Marx, H.; et al. Mass-spectrometry-based draft of the human proteome. *Nature* **2014**, *509* (7502), 582–587.

(4) Wiśniewski, J. R.; Zougman, A.; Nagaraj, N.; Mann, M. Universal sample preparation method for proteome analysis. *Nat. Methods* **2009**, *6* (5), 359–362.

(5) Rolland, T.; Taşan, M.; Charloteaux, B.; Pevzner, S. J.; Zhong, Q.; Sahni, N.; Yi, S.; Lemmens, I.; Fontanillo, C.; Mosca, R.; et al. A Proteome-Scale Map of the Human Interactome Network. *Cell* **2014**, *159* (5), 1212–1226.

(6) Wishart, D. S.; Jewison, T.; Guo, A. C.; Wilson, M.; Knox, C.; Liu, Y.; Djoumbou, Y.; Mandal, R.; Aziat, F.; Dong, E.; et al. HMDB 3.0—The Human Metabolome Database in 2013. *Nucleic Acids Res.* **2013**, *41* (D1), D801–D807.

(7) Ratner, D. M.; Adams, E. W.; Disney, M. D.; Seeberger, P. H. Tools for glycomics: mapping interactions of carbohydrates in biological systems. *Chembiochem* **2004**, *5* (10), 1375–1383.

(8) Lay, J. O., Jr.; Liyanage, R.; Borgmann, S.; Wilkins, C. L. Problems with the "omics." *TrAC-Trend. Anal. Chem.* **2006**, *25* (11), 1046–1056.

(9) Hsu, C. S.; Hendrickson, C. L.; Rodgers, R. P.; McKenna, A. M.; Marshall, A. G. Petroleomics: advanced molecular probe for petroleum heavy ends. *Org. Mass Spectrom.* **2011**, *46* (4), 337–343.

(10) Mullins, O. C.; Sheu, E. Y.; Hammami, A.; Marshall, A. G. Asphaltenes, heavy oils, and petroleomics. **2007**.

(11) Elliott, A. G.; Merenbloom, S. I.; Chakrabarty, S.; Williams, E. R. Single Particle Analyzer of Mass: A Charge Detection Mass Spectrometer with a Multi-Detector Electrostatic Ion Trap. *Int. J. Mass Spectrom.* **2017**, *414*, 45–55.

(12) Hendrickson, C. L.; Quinn, J. P.; Kaiser, N. K.; Smith, D. F.; Blakney, G. T.; Chen, T.; Marshall, A. G.; Weisbrod, C. R.; Beu, S. C. 21 Tesla Fourier Transform Ion Cyclotron Resonance Mass Spectrometer: A National Resource for Ultrahigh Resolution Mass Analysis. *J. Am. Soc. Mass Spectrom.* **2015**, *26* (9), 1626–1632.

(13) Vasicek, L. A.; Ledvina, A. R.; Shaw, J. B.; Griep-Raming, J.; Westphall, M. S.; Coon, J. J.; Brodbelt, J. S. Implementing photodissociation in an Orbitrap mass spectrometer. *J. Am. Soc. Mass Spectrom.* **2011**, *22* (6), 1105–1108.

(14) Macfarlane, R. D.; Torgerson, D. F. 252Cf-plasma desorption time-of-flight mass spectrometry. *Int. J. Mass Spectrom. Ion Phys.* **1976**, *21* (1-2), 81–92.

(15) Macfarlane, R. D. Californium-252 plasma desorption mass spectrometry. *Anal. Chem.* **1983**, *55* (12), 1247A–1264A.

(16) Tanaka, K.; Waki, H.; Ido, Y.; Akita, S.; Yoshida, Y.; Yoshida, T.; Matsuo, T. Protein and polymer analyses up to m/z 100 000 by laser ionization time-of-flight mass spectrometry. *Rapid Commun. Mass Spectrom.* **1988**, *2* (8), 151–153.

(17) Iribarne, J. V.; Thomson, B. A. On the evaporation of small ions from charged droplets. *J. Chem. Phys.* **1976**, *64* (6), 2287–2294.

(18) Fenn, J. B.; Mann, M.; Meng, C. K.; Wong, S. F.; Whitehouse, C. M. Electrospray ionization–principles and practice. *Mass Spectrom. Rev.* **1990**, *9* (1), 37–70.

(19) Hillenkamp, F.; Karas, M.; Beavis, R. C.; Chait, B. T. Matrix-assisted laser

desorption/ionization mass spectrometry of biopolymers. *Anal. Chem.* **1991**, *63* (24), 1193A–1203A.

(20) Uetrecht, C.; Barbu, I. M.; Shoemaker, G. K.; van Duijn, E.; Heck, A. J. R. Interrogating viral capsid assembly with ion mobility-mass spectrometry. *Nat. Chem.* **2011**, *3* (2), 126–132.

(21) Sharon, M.; Robinson, C. V. The role of mass spectrometry in structure elucidation of dynamic protein complexes. *Annu. Rev. Biochem.* **2007**, *76*, 167–193.

(22) McKay, A. R. C.; Ruotolo, B. T.; Ilag, L. L.; Robinson, C. V. Mass measurements of increased accuracy resolve heterogeneous populations of intact ribosomes. *J. Am. Chem. Soc.* **2006**, *128* (35), 11433–11442.

(23) Klein, D. J.; Moore, P. B.; Steitz, T. A. The contribution of metal ions to the structural stability of the large ribosomal subunit. *RNA* **2004**, *10* (9), 1366–1379.

(24) Ruotolo, B. T.; Benesch, J. L. P.; Sandercock, A. M.; Hyung, S.-J.; Robinson, C. V. Ion mobility–mass spectrometry analysis of large protein complexes. *Nat. Protoc.* **2008**, *3* (7), 1139–1152.

(25) Wyttenbach, T.; Bowers, M. T. Structural stability from solution to the gas phase: native solution structure of ubiquitin survives analysis in a solvent-free ion mobility-mass spectrometry environment. *J. Phys. Chem. B* **2011**, *115* (42), 12266–12275.

(26) Freeke, J.; Bush, M. F.; Robinson, C. V.; Ruotolo, B. T. Gas-phase protein assemblies: Unfolding landscapes and preserving native-like structures using noncovalent adducts. *Chem. Phys. Lett.* **2012**, *524*, 1–9.

(27) Clemmer, D. E.; Hudgins, R. Naked protein conformations: Cytochrome *c* in the gas phase. *J. Am. Soc. Mass Spectrom.* **1995**, *117*, 10141–10142.

(28) Jurchen, J. C.; Williams, E. R. Origin of asymmetric charge partitioning in the dissociation of gas-phase protein homodimers. *J. Am. Chem. Soc.* **2003**, *125* (9), 2817–2826.

(29) Suckau, D.; Shi, Y.; Beu, S. C.; Senko, M. W.; Quinn, J. P.; Wampler, F. M.; McLafferty, F. W. Coexisting stable conformations of gaseous protein ions. *Proc. Natl. Acad. Sci. U.S.A.* **1993**, *90* (3), 790–793.

(30) Samalikova, M.; Grandori, R. Protein Charge-State Distributions in Electrospray-Ionization Mass Spectrometry Do Not Appear To Be Limited by the Surface Tension of the Solvent. *J. Am. Chem. Soc.* **2003**, *125* (44), 13352–13353.

(31) Kebarle, P.; Tang, L. From ions in solution to ions in the gas phase - the mechanism of electrospray mass spectrometry. *Anal. Chem.* **1993**, *65* (22), 972–986.

(32) Allen, S. J.; Schwartz, A. M.; Bush, M. F. Effects of polarity on the structures and charge States of native-like proteins and protein complexes in the gas phase. *Anal. Chem.* **2013**, *85* (24), 12055–12061.

(33) Konermann, L.; Ahadi, E.; Rodriguez, A. D.; Vahidi, S. Unraveling the mechanism of electrospray ionization. *Anal. Chem.* **2013**, *85* (1), 2–9.

(34) Karas, M.; Bahr, U.; Dülcks, T. Nano-electrospray ionization mass spectrometry: addressing analytical problems beyond routine. *Fresenius J Anal Chem* **2000**, *366* (6-7), 669–676.

(35) Smith, J. N.; Flagan, R. C.; Beauchamp, J. L. Droplet evaporation and discharge dynamics in electrospray ionization. *J. Phys. Chem. A* **2002**, *106*, 9957–9967.

(36) Hager, D. B.; Dovichi, N. J.; Klassen, J. S.; Kebarle, P. Droplet Electrospray Mass Spectrometry. *Anal. Chem.* **2002**.

(37) Zohra Olumee; John H Callahan, A.; Akos Vertes. Droplet Dynamics Changes in Electrostatic Sprays of Methanol−Water Mixtures. *J. Phys. Chem. B* **1998**.

(38) Doyle, A.; Moffett, D. Behavior of evaporating electrically charged droplets. *J Coll. Sci. Ipm. U. Tok.* **1964**.

(39) Zhou, S.; Cook, K. D. A mechanistic study of electrospray mass spectrometry: charge gradients within electrospray droplets and their influence on ion response. *J. Am. Soc. Mass Spectrom.* **2001**, *12* (2), 206–214.

(40) Duft, D.; Achtzehn, T.; Müller, R.; Huber, B. A.; Leisner, T. Coulomb fission: Rayleigh jets from levitated microdroplets. *Nature* **2003**, *421* (6919), 128.

(41) Gomez, A.; Tang, K. Charge and fission of droplets in electrostatic sprays. *Phys. Fluids* **1994**, *6* (1), 404–414.

(42) Taflin, D. C.; Ward, T. L.; Davis, E. J. Electrified droplet fission and the Rayleigh limit. *Langmuir* **1989**, *5* (2), 376–384.

(43) Iavarone, A. T.; Williams, E. R. Mechanism of Charging and Supercharging Molecules in Electrospray Ionization. *J. Am. Chem. Soc.* **2003**, *125* (8), 2319–2327.

(44) Felitsyn, N.; Peschke, M.; Kebarle, P. Origin and number of charges observed on multiply-protonated native proteins produced by ESI. *Int. J. Mass Spectrom.* **2002**, *219* (1), 39–62.

(45) Marchese, R.; Grandori, R.; Carloni, P.; Raugei, S. A computational model for protein ionization by electrospray based on gas-phase basicity. *J. Am. Soc. Mass Spectrom.* **2012**, *23* (11), 1903–1910.

(46) Konermann, L.; Douglas, D. J. Unfolding of proteins monitored by electrospray ionization mass spectrometry: a comparison of positive and negative ion modes. *J. Am. Soc. Mass Spectrom.* **1998**, *9* (12), 1248–1254.

(47) Ahadi, E.; Konermann, L. Ejection of solvated ions from electrosprayed methanol/water nanodroplets studied by molecular dynamics simulations. *J. Am. Chem. Soc.* **2011**, *133* (24),

9354–9363.

(48) Konermann, L. A minimalist model for exploring conformational effects on the electrospray charge state distribution of proteins. *J. Phys. Chem. B* **2007**, *111* (23), 6534–6543.

(49) Ahadi, E.; Konermann, L. Modeling the behavior of coarse-grained polymer chains in charged water droplets: implications for the mechanism of electrospray ionization. *J. Phys. Chem. B* **2012**, *116* (1), 104–112.

(50) Consta, S.; Malevanets, A. Classification of the ejection mechanisms of charged macromolecules from liquid droplets. *J. Chem. Phys.* **2013**, *138* (4), 044314.

(51) Chowdhury, S. K.; Katta, V.; Chait, B. T. Probing conformational changes in proteins by mass spectrometry. *J. Am. Chem. Soc.* **1990**, *112* (24), 9012–9013.

(52) Gross, D. S.; Schnier, P. D.; Rodriguez-Cruz, S. E.; Fagerquist, C. K.; Williams, E. R. Conformations and folding of lysozyme ions in vacuo. *Proc. Natl. Acad. Sci. U.S.A.* **1996**, *93* (7), 3143–3148.

(53) Shaw, J. B.; Li, W.; Holden, D. D.; Zhang, Y.; Griep-Raming, J.; Fellers, R. T.; Early, B. P.; Thomas, P. M.; Kelleher, N. L.; Brodbelt, J. S. Complete Protein Characterization Using Top-Down Mass Spectrometry and Ultraviolet Photodissociation. *J. Am. Chem. Soc.* **2013**.

(54) Breuker, K.; Oh, H.; Horn, D. M.; Cerda, B. A.; McLafferty, F. W. Detailed unfolding and folding of gaseous ubiquitin ions characterized by electron capture dissociation. *J. Am. Chem. Soc.* **2002**, *124* (22), 6407–6420.

(55) Dole, M.; Mack, L. L.; Hines, R. L.; Mobley, R. C. Molecular Beams of Macroions. *J. Chem. Phys.* **1968**, *49* (5), 2240–2449.

(56) de la Mora, J. F. Electrospray ionization of large multiply charged species proceeds via Dole's charged residue mechanism. *Anal. Chim. Acta* **2000**, *406* (1), 93–104.

(57) Larriba, C.; de la Mora, J. F.; Clemmer, D. E. Electrospray Ionization Mechanisms for Large Polyethylene Glycol Chains Studied Through Tandem Ion Mobility Spectrometry. *J. Am. Soc. Mass Spectrom.* **2014**.

(58) Heck, A. J. R.; Van Den Heuvel, R. H. H. Investigation of intact protein complexes by mass spectrometry. *Mass Spectrom. Rev.* **2004**, *23* (5), 368–389.

(59) Lord Rayleigh. *Philos. Mag.* **1882**, *14*, 184–186.

(60) Williams, E. R. Proton transfer reactivity of large multiply charged ions. *J. Mass. Spectrom.* **1996**, *31* (8), 831–842.

(61) Schnier, P. D.; Gross, D. S.; Williams, E. R. On the maximum charge state and proton transfer reactivity of peptide and protein ions formed by electrospray ionization. *J. Am. Soc. Mass Spectrom.* **1995**, *6* (11), 1086–1097.

(62) Thomson, B. A.; Iribarne, J. V. Field induced ion evaporation from liquid surfaces at atmospheric pressure. *J. Chem. Phys.* **1979**, *71* (11), 4451–4463.

(63) Spencer, E. A. C.; Ly, T.; Julian, R. R. Formation of the serine octamer: Ion evaporation or charge residue? *Int. J. Mass Spectrom.* **2008**, *270* (3), 166–172.

(64) Gamero-Castano, M.; de la Mora, J. F. Mechanisms of electrospray ionization of singly and multiply charged salt clusters. *Anal. Chim. Acta* **2000**.

(65) Wang, G.; Cole, R. B. Charged residue versus ion evaporation for formation of alkali metal halide cluster ions in ESI. *Anal. Chim. Acta* **2000**, *406* (1), 53–65.

(66) Leize, E.; Jaffrezic, A.; Dorsselaer, A. V. Correlation Between Solvation Energies and Electrospray Mass Spectrometric Response Factors. Study by Electrospray Mass Spectrometry of Supramolecular Complexes in Thermodynamic Equilibrium in Solution. *Org. Mass Spectrom.* **1996**, *31* (5), 537–544.

(67) DeMuth, J. C.; McLuckey, S. A. Electrospray droplet exposure to organic vapors: metal ion removal from proteins and protein complexes. *Anal. Chem.* **2015**, *87* (2), 1210–1218.

(68) Hogan, C. J., Jr.; Carroll, J. A.; Rohrs, H. W.; Biswas, P.; Gross, M. L. Charge Carrier Field Emission Determines the Number of Charges on Native State Proteins in Electrospray Ionization. *J. Am. Chem. Soc.* **2008**, *130* (22), 6926–6927.

(69) Hogan, C. J., Jr.; Carroll, J. A.; Rohrs, H. W.; Biswas, P.; Gross, M. L. Combined Charged Residue-Field Emission Model of macromolecular electrospray ionization. *Anal. Chem.* **2009**, *81* (1), 369–377.

(70) Zhuang, X.; Gavriilidou, A. F. M.; Zenobi, R. Influence of Alkylammonium Acetate Buffers on Protein–Ligand Noncovalent Interactions Using Native Mass Spectrometry. *J. Am. Soc. Mass Spectrom.* **2017**, *28* (2), 341–346.

(71) Pagel, K.; Hyung, S.-J.; Ruotolo, B. T.; Robinson, C. V. Alternate dissociation pathways identified in charge-reduced protein complex ions. *Anal. Chem.* **2010**, *82* (12), 5363–5372.

(72) Zhou, M.; Dagan, S.; Wysocki, V. H. Impact of charge state on gas-phase behaviors of noncovalent protein complexes in collision induced dissociation and surface induced dissociation. *Analyst* **2013**, *138* (5), 1353–1362.

(73) Mirza, U. A.; Chait, B. T. Effects of Anions on the Positive Ion Electrospray Ionization Mass Spectra of Peptides and Proteins. *Anal. Chem.* **1994**, *66* (18), 2898–2904.

(74) Pan, P.; McLuckey, S. A. Electrospray ionization of protein mixtures at low pH. *Anal. Chem.* **2003**, *75* (6), 1491–1499.

(75) Verkerk, U. H.; Peschke, M.; Kebarle, P. Effect of buffer cations and of H_3O^+ on the charge

states of native proteins. Significance to determinations of stability constants of protein complexes. *J. Mass. Spectrom.* **2003**, *38* (6), 618–631.

(76) Peschke, M.; Blades, A.; Kebarle, P. Charged states of proteins. Reactions of doubly protonated alkyldiamines with NH_3: Solvation or deprotonation. Extension of two proton cases to multiply protonated globular proteins observed in the gas phase. *J. Am. Chem. Soc.* **2002**, *124* (38), 11519–11530.

(77) Konermann, L.; Rodriguez, A. D.; Liu, J. On the formation of highly charged gaseous ions from unfolded proteins by electrospray ionization. *Anal. Chem.* **2012**, *84* (15), 6798–6804.

(78) Konermann, L. A Simple Model for the Disintegration of Highly Charged Solvent Droplets during Electrospray Ionization. *J. Am. Soc. Mass Spectrom.* **2009**.

(79) Ahadi, E.; Konermann, L. Molecular dynamics simulations of electrosprayed water nanodroplets: internal potential gradients, location of excess charge centers, and "hopping" protons. *J. Phys. Chem. B* **2009**, *113* (20), 7071–7080.

(80) Yue, X.; Vahidi, S.; Konermann, L. Insights into the mechanism of protein electrospray ionization from salt adduction measurements. *J. Am. Soc. Mass Spectrom.* **2014**, *25* (8), 1322–1331.

(81) Flick, T. G.; Williams, E. R. Supercharging with trivalent metal ions in native mass spectrometry. *J. Am. Soc. Mass Spectrom.* **2012**, *23* (11), 1885–1895.

(82) Iavarone, A. T.; Jurchen, J. C.; Williams, E. R. Effects of solvent on the maximum charge state and charge state distribution of protein ions produced by electrospray ionization. *J. Am. Soc. Mass Spectrom.* **2000**, *11* (11), 976–985.

(83) Dobo, A.; Kaltashov, I. A. Detection of multiple protein conformational ensembles in solution via deconvolution of charge-state distributions in ESI MS. *Anal. Chem.* **2001**, *73* (20), 4763–4773.

(84) Loo, J. A.; Loo, R. R. O.; Udseth, H. R.; Edmonds, C. G.; Smith, R. D. Solvent-induced conformational changes of polypeptides probed by electrospray-ionization mass spectrometry. *Rapid Commun. Mass Spectrom.* **1991**, *5* (3), 101–105.

(85) Thomson, B. A. Declustering and fragmentation of protein ions from an electrospray ion source. *J. Am. Soc. Mass Spectrom.* **1997**, *8* (10), 1053–1058.

(86) Iavarone, A. T.; Jurchen, J. C.; Williams, E. R. Supercharged protein and peptide ions formed by electrospray ionization. *Anal. Chem.* **2001**, *73* (7), 1455–1460.

(87) Sterling, H. J.; Cassou, C. A.; Susa, A. C.; Williams, E. R. Electrothermal supercharging of proteins in native electrospray ionization. *Anal. Chem.* **2012**, *84* (8), 3795–3801.

(88) Cassou, C. A.; Sterling, H. J.; Susa, A. C.; Williams, E. R. Electrothermal supercharging in

mass spectrometry and tandem mass spectrometry of native proteins. *Anal. Chem.* **2013**, *85* (1), 138–146.

(89) Tao, L.; McLean, J. R.; McLean, J. A.; Russell, D. H. A collision cross-section database of singly-charged peptide ions. *J. Am. Soc. Mass Spectrom.* **2007**, *18* (7), 1232–1238.

(90) Lomeli, S. H.; Peng, I. X.; Yin, S.; Loo, R. R. O.; Loo, J. A. New reagents for increasing ESI multiple charging of proteins and protein complexes. *J. Am. Soc. Mass Spectrom.* **2010**, *21* (1), 127–131.

(91) Kharlamova, A.; Prentice, B. M.; Huang, T.-Y.; McLuckey, S. A. Electrospray droplet exposure to gaseous acids for the manipulation of protein charge state distributions. *Anal. Chem.* **2010**, *82* (17), 7422–7429.

(92) Kharlamova, A.; McLuckey, S. A. Negative Electrospray Droplet Exposure to Gaseous Bases for the Manipulation of Protein Charge State Distributions. *Anal. Chem.* **2011**, *83* (1), 431–437.

(93) Pitteri, S. J.; Chrisman, P. A.; Hogan, J. M.; McLuckey, S. A. Electron transfer ion/ion reactions in a three-dimensional quadrupole ion trap: reactions of doubly and triply protonated peptides with SO_2. *Anal. Chem.* **2005**, *77* (6), 1831–1839.

(94) Wells, J. M.; McLuckey, S. A. Collision-Induced Dissociation (CID) of Peptides and Proteins. *Methods Enzymol.* **2005**.

(95) Good, D. M.; Wirtala, M.; McAlister, G. C.; Coon, J. J. Performance characteristics of electron transfer dissociation mass spectrometry. *Mol. Cell Proteomics* **2007**, *6* (11), 1942–1951.

(96) Zubarev, R. A.; Kelleher, N. L. Electron capture dissociation of multiply charged protein cations. A nonergodic process. *J. Am. Chem. Soc.* **1998**, *120* (13), 3265–3266.

(97) Breuker, K.; McLafferty, F. W. The thermal unfolding of native cytochrome c in the transition from solution to gas phase probed by native electron capture dissociation. *Angew. Chem. Int. Ed. Engl.* **2005**, *44* (31), 4911–4914.

(98) Brodbelt, J. S. Shedding light on the frontier of photodissociation. *J. Am. Soc. Mass Spectrom.* **2011**, *22* (2), 197–206.

(99) Valentine, S. J.; Anderson, J. G.; Ellington, A. D.; Clemmer, D. E. Disulfide-Intact and -Reduced Lysozyme in the Gas Phase: Conformations and Pathways of Folding and Unfolding. *J. Phys. Chem. B* **1997**, *101* (19), 3891–3900.

(100) Valentine, S. J.; Counterman, A. E.; Clemmer, D. E. Conformer-dependent proton-transfer reactions of ubiquitin ions. *J. Am. Soc. Mass Spectrom.* **1997**, *8*, 954–961.

(101) Sterling, H. J.; Kintzer, A. F.; Feld, G. K.; Cassou, C. A.; Krantz, B. A.; Williams, E. R.

Supercharging protein complexes from aqueous solution disrupts their native conformations. *J. Am. Soc. Mass Spectrom.* **2012**, *23* (2), 191–200.

(102) Lomeli, S. H.; Yin, S.; Ogorzalek Loo, R. R.; Loo, J. A. Increasing charge while preserving noncovalent protein complexes for ESI-MS. *J. Am. Soc. Mass Spectrom.* **2009**, *20* (4), 593–596.

(103) Teo, C. A.; Donald, W. A. Solution additives for supercharging proteins beyond the theoretical maximum proton-transfer limit in electrospray ionization mass spectrometry. *Anal. Chem.* **2014**, *86* (9), 4455–4462.

(104) Sterling, H. J.; Prell, J. S.; Cassou, C. A.; Williams, E. R. Protein conformation and supercharging with DMSO from aqueous solution. *J. Am. Soc. Mass Spectrom.* **2011**, *22* (7), 1178–1186.

(105) Ogorzalek Loo, R. R.; Lakshmanan, R.; Loo, J. A. What protein charging (and supercharging) reveal about the mechanism of electrospray ionization. *J. Am. Soc. Mass Spectrom.* **2014**, *25* (10), 1675–1693.

(106) Loo, J. A.; Loo, R. R. O.; Light, K. J.; Edmonds, C. G.; Smith, R. D. Multiply charged negative ions by electrospray ionization of polypeptides and proteins. *Anal. Chem.* **2002**, *64* (1), 81–88.

(107) Sterling, H. J.; Cassou, C. A.; Trnka, M. J.; Burlingame, A. L.; Krantz, B. A.; Williams, E. R. The role of conformational flexibility on protein supercharging in native electrospray ionization. *Phys. Chem. Chem. Phys.* **2011**, *13* (41), 18288–18296.

(108) Sterling, H. J.; Batchelor, J. D.; Wemmer, D. E.; Williams, E. R. Effects of buffer loading for electrospray ionization mass spectrometry of a noncovalent protein complex that requires high concentrations of essential salts. *J. Am. Soc. Mass Spectrom.* **2010**, *21* (6), 1045–1049.

(109) Sterling, H. J.; Daly, M. P.; Feld, G. K.; Thoren, K. L.; Kintzer, A. F.; Krantz, B. A.; Williams, E. R. Effects of supercharging reagents on noncovalent complex structure in electrospray ionization from aqueous solutions. *J. Am. Soc. Mass Spectrom.* **2010**, *21* (10), 1762–1774.

(110) Sterling, H. J.; Williams, E. R. Real-Time Hydrogen/Deuterium Exchange Kinetics via Supercharged Electrospray Ionization Tandem Mass Spectrometry. *Anal. Chem.* **2010**.

(111) Catalina, M. I.; Van Den Heuvel, R. H. H.; van Duijn, E.; Heck, A. J. R. Decharging of globular proteins and protein complexes in electrospray. *Chem. Eur. J.* **2005**, *11* (3), 960–968.

(112) Verkerk, U. H.; Kebarle, P. Ion-ion and ion-molecule reactions at the surface of proteins produced by nanospray. Information on the number of acidic residues and control of the number of ionized acidic and basic residues. *J. Am. Soc. Mass Spectrom.* **2005**, *16* (8), 1325–1341.

(113) Schnier, P. D.; Gross, D. S.; Williams, E. R. Electrostatic forces and dielectric polarizability of multiply protonated gas-phase cytochrome c ions probed by ion/molecule chemistry. *J. Am. Chem. Soc.* **1995**, *117* (25), 6747–6757.

(114) Le Blanc, J. C. Y.; Wang, J.; Guevremont, R.; Siu, K. W. M. Electrospray mass spectra of protein cations formed in basic solutions. *Org. Mass Spectrom.* **1994**, *29* (11), 587–593.

(115) Loo, R. R. O.; Smith, R. D. Proton transfer reactions of multiply charged peptide and protein cations and anions. *J. Mass. Spectrom.* **1995**, *30*, 339–347.

(116) Cassady, C. J.; Wronka, J.; Kruppa, G. H.; Laukien, F. H.; Hettich, R. Deprotonation reactions of multiply protonated ubiquitin ions. *Rapid Commun. Mass Spectrom.* **1994**, *8* (5), 394–400.

(117) Winger, B. E.; Light-Wahl, K. J.; Smith, R. D. Gas-phase proton transfer reactions involving multiply charged cytochrome c ions and water under thermal conditions. *J. Am. Soc. Mass Spectrom.* **1992**, *3* (6), 624–630.

(118) McLuckey, S. A.; Van Berkel, G. J.; Glish, G. L. Reactions of dimethylamine with multiply charged ions of cytochrome c. *J. Am. Chem. Soc.* **1990**, *112* (14), 5668–5670.

(119) McLuckey, S. A.; Stephenson, J. L. Ion/ion chemistry of high-mass multiply charged ions. *Mass Spectrom. Rev.* **1998**.

(120) Stephenson, J. L.; McLuckey, S. A. Ion/ion reactions in the gas phase: Proton transfer reactions involving multiply-charged proteins. *J. Am. Chem. Soc.* **1996**, *118* (31), 7390–7397.

(121) Lermyte, F.; Williams, J. P.; Brown, J. M.; Martin, E. M.; Sobott, F. Extensive Charge Reduction and Dissociation of Intact Protein Complexes Following Electron Transfer on a Quadrupole-Ion Mobility-Time-of-Flight MS. *J. Am. Soc. Mass Spectrom.* **2015**, *26* (7), 1068–1076.

(122) Susa, A. C.; Mortensen, D. N.; Williams, E. R. Effects of Cations on Protein and Peptide Charging in Electrospray Ionization from Aqueous Solutions. *J. Am. Soc. Mass Spectrom.* **2014**, *25* (6), 918–927.

(123) Peruzzi, N.; Ninham, B. W.; Nostro, Lo, P.; Baglioni, P. Hofmeister Phenomena in Nonaqueous Media: The Solubility of Electrolytes in Ethylene Carbonate. *J. Phys. Chem. B* **2012**.

(124) Baldwin, R. L. How Hofmeister ion interactions affect protein stability. *Biophys. J.* **1996**, *71* (4), 2056–2063.

(125) Zhu, M. M.; Rempel, D. L.; Zhao, J.; Giblin, D. E.; Gross, M. L. Probing Ca2+-induced conformational changes in porcine calmodulin by H/D exchange and ESI-MS: effect of cations and ionic strength. *Biochemistry* **2003**, *42* (51), 15388–15397.

(126) van den Bremer, E. T. J.; Jiskoot, W.; James, R.; Moore, G. R.; Kleanthous, C.; Heck, A. J. R.; Maier, C. S. Probing metal ion binding and conformational properties of the colicin E9 endonuclease by electrospray ionization time-of-flight mass spectrometry. *Protein Sci.* **2002**, *11* (7), 1738–1752.

(127) Maret, W. New perspectives of zinc coordination environments in proteins. *J. Inorg. Biochem.* **2012**, *111*, 110–116.

(128) Zhang, Y.; Cremer, P. S. Chemistry of Hofmeister anions and osmolytes. *Annu. Rev. Phys. Chem.* **2010**, *61* (1), 63–83.

(129) Lodish, H.; Berk, A.; Zipursky, S. L.; Matsudaira, P.; Baltimore, D.; Darnell, J. *Molecular Cell Biology*, 4 ed.; W.H. Freeman: New York, 2000.

(130) Hernández, H.; Robinson, C. V. Determining the stoichiometry and interactions of macromolecular assemblies from mass spectrometry. *Nat. Protoc.* **2007**, *2* (3), 715–726.

(131) Wang, G.; Cole, R. B. Effect of solution ionic strength on analyte charge state distributions in positive and negative ion electrospray mass spectrometry. *Anal. Chem.* **1994**, *66* (21), 3702–3708.

(132) Pan, P.; McLuckey, S. A. The effect of small cations on the positive electrospray responses of proteins at low pH. *Anal. Chem.* **2003**, *75* (20), 5468–5474.

(133) Iavarone, A. T.; Udekwu, O. A.; Williams, E. R. Buffer loading for counteracting metal salt-induced signal suppression in electrospray ionization. *Anal. Chem.* **2004**, *76* (14), 3944–3950.

(134) Xiang, F.; Lin, Y.; Wen, J.; Matson, D. W. An integrated microfabricated device for dual microdialysis and on-line ESI-ion trap mass spectrometry for analysis of complex biological samples. *Anal. Chem.* **1999**, *71* (8), 1485–1490.

(135) Prodanov, M.; Garrido, I.; Vacas, V.; Lebrón-Aguilar, R.; Dueñas, M.; Gómez-Cordovés, C.; Bartolomé, B. Ultrafiltration as alternative purification procedure for the characterization of low and high molecular-mass phenolics from almond skins. *Anal. Chim. Acta* **2008**, *609* (2), 241–251.

(136) Gamba, G. Molecular physiology and pathophysiology of electroneutral cation-chloride cotransporters. *Physiol. Rev.* **2005**, *85* (2), 423–493.

(137) Toyoshima, C.; Nomura, H. Structural changes in the calcium pump accompanying the dissociation of calcium. *Nature* **2002**, *418* (6898), 605–611.

(138) Valero, E.; De Bonis, S.; Filhol, O.; Wade, R. H.; Langowski, J.; Chambaz, E. M.; Cochet, C. Quaternary structure of casein kinase 2. Characterization of multiple oligomeric states and relation with its catalytic activity. *J. Biol. Chem.* **1995**, *270* (14), 8345–8352.

(139) Clarke, D. J.; Campopiano, D. J. Desalting large protein complexes during native electrospray mass spectrometry by addition of amino acids to the working solution. *Analyst*

2015, *140* (8), 2679–2686.

(140) Flick, T. G.; Cassou, C. A.; Chang, T. M.; Williams, E. R. Solution additives that desalt protein ions in native mass spectrometry. *Anal. Chem.* **2012**, *84* (17), 7511–7517.

(141) Cassou, C. A.; Williams, E. R. Desalting protein ions in native mass spectrometry using supercharging reagents. *Analyst* **2014**, *139* (19), 4810–4819.

(142) Flick, T. G.; Merenbloom, S. I.; Williams, E. R. Effects of Metal Ion Adduction on the Gas-Phase Conformations of Protein Ions. *J. Am. Soc. Mass Spectrom.* **2013**, *24* (11), 1654–1662.

(143) Hu, J.; Guan, Q.-Y.; Wang, J.; Jiang, X.-X.; Wu, Z.-Q.; Xia, X.-H.; Xu, J.-J.; Chen, H.-Y. Nanoemitters Suppress the Formation of Metal Adduct Ions in Electrospray Ionization Mass Spectrometry. *Anal. Chem.* **2017**.

(144) Schmidt, A.; Karas, M.; Dülcks, T. Effect of different solution flow rates on analyte ion signals in nano-ESI MS, or: when does ESI turn into nano-ESI? *J. Am. Soc. Mass Spectrom.* **2003**, *14* (5), 492–500.

(145) Susa, A. C.; Xia, Z.; Williams, E. R. Small Emitter Tips for Native Mass Spectrometry of Proteins and Protein Complexes from Nonvolatile Buffers That Mimic the Intracellular Environment. *Anal. Chem.* **2017**, *89* (5), 3116–3122.

Chapter 2

Effects of Cations on Protein and Peptide Charging in Electrospray Ionization from Aqueous Solutions

This chapter is reproduced with permission from:

Anna C. Susa, Daniel N. Mortensen, Evan R. Williams
"Effects of Cations on Protein and Peptide Charging in Electrospray Ionization from Aqueous Solutions"
Journal of the American Society for Mass Spectrometry, **2014**, *25*(6): 918–927

2.1 Abstract

The effects of eight different cations with ionic radii between 69 and 337 pm on the charging of peptides and proteins with electrospray ionization from aqueous acetate salt solutions are reported. Significant adduction occurs for all cations except NH_4^+, and the average protein charge is lower when formed from solutions containing salts compared to solutions without salts added. Circular dichroism and ion mobility results show the protein conformations are different in pure water compared to salt solutions, which likely affects the extent of charging. The average charge of protein and peptide ions formed from solutions with Li^+ and Cs^+, which have Gibbs solvation free energies (GSFEs) that differ by 225 kJ/mol, is similar. Lower charge states are typically formed from solutions with tetramethylammonium and tetraethylammonium that have lower GSFE values. Loss of the larger cations that have the lowest GSFEs is facile when adducted protein ions are collisionally activated resulting in the formation of lower analyte charge states. This reaction pathway provides a route to produce abundant singly protonated protein ions under native mass spectrometry conditions. The average protein and peptide charge with NH_4^+ is nearly the same as that with Rb^+ and K^+, cations with similar GSFE and ionic radii. This indicates that proton transfer from NH_4^+ to proteins plays an insignificant role in the extent of protein charging in native mass spectrometry.

2.2 Introduction

Electrospray ionization (ESI) is widely used to produce intact, multiply charged gas-phase macromolecular ions directly from solution for analysis by mass spectrometry (MS).[1,2] Multiple charging has the advantage that the mass-to-charge (m/z) ratios of the intact molecular ions are typically within the upper range of most mass spectrometers. The extent of charging depends on many factors, including solution-phase conformation,[3-5] solvent surface tension,[6,7] basicities of the analyte and solvent,[1,2,7,8] instrumental parameters,[3-5,9] and other factors. Broad distributions of high charge states are formed from solutions in which proteins are denatured, whereas more narrow distributions of low charge states are formed from aqueous buffered solutions where proteins have native or native-like conformations. The extent of charging from either denaturing or buffered aqueous solutions can

be significantly increased by supercharging[6,7,10-19] or decreased by addition of bases either in solution[7] or in the gas phase.[20,21]

Several ESI ion formation mechanisms have been proposed to account for the observed charging, including the charge residue mechanism (CRM),[22] the ion evaporation mechanism (IEM),[23] and the combined charge residue field emission model (CCRFEM),[24] which incorporates aspects of both of the former mechanisms. Highly charged droplets that are produced by ESI can undergo solvent evaporation and Rayleigh fission to form smaller, highly charged droplets that carry away a significant fraction of the original droplet charge.[25,26] In the IEM, gas-phase ions are produced from the ESI droplet when the electrostatic energy at the surface of the droplet overcomes the Gibbs free energy barrier for the process

$$X^+(aq) \rightarrow X^+(H_2O)_n(g)$$

where X^+ is the ion of interest and n is the number of water molecules.[23,27] In the CRM, gas-phase ions are produced by solvent evaporation in the late stages of the droplet lifetime.[22] Globular protein and polymer charging is related to the Rayleigh limit charge, Z_R, of droplets roughly the same size as the analyte molecule, a result that is consistent with the CRM for ion formation under native conditions.[6,28] In contrast, much less charge would be expected if these ions were produced by the IEM.[6]

Ions, or buffers commonly used in native ESI mass spectrometry, can also affect charging of proteins and peptides, an effect related to the ionic strength as well as charge state of the ions.[29-34] Ammonium acetate is extensively used as a buffer in native ESI mass spectrometry. The extent of protein charging from aqueous ammonium acetate solution is often thought to be determined by proton transfer from NH_4^+ to the protein.[2,35-49] It was proposed that "NH_4^+ ions present at the surface of the shrinking water droplet, which are part of the excess charge on the droplet, are expected to attach themselves to the basic sites and ultimately lead to their protonation".[35] However, other results indicate that cations typically adduct to acidic sites such as carboxyl groups.[50,51] In the CCRFEM, small ions that reside at the droplet surface evaporate from the droplet at a rate determined by their solvation energy and the electric field strength at the droplet surface, whereas macromolecules are located in the interior of the droplet and ionize by the CRM.[24] Salts with low solvation energies carry away some of the droplet surface charge resulting in fewer charges available to the macromolecule.[24]

Here, the effects of cations with a wide range in Gibbs solvation free energy (GSFE) values in aqueous acetate solutions on protein and peptide charge are investigated. The extent of charging trends with the GSFE, but loss of large cations with low GSFE values readily occurs from adducted molecular ions in the gas phase resulting in formation of lower charge states. This dissociation pathway results in a facile method to produce singly protonated protein ions in native mass spectrometry. These results also show that proton transfer reactions from protonated ammonia to proteins and peptides do not play a significant role in the extent of charging in native mass spectrometry.

2.3 Experimental

Data were acquired using either a Waters Q-TOF Premier hybrid mass spectrometer or a Waters Synapt G2 High Definition mass spectrometer (Waters, Milford, MA, USA) equipped with a Z-spray nanoelectrospray (nano-ESI) ion source. Peptide or protein solutions (50 μM) with 25 mM acetate salts (unless otherwise noted) were prepared using Millipore Milli-Q water. The pH of all protein and peptide solutions except those in cesium acetate and rubidium acetate solutions ranges from 6.5 to 6.9. The pH of the protein and peptides in cesium and rubidium acetate solutions is 5.0,

likely a result of different suppliers for these salts. Nano-ESI emitters, made by pulling borosilicate glass capillaries (1.0 mm o.d./0.78 mm i.d.; Sutter Instruments, Novato, CA, USA) to a tip i.d. of approximately 1 m with a Flaming/Brown micropipette puller (model P-87; Sutter Instruments), were filled with ~5 μL of sample. A 1.0-1.5 kV potential was applied to a platinum wire (0.127 mm diameter, Sigma, St. Louis, MO, USA) that is in contact with the solution to initiate ion formation by nano-ESI. Gentle source conditions that minimized ion activation were used. For ion mobility experiments, the traveling wave ion mobility cell was operated at a He flow rate of 180 mL/min, an IMS gas (N_2) flow rate of 90 mL/min, a traveling wave velocity of 1000 m/s, and a wave height of 40 V.

The average charge was calculated as an abundance weighted sum of all individual charge states divided by the total ion abundance for all charge states. The uncertainties correspond to the standard deviation of three replicate measurements from three separate ESI emitters. Angiotensin II, bradykinin, substance P, bovine ubiquitin, egg white lysozyme, β-lactoglobulin, and ammonium acetate were obtained from Sigma (St. Louis, MO, USA); Substance P (free acid) from GenScript (Piscataway, NJ, USA); Substance P methyl ester from American Peptide Company (Sunnyvale, CA, USA); Lithium acetate, sodium acetate, potassium acetate from Fisher Scientific (Pittsburgh, PA, USA); Tetramethylammonium acetate and tetraethylammonium acetate from MP Biomedicals (Solon, OH, USA); Cesium acetate and rubidium acetate from Alfa Aesar (Ward Hall, MA, USA). All chemicals were used without further purification.

Circular dichroism (CD) measurements were performed using a Jasco 810 spectropolarimeter (JASCO, Inc., Easton, MD, USA). Solutions were stirred with a Teflon stir bar in a 1.0 cm quartz cuvette at room temperature during wavelength scan analysis from 190 to 260 nm.

2.4 Results and Discussion

2.4.1 Effects of cations on protein and peptide charge

Ions of eight different proteins and peptides were formed by nano-ESI from aqueous solutions containing nine different acetate salt solutions to determine how cations affect the charge states that are produced. Protein and peptide ions formed from these solutions are expected to have native or native-like structures. These biopolymers have pI values between 4.8 and 12.0,[52] and the Gibbs solvation free energies of the different cations span a 475 kJ/mol range.[53] Extensive cation adduction generally occurs for all protein and peptide ions formed from these acetate salt solutions, with the most adduction occurring with sodium and potassium (Supplemental Table 2.1). Protonated molecular ions with no NH_4^+ adducts are produced with ammonium acetate, but with the other cations, minimal or no protonated ions are formed. For example, over 30 Na^+ adduct to the 5+ charge state of ubiquitin formed from sodium acetate solution, whereas no NH_4^+ adducts to this same charge state with ammonium acetate (Figure 2.1). Alkali metal acetate and alkylammonium acetate clusters are also abundant, especially below m/z ~1500 (Figure 2.1). Ammonium acetate clusters are not observed.

The Rayleigh limit charge of a water droplet of the same size as each ion was estimated by approximating the molecules as spheres with densities of 1 mg/mL[6,28] ($Z_{R,m}$) and also by using gas-phase collisional cross sections (σ) [20,54-56] of the lowest charge state reported for the molecular ions to obtain the radius approximating the ion as a sphere ($Z_{R,\sigma}$). These values, along with the maximum (Z_{max}) and average (Z_{ave}) charge of these ions formed from water without salts added and aqueous solutions with NH_4^+ or Rb^+ are given in Table 2.1. The charge of protein and peptide ions formed from NH_4^+ and Rb^+ acetate solutions are compared because the ionic radii of NH_4^+ and Rb^+ are similar (148 pm and 149 pm, respectively) as are their GSFEs (−285 kJ/mol and −275 kJ/mol,

respectively; all values are relative to a GSFE of tetraethylammonium (TEA^+) which is arbitrarily assigned a value of zero).[53] $Z_{R,\sigma}$ is consistently larger than $Z_{R,m}$ by an average of 27 % and these values provide an indication of the range of uncertainties in estimating the charging predicted by the CRM. Z_{max} for protein and peptide ions formed from water is within one charge of $Z_{R,\sigma}$ except for β-lactoglobulin where Z_{max} is much lower than $Z_{R,\sigma}$. For the biopolymer ions formed from pure water, Z_{max} is 83 % of $Z_{R,\sigma}$ and 106 % of $Z_{R,m}$, respectively. Lower charge states of biopolymer ions are produced from ammonium acetate and rubidium acetate solutions; Z_{max} is 75 and 69 % of $Z_{R,\sigma}$ for these respective solutions, and Z_{max} is 95 and 88 % of $Z_{R,m}$. These results are consistent with those of De la Mora who reported that the Z_{max} and Z_{ave} of protein ions formed from water or ammonium acetate are within 60 to 110 % of Z_R.[28] Results for dendrimers showed a correlation between ion charging in different solvents and Z_R calculated using the surface tension of the different solvents.[6] These results provide support for large globular protein ions being formed by the CRM. In contrast, ions formed by the IEM would have significantly less charge.[6]

The average protein charge as a function of the relative Gibbs solvation free energy of the cations is shown in Figure 2.2. The dashed lines in the figures correspond to the average charge of these protein ions formed from aqueous solutions without salts added, which are higher than those from solutions containing acetate salts, although the effects of salts are minimal for β-lactoglobulin (Figure 2.2). The average protein ion charge decreases by 4 ± 1 % from Li^+ (GSFE is −475 kJ/mol) to Cs^+ (−250 kJ/mol), a range of 225 kJ/mol in Gibbs solvation free energy. With tetramethylammonium (TMA^+) and TEA^+ acetate, which have the lowest Gibbs solvation free energies,[53] the average charge is much lower. The most significant change in protein charging occurs between Cs^+ and TMA^+. Protein ions formed from TMA^+ and TEA^+ acetate solutions have on average 32 and 43 % less charge, respectively, than those formed from Cs^+ acetate solutions. The lower charging for protein ions formed from solutions with salts could be a result of cation evaporation from the ESI droplet lowering the overall charge available for the protein as would be the case for the CCRFEM.[24]

The relative ion evaporation rates for alkali metal and alkylammonium ions differ significantly and correlate with the Gibbs solvation free energies (GSFEs) of the ions at low concentrations (< 10−5 M), but the differences in ion evaporation rates for the different ions is significantly less at high concentrations (> 10−5 M) and the correlation with the GSFEs of the cations is low.[57-59] The relative rates of ion evaporation for the alkali metals do not depend strongly on GSFE at high concentration, and the rate of evaporation for Li^+ is higher than that of Cs^+,[27,58] which is the opposite of the trend reported at low salt concentrations. The lower charging of protein ions formed from Cs^+ solutions compared to that from Li^+ solutions is inconsistent with the relative ion evaporation rates reported for these alkali metal ions at high concentrations [27,58] if the protein ions are formed by the CCRFEM. The relative rate of ion evaporation of TEA^+ is approximately 5 times that of Cs^+ at high concentrations,[58] which is consistent with the CCRFEM for the formation of lower protein charge from the alkylammonium acetate versus the alkali metal ion acetate solutions.

Some studies suggest that peptide ions are produced by the IEM[60-62] whereas others indicated the possibility that peptide ions are produced by the CRM.[6,62] In contrast to proteins, the average charge for peptide ions formed from water without salts added can be lower (three different forms of substance P), higher (angiotensin II) or similar (bradykinin) to the average charge when the alkali metal or ammonium acetate salts are added (Figure 2.3). The average charge of all peptide ions, except $SubPNH_2$, is lower when these ions are formed from TMA^+ and TEA^+ acetate solutions compared to the average charge of these ions formed from the other solutions. There is no significant dependence of the average charge of $SubPNH_2$ ions on the GSFE of the cations. The protein and most peptide ions investigated here follow a similar trend, in which similar charge states are formed from ammonium and alkali metal ion acetate solutions and lower charge states are formed from

alkylammonium acetate solutions. The higher average charge of angiotensin II ions formed from alkali metal ion and ammonium acetate salt solutions than from pure water suggests that evaporation of small cations does not play a significant role in the charging of these ions.

2.4.2 Effects of protein and peptide structure on charge

The shapes of molecules in solution can significantly affect the charge of these ions in ESI. The effects of salts on the secondary structure of ubiquitin (Figure 2.4), β-lactoglobulin and lysozyme (Supplemental Figures 2.2 and 2.3) were investigated using circular dichroism (CD) in the far-UV region, which probes α-helical and β-sheet content. The CD spectrum of ubiquitin in water without salts added is distinctly different from the CD spectra of ubiquitin in 25 mM ammonium acetate and 25 mM sodium acetate solutions. There is greater ellipticity at 208 nm in water, indicative of more α-helical structure,[63] than when salts are present. There are more subtle differences in the CD spectra of ubiquitin in ammonium acetate and sodium acetate, indicating that the identity of the cation has only a small influence on the secondary structure of ubiquitin in these solutions. CD spectra of β-lactoglobulin and lysozyme (Supplemental Figures 2.2 and 2.3) in water without salts added and water with either ammonium acetate or sodium acetate added show similar trends. The CD signal for lysozyme in water has greater positive ellipticity between 225 and 230 nm, indicative of more α-helical structure[63] (Supplemental Figure 2.3) and the signal for β-lactoglobulin in water is less intense at 217 nm than the corresponding signal of β-lactoglobulin in ammonium acetate and sodium acetate. These CD results show that these proteins have measurable differences in their secondary structure in water without added salts compared to when ammonium acetate or sodium acetate is in the solution and that the identity of the cation also has subtle effects on secondary structure in solution.

Ion mobility spectrometry (IMS) was also used to determine whether ubiquitin ions formed from water without salts and with ammonium acetate or sodium acetate retain different conformations in the gas phase. Arrival time distributions of $(U + 6H)^{6+}$ formed from water and from ammonium acetate and for $(U + 4Na + 2H)^{6+}$ formed from sodium acetate solutions are shown in Figure 2.5. The arrival time distributions of $(U + 6H)^{6+}$ formed from ammonium acetate have two broad features centered at 10 and 14 ms, whereas the arrival time distributions for the same ions formed from water has a very broad feature at 13.5 ms with a less abundant undefined shoulder at 10 ms. The arrival time distributions of $(U + 6H)^{6+}$ formed from these two solutions show a distinct range of conformer families with the more compact conformers most abundant in ammonium acetate solution. These data clearly show that the gas-phase conformations of protonated ubiquitin 6+ formed from water and ammonium acetate solutions are different, and therefore the solution-phase structures of these ions are most likely different as well, a result consistent with the CD measurements. The greater abundance of more compact conformers from ammonium acetate solution is also consistent with the lower charging observed from this solution.

No $(U + 6H)^{6+}$ is formed from the sodium acetate solution, but the arrival time distribution of $(U + 4Na + 2H)^{6+}$ has a feature centered at 9 ms with a shoulder at 10.5 ms. This indicates that the partially sodiated ions are even more compact than the compact conformers of the fully protonated ions with the same charge state formed from water or ammonium acetate. Nonspecific cation adduction to gaseous protein ions typically results in compaction of structure compared to the protonated form, even when the ions are formed from the same solution.[64] The CD results show that the protein conformation in aqueous solutions without salts added is different than in ammonium acetate solutions. IMS results show that this conformational difference in solution translates to a difference in the conformation of gas-phase ions. The difference in solution-phase conformation of proteins in solutions without salts versus with salts added likely contributes significantly to the difference in protein charging from these solutions.

CD spectra were also obtained for angiotensin II and the three forms of SubP in water with and without salts added to determine if the salts affect the secondary structure of these peptides. The CD signal for these peptides in water without salts added is the same as that with ammonium acetate or sodium acetate added (Supplemental Figures 2.1 and 2.4) indicating that there is not a significant difference in the secondary structure of these peptides with and without salts. The C-termini of the three forms of SubP differ and this affects the relative charging of these peptides from acetate solutions and water. This indicates that the primary structure of the peptide plays a role in the effect of cations on the extent of charging.

2.4.3 Effect of internal energy on protein charge

Energetic collision of multiply charged ions with gases can lower the charge states in ESI.[65] The effects of collisional activation on the average charge of ubiquitin ions formed from various acetate salt solutions and from pure water as a function of collision voltage are shown in Figure 2.6a. For K^+, Rb^+, Cs^+, TMA^+, and TEA^+ acetate solutions, the average charge decreases with increasing collision voltage. For example, the average charge of ubiquitin ions formed from TEA^+ acetate decreases from 2.95 ± 0.02 to 1.03 ± 0.04, at collision voltages of 0 and 70 V, respectively. In contrast, there is a minimal decrease in the average charge of ubiquitin ions formed from water without salts added, and aqueous solutions with Li^+, Na^+ or NH_4^+ over the same range of collision voltages. The average charge of ubiquitin ions formed from solutions with TMA^+ and TEA^+ is lower than with the other ions at 0 V. Based on results at high collision voltage, it is likely that some collisional activation that occurs in the source, even with soft conditions, lowers the charge from that originally produced by ESI.

The decrease in average charge with increasing collision energy can be attributed to two dissociation pathways: loss of adducted cations and preferential fragmentation of the high charge ions. Loss of TEA^+ and TMA^+ from ubiquitin is facile whereas loss of Li^+ or Na^+ does not occur prior to backbone fragmentation at higher collision energy. For example, collisional activation of $(U + 7Cs - 2H)^{5+}$ at 60 V results in the sequential loss of Cs^+ to form $(U + 6Cs - 2H)^{4+}$ and $(U + 5Cs - 2H)^{3+}$ exclusively whereas collisional activation of $(U + 7Na - 2H)^{5+}$ at the same voltage results in b_2^+, b_3^+, y_3^+ and y_4^+ fragments but no loss of Na^+. High charge states of ubiquitin ions formed from water, ammonium acetate, sodium acetate and lithium acetate solutions fragment to form *b* and *y* ions at collision energies of ~30 V and higher. In contrast, b and y ions from ubiquitin ions generated from the other acetate salt solutions start to form between 50 - 80 V. These results are consistent with the loss of the larger cations taking away internal energy and thus more internal energy deposition is required to produce backbone cleavage.

The binding energies of these cations to gaseous proteins and peptides are not known, but the gas phase binding energies of water molecules to these cations have been reported.[66-69] The binding energies of a water molecule to Li^+, Na^+, NH_4^+, K^+, Rb^+, Cs^+, TMA^+ and TEA^+ are 142, 100, 83, 75, 67, 57, 38 and 29 kJ/mol, respectively.[67-69] This ordering is nearly the same as the GSFE values of these cations. We expect there to be a similar trend in the binding energies of these cations to peptides and proteins. Larger cations should be bound less strongly to the peptide or protein and should be more readily lost. The higher collision voltage necessary to form *b* and *y* ions for the large cations can be attributed to the energy lost as a result of breaking the bond between the cation and protein; additional energy must be added to form b and y fragments.

Hogan et al.[24] found that the charge states of several protein ions formed by ESI from triethylammonium bicarbonate solutions are lower than the charge states of the corresponding ions formed from ammonium acetate solutions. Triethylammonium evaporates more rapidly from a droplet than ammonium HoganJr:2009ct} and could lower droplet charge and the overall charge of

the protein. However, TEA^+ adducts much less strongly to the protein ion and is easily lost as a result of gas-phase collisional activation, which also lowers the overall charge of the protein ion.

2.4.4 Effects of cation proton transfer reactivity on protein and peptide charge

Adduction of basic molecules, such as diethylamine, in the ESI solution can result in lower charging of proteins [7,44,70,71] as a result of these molecules preferentially carrying away charges as a result of proton transfer from the protein to the basic molecules. Charging of proteins and protein complexes from aqueous ammonium acetate solutions is often attributed to proton transfer from NH_4^+ to the protein.[2,35-49] The GSFE of NH_4^+ (285 kJ/mol) is between that of K^+ (295 kJ/mol) and Rb+ (275 kJ/mol) and the ionic radius is nearly the same as Rb^+. The average charge of the protein ions formed from NH_4^+ (25 mM solution) is higher than that of Rb^+ and K^+ by 5 ± 2 % and 5 ± 1 %, respectively. Neither Rb^+ nor K^+ can undergo proton transfer reactions, and this difference in protein charging for solutions containing NH_4^+ versus Rb^+ or K^+ is minor. The initial pH of the rubidium acetate solutions is slightly lower than that of the ammonium and potassium solutions, but the similar results from Rb^+ and K^+ solutions suggest that this difference in initial solution pH has a negligible effect on the protein and peptide ion charge. Higher concentrations of ammonium acetate have little effect on protein or peptide charge. The average charge of proteins and peptides is 2 ± 1 % and 1 ± 1 % lower, respectively, when these ions are formed from 100 mM ammonium acetate solutions compared to 25 mM. The negligible difference in charging from solutions containing NH_4^+ versus Rb^+ or K^+, and the minimal effect of NH_4^+ concentration on protein charge indicates that proton transfer of NH_4^+ to the protein ion is insignificant in the extent of protein charging in native mass spectrometry. However, while interaction of NH_4^+ to deprotonated acidic sites in the protein can reduce the number of cation adducts,[35,38,72,73] such as sodium, and proton transfer from NH_4^+ to the acidic sites may occur, our results indicate that this does not result in a significant change in the overall net charge on the protein ions.

2.4.5 Generating singly charged and neutral proteins

Low charge state ions of proteins and protein complexes are often more compact and more stable to induced conformation changes and gas phase collisional cross sections of low charge states of proteins are often similar to cross sections calculated from crystal structures.[20,74,75] The charge states of proteins can be reduced by several different methods, including ion-ion,[76] ion-electron,[77,78] or ion-molecule reactions.[21,44] Low charge state ions can also be readily formed by collisionally activating protein or peptide ions complexed with TMA^+ and TEA^+. For example, collisional activation of $(U + 2TMA + H)^{3+}$ results in nearly exclusive formation of $(U + TMA + H)^{2+}$ and $(U + H)^{1+}$ at 40 V and 80 V collision energies, respectively (Figure 2.6b). The $(U + H)^{1+}$ ion can be formed from $(U + TMA + H)^{2+}$ with a 96 % yield at the latter collision voltage. Similarly, $(M + H)^{1+}$ of several other protein ions, including cytochrome *c*, myoglobin, and melittin can be formed from a native ESI solution using this method. Because some of the collisional energy deposited into the ion is required to break the noncovalent interaction of the cation and the protein, this method to produce singly protonated ions may not significantly perturb the structures of large proteins and protein complexes.

The number of TMA^+ or TEA^+ adducts is often greater than the net ion charge (Figure 2.1). When the number of adducts is equal to the net charge state of the ion, the protein molecule itself has a net charge of zero. Similarly, the protein molecule has a net negative charge when the number of positively charged adducts exceeds the overall net charge of the adducted protein ion. Isolating and collisionally activating these positively charged ions that are generated by ESI would lead to a negatively charged or neutral beam of protein molecules that is selected for both mass and energy.

2.5 Conclusions

The effects of different cations on the charge states of protein and peptide ions produced in electrospray ionization from aqueous acetate solutions were investigated. The charge states of three proteins formed from aqueous solutions without added acetate salts are higher than those formed from solutions with added salts whereas the charge states of peptides can be higher, lower or the same as those formed with added salts. Results from circular dichroism measurements show that the protein secondary structure differs in aqueous solutions without salts added compared to solutions containing either sodium or ammonium acetate. Ion mobility results show that protonated molecular ions with the same charge state formed from water and aqueous ammonium acetate solutions differ, indicating that the solution-phase structures differ as well. These results indicate that the origin of the difference in protein charging with and without salts is an effect of differences in protein conformation in these solutions.

Collisional activation of proteins adducted to the larger cations that have low Gibbs solvation free energies produces facile loss of the cations resulting in intact protein ions with fewer charges. This dissociation pathway may account for the substantially lower protein charging from solutions containing cations such as TMA^+ and TEA^+. The protein ions formed from TMA^+ and TEA^+ solutions are less charged than those formed from ammonium or alkali metal ion solutions even at conditions where no intentional collisional activation occurs. This suggests that the CCRFEM may also contribute to the lower charging observed.

Although charging depends on the ionic strength of the aqueous solution, similar extents of protein and peptide charging containing equal concentrations of either ammonium acetate or rubidium acetate indicate that proton transfer from protonated ammonia to proteins and peptides does not play a significant role in the extent of charging in native mass spectrometry.

Formation of singly protonated protein ions from higher charge state ions that are adducted to larger cations is readily achieved by collisional activation to induce loss of the charged cation, leaving the intact singly protonated protein ion. This method can not only produce protein ions with just one charge, but should also provide a route to generating either beams of neutral protein molecules or protein anions that are selected for both mass and kinetic energy from multiply charged positive ions formed by ESI.

2.6 Acknowledgments

The authors thank the National Institutes of Health (grant no. R01GM097357) for generous financial support. The authors also thank Dr. Haichuan Liu and Professor Ewa Witkowska of the UCSF Sandler-Moore Mass Spectrometry Core Facility for the use of the Synapt G2 instrument and Professor Bryan A. Krantz for the use of the circular dichroism spectropolarimeter. The authors also thank Catherine A. Cassou for helpful discussions.

2.7 References

(1) Fenn, J. B.; Mann, M.; Meng, C. K.; Wong, S. F.; Whitehouse, C. M. Electrospray ionization–principles and practice. *Mass Spectrom. Rev.* **1990**, *9* (1), 37–70.

(2) Kebarle, P.; Verkerk, U. H. Electrospray: from ions in solution to ions in the gas phase, what we know now. *Mass Spectrom. Rev.* **2009**, *28* (6), 898–917.

(3) Chowdhury, S. K.; Katta, V.; Chait, B. T. Probing conformational changes in proteins by mass spectrometry. *J. Am. Chem. Soc.* **1990**, *112* (24), 9012–9013.

(4) Dobo, A.; Kaltashov, I. A. Detection of multiple protein conformational ensembles in solution via deconvolution of charge-state distributions in ESI MS. *Anal. Chem.* **2001**, *73* (20), 4763–4773.

(5) Loo, J. A.; Loo, R. R. O.; Udseth, H. R.; Edmonds, C. G.; Smith, R. D. Solvent-induced conformational changes of polypeptides probed by electrospray-ionization mass spectrometry. *Rapid Commun. Mass Spectrom.* **1991**, *5* (3), 101–105.

(6) Iavarone, A. T.; Williams, E. R. Mechanism of Charging and Supercharging Molecules in Electrospray Ionization. *J. Am. Chem. Soc.* **2003**, *125* (8), 2319–2327.

(7) Iavarone, A. T.; Jurchen, J. C.; Williams, E. R. Effects of solvent on the maximum charge state and charge state distribution of protein ions produced by electrospray ionization. *J. Am. Soc. Mass Spectrom.* **2000**, *11* (11), 976–985.

(8) Schnier, P. D.; Gross, D. S.; Williams, E. R. Electrostatic forces and dielectric polarizability of multiply protonated gas-phase cytochrome c ions probed by ion/molecule chemistry. *J. Am. Chem. Soc.* **1995**, *117* (25), 6747–6757.

(9) Thomson, B. A. Declustering and fragmentation of protein ions from an electrospray ion source. *J. Am. Soc. Mass Spectrom.* **1997**, *8* (10), 1053–1058.

(10) Iavarone, A. T.; Jurchen, J. C.; Williams, E. R. Supercharged protein and peptide ions formed by electrospray ionization. *Anal. Chem.* **2001**, *73* (7), 1455–1460.

(11) Sterling, H. J.; Cassou, C. A.; Trnka, M. J.; Burlingame, A. L.; Krantz, B. A.; Williams, E. R. The role of conformational flexibility on protein supercharging in native electrospray ionization. *Phys. Chem. Chem. Phys.* **2011**, *13* (41), 18288–18296.

(12) Sterling, H. J.; Batchelor, J. D.; Wemmer, D. E.; Williams, E. R. Effects of buffer loading for electrospray ionization mass spectrometry of a noncovalent protein complex that requires high concentrations of essential salts. *J. Am. Soc. Mass Spectrom.* **2010**, *21* (6), 1045–1049.

(13) Sterling, H. J.; Cassou, C. A.; Susa, A. C.; Williams, E. R. Electrothermal supercharging of proteins in native electrospray ionization. *Anal. Chem.* **2012**, *84* (8), 3795–3801.

(14) Sterling, H. J.; Prell, J. S.; Cassou, C. A.; Williams, E. R. Protein conformation and supercharging with DMSO from aqueous solution. *J. Am. Soc. Mass Spectrom.* **2011**, *22* (7), 1178–1186.

(15) Cassou, C. A.; Sterling, H. J.; Susa, A. C.; Williams, E. R. Electrothermal supercharging in mass spectrometry and tandem mass spectrometry of native proteins. *Anal. Chem.* **2013**, *85* (1), 138–146.

(16) Sterling, H. J.; Kintzer, A. F.; Feld, G. K.; Cassou, C. A.; Krantz, B. A.; Williams, E. R. Supercharging protein complexes from aqueous solution disrupts their native conformations. *J. Am. Soc. Mass Spectrom.* **2012**, *23* (2), 191–200.

(17) Lomeli, S. H.; Yin, S.; Ogorzalek Loo, R. R.; Loo, J. A. Increasing charge while preserving noncovalent protein complexes for ESI-MS. *J. Am. Soc. Mass Spectrom.* **2009**, *20* (4), 593–596.

(18) Lomeli, S. H.; Peng, I. X.; Yin, S.; Loo, R. R. O.; Loo, J. A. New reagents for increasing ESI multiple charging of proteins and protein complexes. *J. Am. Soc. Mass Spectrom.* **2010**, *21* (1), 127–131.

(19) Hall, Z.; Robinson, C. V. Do charge state signatures guarantee protein conformations? *J. Am. Soc. Mass Spectrom.* **2012**, *23* (7), 1161–1168.

(20) Valentine, S. J.; Counterman, A. E.; Clemmer, D. E. Conformer-dependent proton-transfer reactions of ubiquitin ions. *J. Am. Soc. Mass Spectrom.* **1997**, *8*, 954–961.

(21) Williams, E. R. Proton transfer reactivity of large multiply charged ions. *J. Mass. Spectrom.* **1996**, *31* (8), 831–842.

(22) Dole, M.; Mack, L. L.; Hines, R. L.; Mobley, R. C. Molecular Beams of Macroions. *J. Chem. Phys.* **1968**, *49* (5), 2240–2449.

(23) Iribarne, J. V.; Thomson, B. A. On the evaporation of small ions from charged droplets. *J. Chem. Phys.* **1976**, *64* (6), 2287–2294.

(24) Hogan, C. J., Jr.; Carroll, J. A.; Rohrs, H. W.; Biswas, P.; Gross, M. L. Combined Charged Residue-Field Emission Model of macromolecular electrospray ionization. *Anal. Chem.* **2009**, *81* (1), 369–377.

(25) Duft, D.; Achtzehn, T.; Müller, R.; Huber, B. A.; Leisner, T. Coulomb fission: Rayleigh jets from levitated microdroplets. *Nature* **2003**, *421* (6919), 128.

(26) Smith, J. N.; Flagan, R. C.; Beauchamp, J. L. Droplet evaporation and discharge dynamics in electrospray ionization. *J. Phys. Chem. A* **2002**, *106*, 9957–9967.

(27) Thomson, B. A.; Iribarne, J. V. Field induced ion evaporation from liquid surfaces at atmospheric pressure. *J. Chem. Phys.* **1979**, *71* (11), 4451–4463.

(28) de la Mora, J. F. Electrospray ionization of large multiply charged species proceeds via Dole's charged residue mechanism. *Anal. Chim. Acta* **2000**, *406* (1), 93–104.

(29) Wang, G.; Cole, R. B. Effect of solution ionic strength on analyte charge state distributions in positive and negative ion electrospray mass spectrometry. *Anal. Chem.* **1994**, *66* (21), 3702–3708.

(30) Wang, G.; Cole, R. B. Effects of solvent and counterion on ion pairing and observed charge states of diquaternary ammonium salts in electrospray ionization mass spectrometry. *J. Am. Soc. Mass Spectrom.* **1996**, *7*, 1050–1058.

(31) Flick, T. G.; Williams, E. R. Supercharging with trivalent metal ions in native mass spectrometry. *J. Am. Soc. Mass Spectrom.* **2012**, *23* (11), 1885–1895.

(32) Zhu, M. M.; Rempel, D. L.; Zhao, J.; Giblin, D. E.; Gross, M. L. Probing Ca2+-induced conformational changes in porcine calmodulin by H/D exchange and ESI-MS: effect of cations and ionic strength. *Biochemistry* **2003**, *42* (51), 15388–15397.

(33) Liu, H.; Håkansson, K. Divalent metal ion-peptide interactions probed by electron capture dissociation of trications. *J. Am. Soc. Mass Spectrom.* **2006**, *17* (12), 1731–1741.

(34) Ly, T.; Julian, R. R. Protein-metal interactions of calmodulin and α-synuclein monitored by selective noncovalent adduct protein probing mass spectrometry. *J. Am. Soc. Mass Spectrom.* **2008**, *19* (11), 1663–1672.

(35) Felitsyn, N.; Peschke, M.; Kebarle, P. Origin and number of charges observed on multiply-protonated native proteins produced by ESI. *Int. J. Mass Spectrom.* **2002**, *219* (1), 39–62.

(36) Kebarle, P. A brief overview of the present status of the mechanisms involved in electrospray mass spectrometry. *J. Mass. Spectrom.* **2000**, *35* (7), 804–817.

(37) Hautreux, M.; Hue, N.; Fou de Kerdaniel, Du, A.; Zahir, A.; Malec, V.; Laprévote, O. Under non-denaturing solvent conditions, the mean charge state of a multiply charged protein ion formed by electrospray is linearly correlated with the macromolecular surface. *Int. J. Mass Spectrom.* **2004**, *231* (2-3), 131–137.

(38) Prakash, H.; Kansara, B. T.; Mazumdar, S. Effects of salts on the charge-state distribution and the structural basis of the most-intense charge-state of the gaseous protein ions produced by electrospray ionization. *Int. J. Mass Spectrom.* **2010**, *289* (2-3), 84–91.

(39) Konermann, L.; Ahadi, E.; Rodriguez, A. D.; Vahidi, S. Unraveling the mechanism of electrospray ionization. *Anal. Chem.* **2013**, *85* (1), 2–9.

(40) Ho, Y.; Chen, J.; Hu, T. Elucidating factors manipulated the formation of multiply charged protein homomultimeric complexes by electrospray ionization. *J. Chin. Chem. Soc.-Taip.* **2007**, *54*, 391–400.

(41) Verkerk, U. H.; Peschke, M.; Kebarle, P. Effect of buffer cations and of H_3O^+ on the charge states of native proteins. Significance to determinations of stability constants of protein complexes. *J. Mass. Spectrom.* **2003**, *38* (6), 618–631.

(42) Verkerk, U. H.; Kebarle, P. Ion-ion and ion-molecule reactions at the surface of proteins produced by nanospray. Information on the number of acidic residues and control of the number of ionized acidic and basic residues. *J. Am. Soc. Mass Spectrom.* **2005**, *16* (8), 1325–1341.

(43) Heck, A. J. R.; Van Den Heuvel, R. H. H. Investigation of intact protein complexes by mass spectrometry. *Mass Spectrom. Rev.* **2004**, *23* (5), 368–389.

(44) Catalina, M. I.; Van Den Heuvel, R. H. H.; van Duijn, E.; Heck, A. J. R. Decharging of globular proteins and protein complexes in electrospray. *Chem. Eur. J.* **2005**, *11* (3), 960–968.

(45) Hiraoka, K.; Asakawa, Y.; Kawashima, Y.; Okazaki, S.; Nakamura, M.; Yamamoto, Y.; Takamizawa, A. The effect of the presence of foreign salts on the formation of gaseous ions for electrospray and laser spray. *Rapid Commun. Mass Spectrom.* **2004**, *18* (20), 2437–2442.

(46) Peschke, M.; Blades, A.; Kebarle, P. Charged states of proteins. Reactions of doubly protonated alkyldiamines with NH_3: Solvation or deprotonation. Extension of two proton cases to multiply protonated globular proteins observed in the gas phase. *J. Am. Chem. Soc.* **2002**, *124* (38), 11519–11530.

(47) Peschke, M.; Verkerk, U. H.; Kebarle, P. Features of the ESI mechanism that affect the observation of multiply charged noncovalent protein complexes and the determination of the association constant by the titration method. *J. Am. Soc. Mass Spectrom.* **2004**, *15* (10), 1424–1434.

(48) Watt, S. J.; Sheil, M.; Beck, J. L.; Prosselkov, P.; Otting, G.; Dixon, N. E. Effect of protein stabilization on charge state distribution in positive and negative ion electrospray ionization mass spectra. *J. Am. Soc. Mass Spectrom.* **2007**, *18* (9), 1605–1611.

(49) Grandori, R. Origin of the conformation dependence of protein charge-state distributions in electrospray ionization mass spectrometry. *J. Mass. Spectrom.* **2003**, *38* (1), 11–15.

(50) Hu, P.; Gross, M. L. Strong interactions of anionic peptides and alkaline earth metal ions: metal-ion-bound peptides in the gas phase. *J. Am. Chem. Soc.* **1992**, *114*, 9153–9160.

(51) Flick, T. G.; Merenbloom, S. I.; Williams, E. R. Effects of Metal Ion Adduction on the Gas-Phase Conformations of Protein Ions. *J. Am. Soc. Mass Spectrom.* **2013**, *24* (11), 1654–1662.

(52) UniProt Consortium. Update on activities at the Universal Protein Resource (UniProt) in 2013. *Nucleic Acids Res.* **2013**, *43* (Database issue), D43–D47.

(53) Marcus, Y. Thermodynamics of solvation of ions. Part 5. Gibbs free energy of hydration at 298.15 K. *Faraday Trans.* **1991**, *87* (18), 2995–2999.

(54) Valentine, S. J.; Anderson, J. G.; Ellington, A. D.; Clemmer, D. E. Disulfide-Intact and -Reduced Lysozyme in the Gas Phase: Conformations and Pathways of Folding and Unfolding. *J. Phys. Chem. B* **1997**, *101* (19), 3891–3900.

(55) Wyttenbach, T.; Helden, von, G.; Bowers, M. T. Gas-phase conformation of biological molecules: Bradykinin. *J. Am. Chem. Soc.* **1996**, *118* (35), 8355–8364.

(56) Bush, M. F.; Hall, Z.; Giles, K.; Hoyes, J.; Robinson, C. V.; Ruotolo, B. T. Collision cross sections of proteins and their complexes: a calibration framework and database for gas-phase structural biology. *Anal. Chem.* **2010**, *82* (22), 9557–9565.

(57) Kebarle, P.; Tang, L. From ions in solution to ions in the gas phase - the mechanism of electrospray mass spectrometry. *Anal. Chem.* **1993**, *65* (22), 972–986.

(58) Tang, L.; Kebarle, P. Dependence of ion intensity in electrospray mass spectrometry on the concentration of the analytes in the electrosprayed solution. *Anal. Chem.* **1993**, *65*, 3654–3668.

(59) Wang, G.; Cole, R. B. Charged residue versus ion evaporation for formation of alkali metal halide cluster ions in ESI. *Anal. Chim. Acta* **2000**, *406* (1), 53–65.

(60) Nguyen, S.; Fenn, J. B. Gas-phase ions of solute species from charged droplets of solutions. *Proc. Natl. Acad. Sci. U.S.A.* **2007**, *104* (4), 1111–1117.

(61) Spencer, E. A. C.; Ly, T.; Julian, R. R. Formation of the serine octamer: Ion evaporation or charge residue? *Int. J. Mass Spectrom.* **2008**, *270* (3), 166–172.

(62) Ahadi, E.; Konermann, L. Modeling the behavior of coarse-grained polymer chains in charged water droplets: implications for the mechanism of electrospray ionization. *J. Phys. Chem. B* **2012**, *116* (1), 104–112.

(63) Kelly, S. M.; Jess, T. J.; Price, N. C. How to study proteins by circular dichroism. *BBA-Proteins and Proteom.* **2005**, *1751* (2), 119–139.

(64) Merenbloom, S. I.; Flick, T. G.; Daly, M. P.; Williams, E. R. Effects of select anions from the Hofmeister series on the gas-phase conformations of protein ions measured with traveling-wave ion mobility spectrometry/mass spectrometry. *J. Am. Soc. Mass Spectrom.* **2011**, *22* (11), 1978–1990.

(65) Engel, B. J.; Pan, P.; Reid, G. E.; Wells, J. M.; McLuckey, S. A. Charge state dependent fragmentation of gaseous protein ions in a quadrupole ion trap: bovine ferri-, ferro-, and apo-cytochrome *c*. *Int. J. Mass Spectrom.* **2002**, *219* (1), 171–187.

(66) Meot-Ner Mautner, M. Update 1 of: Strong ionic hydrogen bonds. *Chem. Rev.* **2012**, *112* (10), PR22–PR103.

(67) Dzidic, I.; Kebarle, P. Hydration of the alkali ions in the gas phase. Enthalpies and entropies of reactions $M^+(H_2O)_{n-1} + H_2O = M^+(H_2O)_n$. *J. Phys. Chem.* **1970**, *74*, 1466–1474.

(68) Meot-Ner Mautner, M. The ionic hydrogen bond and ion solvation. 2. Solvation of onium ions by one to seven water molecules. Relations between monomolecular, specific, and bulk hydrogen. *J. Am. Chem. Soc.* **1984**, *106* (5), 1265–1272.

(69) Meot-Ner Mautner, M.; Deakyne, C. A. Unconventional Ionic Hydrogen Bonds. 1. $CH^{\delta+}$--X. Complexes of Quaternary Ions with n- and pi-Donors. *J. Am. Chem. Soc.* **1985**, *107* (2), 469–474.

(70) Pagel, K.; Hyung, S.-J.; Ruotolo, B. T.; Robinson, C. V. Alternate dissociation pathways identified in charge-reduced protein complex ions. *Anal. Chem.* **2010**, *82* (12), 5363–5372.

(71) Lemaire, D.; Marie, G.; Serani, L.; Laprévote, O. Stabilization of gas-phase noncovalent macromolecular complexes in electrospray mass spectrometry using aqueous triethylammonium bicarbonate buffer. *Anal. Chem.* **2001**, *73* (8), 1699–1706.

(72) Flick, T. G.; Cassou, C. A.; Chang, T. M.; Williams, E. R. Solution additives that desalt protein ions in native mass spectrometry. *Anal. Chem.* **2012**, *84* (17), 7511–7517.

(73) Iavarone, A. T.; Udekwu, O. A.; Williams, E. R. Buffer loading for counteracting metal salt-induced signal suppression in electrospray ionization. *Anal. Chem.* **2004**, *76* (14), 3944–3950.

(74) Zhou, M.; Dagan, S.; Wysocki, V. H. Impact of charge state on gas-phase behaviors of noncovalent protein complexes in collision induced dissociation and surface induced dissociation. *Analyst* **2013**, *138* (5), 1353–1362.

(75) Clemmer, D. E.; Hudgins, R. Naked protein conformations: Cytochrome *c* in the gas phase. *J. Am. Soc. Mass Spectrom.* **1995**, *117*, 10141–10142.

(76) Pitteri, S. J.; Chrisman, P. A.; Hogan, J. M.; McLuckey, S. A. Electron transfer ion/ion reactions in a three-dimensional quadrupole ion trap: reactions of doubly and triply protonated peptides with SO_2. *Anal. Chem.* **2005**, *77* (6), 1831–1839.

(77) Scalf, M.; Westphall, M. S.; Smith, L. M. Charge Reduction Electrospray Mass Spectrometry. *Anal. Chem.* **2000**, *72*, 52–60.

(78) Horn, D. M.; Breuker, K.; Frank, A. J.; McLafferty, F. W. Kinetic intermediates in the folding of gaseous protein ions characterized by electron capture dissociation mass spectrometry. *J. Am. Chem. Soc.* **2001**, *123* (40), 9792–9799.

2.8 Tables and Figures

Table 2.1. $Z_{R,\sigma}$ and $Z_{R,m}$ for water droplet the same size as ion of interest compared to Z_{max} and Z_{ave} for ions formed from aqueous solutions without salts added, or with 25 mM NH_4^+ or Rb^+.

			Water, no salts added		NH_4^+		Rb^+	
Protein/peptide	$Z_{R,\sigma}$	$Z_{R,m}$	Z_{max}	Z_{ave}	Z_{max}	Z_{ave}	Z_{max}	Z_{ave}
Ubiquitin	9.5+	7.4+	10+	6.5+	6+	5.4+	5+	5.0+
Lysozyme	12+	9.4+	11+	9.4+	9+	7.7+	9+	7.5+
β-Lactoglobulin	14+	11+	10+	8.0+	9+	7.9+	8+	7.4+
Angiotensin II	3.3+	2.6+	2+	1.8+	2+	1.9+	2+	1.8+
Bradykinin	3.2+	2.6+	3+	2.0+	3+	2.0+	2+	2.0+
$SubPNH_2$	3.7+	2.9+	3+	2.7+	3+	2.1+	3+	2.2+
SubPOH	3.7+	2.9+	3+	2.2+	3+	2.0+	3+	2.0+
SubPOMe	3.7+	2.9+	3+	2.9+	3+	2.1+	3+	2.2+

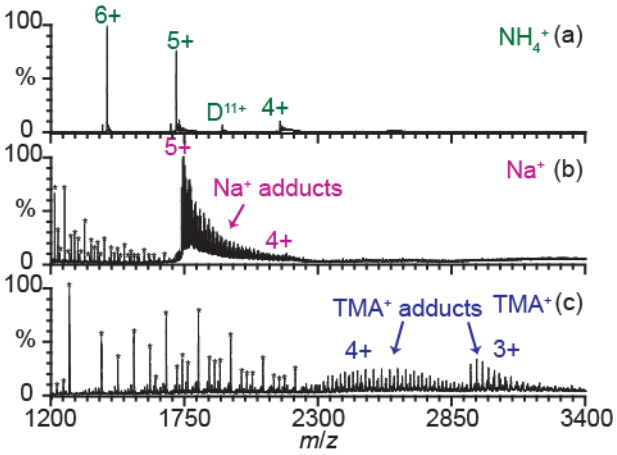

Figure 2.1. Nano-ESI mass spectra of 50 μM bovine ubiquitin ions formed from 25 mM aqueous solutions of (a) ammonium acetate, (b) sodium acetate, and (c) tetramethylammonium acetate. (*) indicate (b) sodium acetate or (c) tetramethylammonium acetate clusters, some of which are multiply charged.

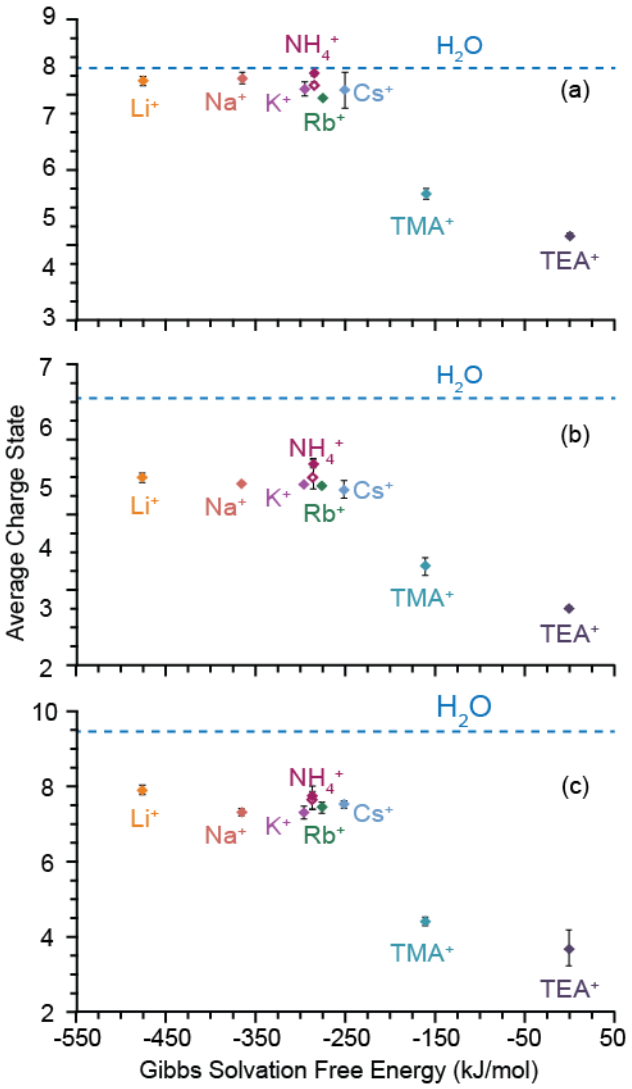

Figure 2.2. Average charge state of 50 μM (a) β-lactoglobulin, (b) bovine ubiquitin, and (c) egg-white lysozyme formed from 25 mM (solid diamond) or 100 mM (solid diamond) acetate salt solutions and water (dashed line) plotted as a function of relative Gibbs solvation free energy of the cation (referenced to TEA^+, which is assigned a value of zero).

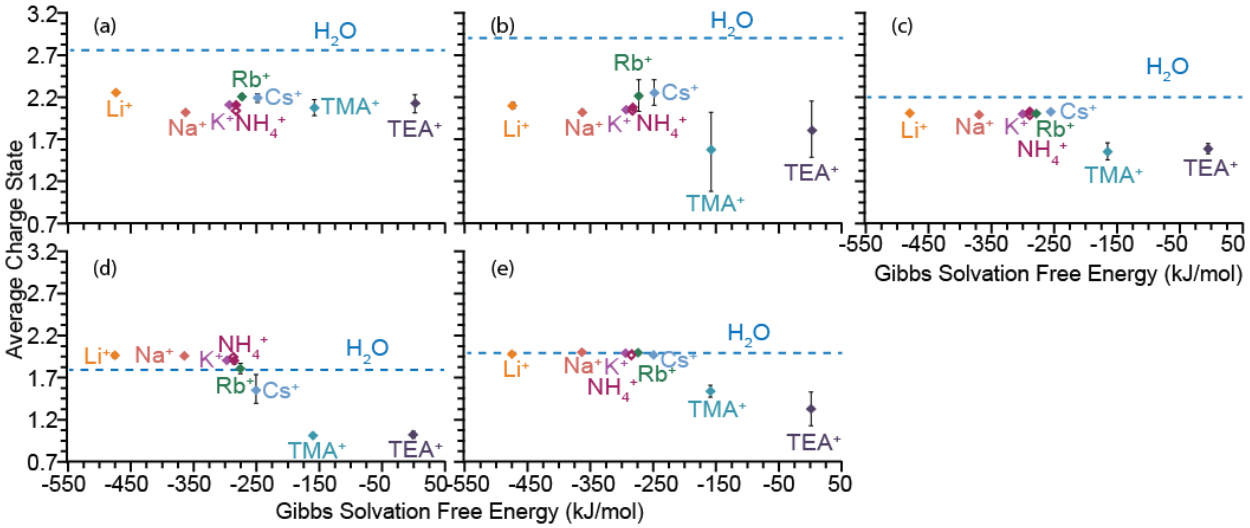

Figure 2.3. Average charge state of 50 μM (a) SubPNH$_2$, (b) SubPOMe, (c) SubPOH, (d) angiotensin II, and (e) bradykinin formed from 25 mM (solid diamond) or 100 mM (solid diamond) acetate salt solutions and water (dashed line) plotted as a function of relative Gibbs solvation free energy of the cation (referenced to TEA+, which is assigned a value of zero).

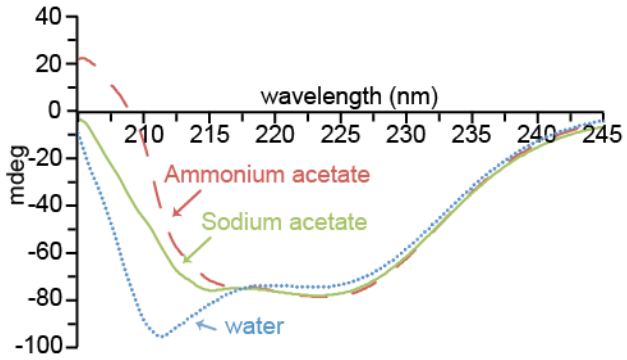

Figure 2.4. Circular dichroism spectra for 25 μM ubiquitin in 25 mM sodium acetate (green line), 25 mM ammonium acetate (red dashed line), and water (blue dotted line).

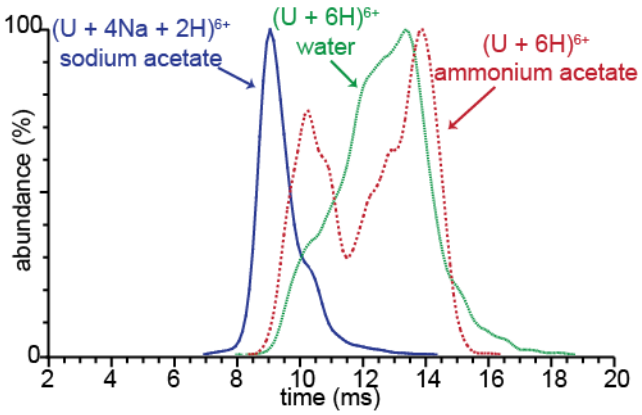

Figure 2.5. Ion mobility arrival time distributions of ubiquitin $(U + 6H)^{6+}$ formed from water (green dotted line), 25 mM ammonium acetate (red solid line) and $(U + 4Na + 2H)^{6+}$ formed from 25 mM sodium acetate (blue dashed line).

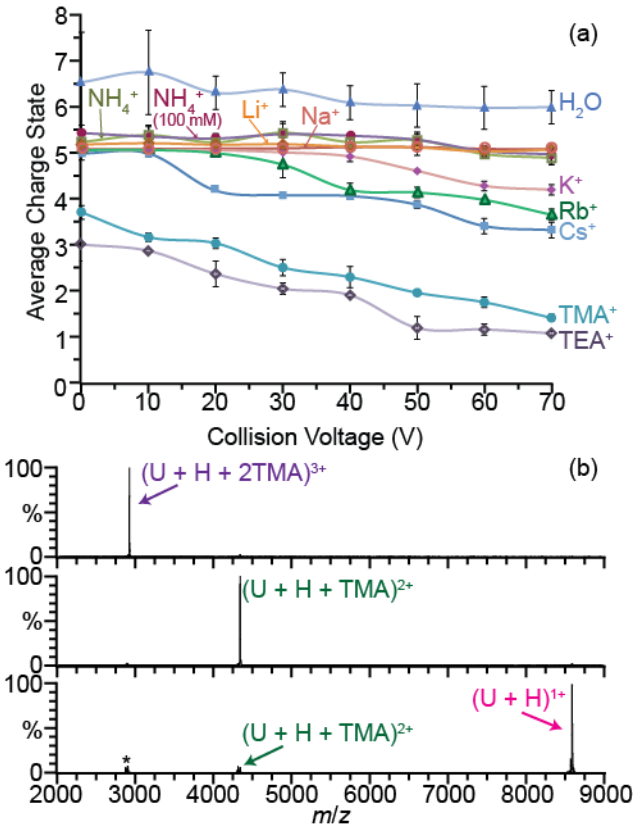

Figure 2.6. (a) Average charge of ubiquitin ions formed from 25 mM (unless otherwise noted) acetate salt solutions from collision voltages 0 to 70 V. (b) Collisional activation of $(U + H + 2TMA)^{3+}$ at 0 V (top) to form $(U + H + TMA)^{2+}$ at 40 V (middle) and $(U + H)^{1+}$ at 80 V (bottom). (*) indicates stable low abundance cluster ions at same m/z as precursor that are also isolated at 0 V.

2.9 Supplemental Information

Supplemental Table 2.1. Average number of cation adducts per charge state of each protein/peptide ion.

		Average number of adducts							
protein/peptide	***Charge state***	***Li^+***	***Na^+***	***K^+***	***Rb^+***	***NH_4^+***	***Cs^+***	***TMA^+***	***TEA^+***
angiotensin II	1+	0.7	0.7	0.7	1.3	0.0	1.0	2.3	2.0
	2+	4.0	4.0	4.3	4.0	0.0	2.7		0.3
bradykinin	1+	1.0	0.0	0.0	1.0	0.0	2.0	2.0	2.0
	2+	4.0	4.0	2.0	4.0	0.0	4.0	0.0	0.0
SubP	1+					0.0		1.0	1.0
	2+	1.7	2.0	1.7	2.0	0.0	2.0	0.0	0.0
	3+	1.0		1.0	0.0	0.0	0.0	0.0	0.0
SubPOMe	1+	0.3				0.0		1.0	1.0
	2+	2.0	3.0	3.0	2.0	0.0	3.0	0.0	0.0
	3+	0.0	0.0	0.0	0.0	0.0	0.0	0.0	0.0
SubPOH	1+		0.0			0.0	0.0	2.0	2.0
	2+	3.0	3.0	3.0	3.0	0.0	2.7	0.0	0.0
	3+			0.0	0.0	0.0	0.0		
ubiquitin	2+								
	3+							12.0	5.7
	4+		0.7		0.3	0.0	0.7	28.0	11.7
	5+	5.8	26.7	14.7	9.0	0.0	10.3		
	6+	6.7	1.7	0.3		0.0			
lysozyme	3+								7.0
	4+							10.0	7.7
	5+							2.0	
	6+		1.0	5.3	3.0	0.0	3.0	0.0	
	7+	3.7	26.7	7.7	5.7	0.0	5.7		
	8+	1.0	9.3	4.7	4.7	0.0	2.0		
	9+	1.0	2.0	3.0	3.0	0.0	1.0		
	10+	0.0							
β-lactoglobulin	4+								3.0
	5+							9.0	6.7
	6+	0.3	20.1			0.0		12.0	
	7+	3.0	20.0	24.7	11.0	0.0	10.0		
	8+	5.0	36.7	35.1	9.7	0.0	5.5		
	9+	0.0				0.0	2.0		
	10+	0.0							

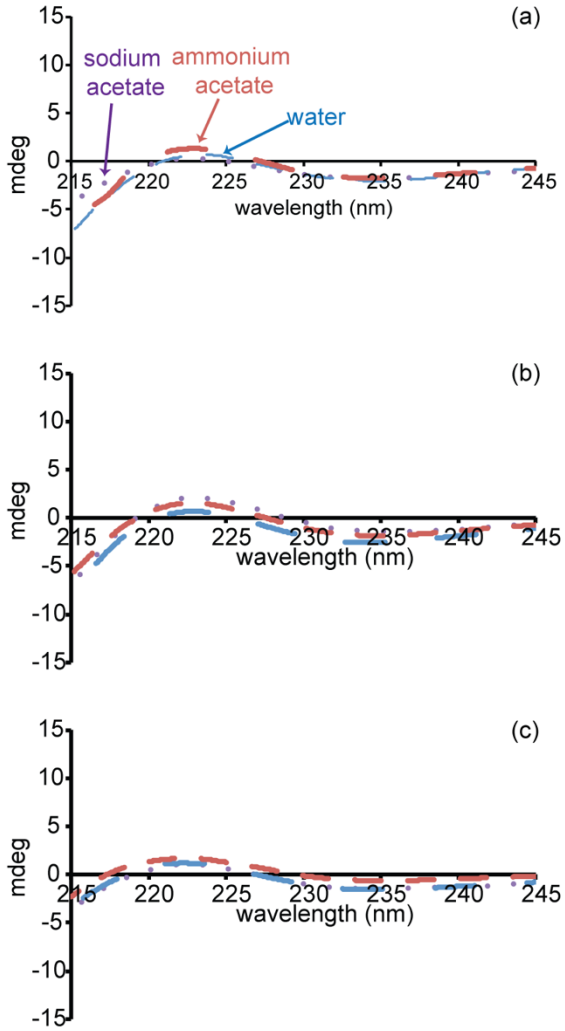

Supplemental Figure 2.1. CD spectra of 50 μM (a) SubPOH, (b) SubPNH$_2$, and (c) SubPOMe in water (blue dashed line), 25 mM sodium acetate (purple dotted line) and 25 mM ammonium acetate (red dashed line).

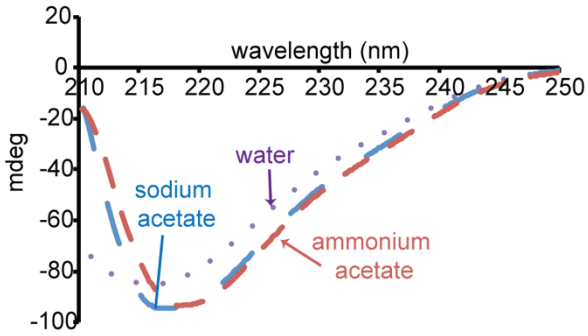

Supplemental Figure 2.2. CD spectra of 25 μM β-lactoglobulin in water (blue dashed line), 25 mM sodium acetate (purple dotted line) and 25 mM ammonium acetate (red dashed line).

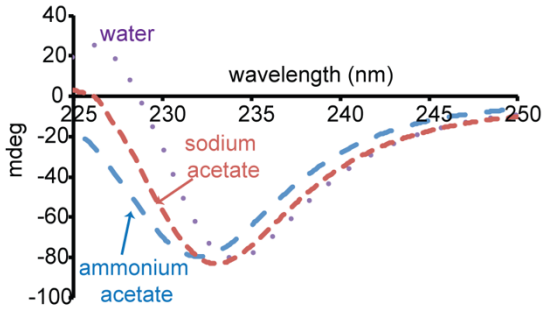

Supplemental Figure 2.3. CD spectra of 25 μM lysozyme in water (purple dotted line), 25 mM sodium acetate (red dashed line) and 25 mM ammonium acetate (blue dashed line).

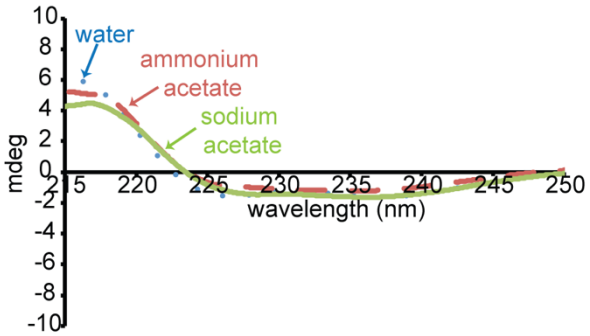

Supplemental Figure 2.4. CD spectra of 25 μM angiotensin II in water (blue dotted line), 25 mM ammonium acetate (red dashed line) and 25 mM sodium acetate (green line).

Chapter 3

Charging of Proteins in Native Mass Spectrometry

This chapter is reproduced with permission from:

Anna C. Susa, Zijie Xia, Henry Y. H. Tang, John A. Tainer, Evan R. Williams
"Charging of Proteins in Native Mass Spectrometry"
Journal of the American Society for Mass Spectrometry, **2017**, *28*(2): 332-340

3.1 Abstract

Factors that influence the charging of protein ions formed by electrospray ionization from aqueous solutions in which proteins have native structures and function were investigated. Protein ions ranging in molecular weight from 12.3 to 79.7 kDa and pI values from 5.4 to 9.6 were formed from different solutions and reacted with volatile bases of gas-phase basicities higher than that of ammonia in the cell of a Fourier-transform ion cyclotron resonance mass spectrometer. The charge-state distribution of cytochrome *c* ions formed from aqueous ammonium or potassium acetate is the same. Moreover, ions formed from these two solutions do not undergo proton transfer to 2-fluoropyridine, which is 8 kcal/mol more basic than ammonia. These results provide compelling evidence that proton-transfer between ammonia and protein ions does not limit protein ion charge in native electrospray ionization. Both circular dichroism and ion mobility measurements indicate that there are differences in conformation of proteins in pure water and aqueous ammonium acetate, and these differences can account for the difference in the extent of charging and proton-transfer reactivities of protein ions formed from these solutions. The extent of proton-transfer of the protein ions with higher gas-phase basicity bases trends with how closely the protein ions are charged to the value predicted by the Rayleigh limit for spherical water droplets approximately the same size as the proteins. These results indicate that droplet charge limits protein ion charge in native mass spectrometry and are consistent with these ions being formed by the charged residue mechanism.

3.2 Introduction

Many factors affect the extent of charging of intact gas-phase macromolecular ions formed by electrospray ionization (ESI),[1-19] but the conformation of a molecule in solution is one of the most significant.[3-5] Broad distributions of highly charged protein ions are formed from solutions in which proteins are denatured, such as water/methanol/acid solutions. In contrast, narrower distributions of lower charge states are formed from buffered aqueous solutions in which proteins are in native or native-like conformations.[3] Other factors, such as surface tension of the ESI droplet,[6,7] instrumental parameters,[3-5,8] supercharging methods,[7,9-13] and gaseous reactions with acid or base vapors[16-19] can also affect the extent of charging of protein ions formed by ESI. The maximum extent of charging of denatured and supercharged protein ions can be limited by the proton-transfer reactivity of the ion relative to that of the electrospray solvent or other molecules in solution.[6,18,19]

Factors that limit the extent of charging of protein ions formed from buffered aqueous solutions by ESI are debated,[15,20-27] and several mechanisms for ion formation of protein ions from

buffered aqueous solutions have been proposed.[23,28-30] In the charged residue mechanism (CRM) for ion formation, multiply charged gas-phase ions are formed by solvent evaporation in the late stages of droplet lifetime.[28] De la Mora[15] and others[7,31,32] showed that the extent of charging of globular macromolecular ions formed from aqueous solutions is close to the number of charges predicted by the Rayleigh limit (Z_R) for a water droplet that is approximately the same size as the macromolecule. The maximum charge of globular protein and dendrimer ions from 6 to 1400 kDa formed from aqueous solutions was between 65 to 110 % of Z_R and proportional to the square root of the molecular weight, suggesting the formation of globular ions from 6 to 1400 kDa follows the CRM.[15] The maximum charge of polyethylene glycol (PEG) ions with molecular weights greater than 50 kDa exceeded Z_R, suggesting that these ions are formed from nonspherical droplets that fail to undergo Coulombic fissions because the PEG backbone is highly charged.[15] In the chain ejection model (CEM), folded native protein ions are formed by the CRM, but highly charged unfolded protein ions are ejected from the ESI droplet before complete desolvation occurs.[20,33-36]

Salts, or buffers commonly used in native ESI mass spectrometry, can also affect the extent of charging on protein ions formed from aqueous solutions.[22,37-40] In the combined charged residue-field emission model (CCRFEM) for ion formation, small ions residing at the droplet surface evaporate from the droplet at a rate determined by the electric field strength at the droplet surface and ion solvation energies, and macromolecules located in the interior of the droplet ionize by the CRM.[29] In the CCRFEM, buffer ions with low solvation energies evaporate, carrying away charge from the ESI droplet, such that less charge remains on the macromolecules in the droplet after solvent evaporation.[29] Recently, Allen et al.[31] reported that protein ions formed from buffered aqueous ESI solutions with molecular weights less than 130 kDa were charged less than Z_R, but protein ions with molecular weights greater than 130 kDa were charged closer to Z_R. The authors suggested that this is consistent with charge-carrier emission of buffer ions limiting the charge of protein ions with molecular weights less than 130 kDa formed from buffered aqueous ESI solutions.[31]

It has also been proposed that the extent of charging of proteins from native solutions is limited by proton-transfer reactivity between protein ions and commonly added salts, such as ammonium acetate or ammonium bicarbonate, which are extensively used as buffers in aqueous ESI solutions. [2,23,26,41-49] Kebarle and coworkers suggested that charging of protein ions formed by ESI from aqueous ammonium salt solutions is limited by proton-transfer between the protein ion and ammonium or ammonia at the surface of the ESI droplet in the final stages of solvent evaporation. [23,41,47] In this mechanism, NH_3 formed in the last stages of the ESI process can accept a proton from the protein resulting in less highly charged ions.[41]

Adding basic molecules directly to aqueous ESI solutions can result in lower protein ion charging[49,50] either as a result of proton-transfer reactions or competition for protons in the ionization process. Protein ions formed from aqueous solutions can be denatured by exposing the ESI droplet to gaseous acids or bases which increase the charging as a result of the change in protein conformation.[16,17] The proton-transfer reactivities of protein ions with volatile bases, formed by ESI from solutions in which the proteins are denatured, have been investigated experimentally [4,18,51-56] and modeled computationally.[14,19,26,41,47,56] Proton-transfer reactions between protein ions and volatile basic molecules show that the apparent gas-phase basicity of high charge state ions is lower than that of low charge state ions,[14,18,52,56] and that proton-transfer rates between protein ions and basic molecules depend on temperature[51,57,58] Conformation also affects the proton-transfer reactivity of protein ions.[14,52,56] The apparent gas-phase basicity of disulfide-intact lysozyme ions formed from solutions in which the protein conformation is compact is lower than that of disulfide-reduced lysozyme ions of the same charge state formed from solutions in which the protein is denatured.[56]

Here, we investigate factors that limit the extent of charging of protein ions formed from buffered aqueous solutions using proton-transfer reactions with volatile molecules more basic than

ammonia, circular dichroism and ion mobility mass spectrometry. Cytochrome *c* has nearly identical secondary structure in solutions of aqueous ammonium acetate or potassium acetate, and the charge-state distributions of cytochrome *c* ions formed from these solutions are similar. Moreover, the protein ions formed from these solutions do not react with 2-fluoropyridine which is 8 kcal/mol more basic NH_3. These results show that charging of protein ions in native mass spectrometry is not limited by the presence of NH_4^+ or NH_3 in solution. The extent of the proton-transfer reactivities of protein ions formed from native aqueous solutions depends on conformation and how closely the ions are charged to Z_R. These results indicate that the charge on the ESI droplets limits the extent of charging of the molecular ions of proteins in native mass spectrometry.

3.3 Experimental

3.3.1 Proton-transfer reactions

Mass spectral data were acquired using a 9.4 T Fourier-transform ion cyclotron resonance (FT-ICR) mass spectrometer that is described elsewhere [59]. Protein ions were formed from aqueous ammonium acetate, potassium acetate or pure water solutions by nanoelectrospray ionization using borosilicate capillaries (1.0 mm o.d./0.78 mm i.d., Sutter Instruments, Novato, CA, USA) that were pulled to a tip i.d. of 0.8 μm or 1.6 μm with a Flaming/Brown micropipette puller (Model P-87, Sutter Instruments, Novato, CA, USA). Tip diameters were measured with a scanning electron microscope (Hitachi TM-1000 SEM, Schaumburg, IL, USA) at the Electron Microscope Laboratory at UC Berkeley. Nanoelectrospray was initiated by applying a potential of about +0.7 to 1.2 kV to a 0.127 mm diameter platinum wire inserted into the capillary and in contact with the sample solution.

Volatile bases were degassed using several freeze-pump-thaw cycles and introduced into the mass spectrometer through a sapphire leak valve to a vacuum chamber pressure of 1.0×10^{-8} Torr (base pressure is ~3×10^{-10} Torr) measured using an ion gauge located remotely from the ion cell. The ion gauge was not calibrated to the pressure of the volatile basic molecules in the ion cell. Rate constants of cytochrome *c* ions formed from water/methanol/acetic acid and reacted with pyridine are within 35-85% of those reported by Schnier et al.[14] Protein ions were reacted in the cell with 2-fluoropyridine (2-FP), pyridine, diethylamine (DEA) and dipropylamine (DPA) for up to 120 s.
Lyophilized protein powders of equine cytochrome *c*, bovine carbonic anhydrase, jack bean concanavalin A, human holo-transferrin, equine myoglobin, 2-FP, DEA, DPA, ammonium acetate, potassium acetate and sodium acetate are from Sigma (St. Louis, MO) and pyridine is from Fisher Scientific (Waltham, MA). Protein solutions were prepared at 10 μM in Millipore Milli-Q water, 10 mM ammonium acetate, 10 mM potassium acetate, or 10 mM sodium acetate, except for holo-transferrin where 200 mM ammonium acetate was used to maintain sufficient ion signal.

3.3.2 Ion mobility mass spectrometry

Arrival time distributions and mass spectral data were acquired using a Waters Synapt G2 (Waters, Milford, MA, USA) that is located at University of California, San Francisco. The traveling wave ion mobility cell was operated with a constant wave velocity of 800 m/s, wave height of 40 V, helium flow rate of 180 mL/min, and IMS (N_2) flow rate of 90 mL/min. The time of flight mass analyzer was operated in sensitivity mode ("V"). Calculated collision cross sections were obtained from the arrival time distributions using the procedure described by Bush et al.[60] Cytochrome *c*, ubiquitin, bovine serum albumin, avidin, β-lactoglobulin, and concanavalin A were used as calibrant ions. Arrival times were assigned as the center of the full-width at half-maximum for the arrival time

distribution for each ion. Average collision cross sections, CCS_{av}, were calculated as an average weighted sum of the collision cross sections for each charge-state distribution.

The charge-state distributions of protein ions obtained with the FT-ICR and Synapt mass spectrometers are similar, except for carbonic anhydrase ions formed from pure water. Charge states up to the 19+ and 15+ were observed with these respective instruments. The higher charging with the FT-ICR mass spectrometer is likely due to more droplet heating in this instrument which can result in some unfolding of the protein in the droplet prior to ion formation.[10]

3.3.3 Circular dichroism

Circular dichroism (CD) data were acquired using a Jasco Model 815 spectropolarimeter (JASCO, Inc., Easton, MD, USA). Wavelength scans from 190 to 260 nm at 20 °C were acquired for solutions containing 10 μM cytochrome *c* in pure water, 10 mM ammonium acetate, potassium acetate, and sodium acetate.

3.4 Results and Discussion

3.4.1 Effects of protein conformation on protein ion charging

The average charge of cytochrome *c* and carbonic anhydrase ions formed from pure water is higher than that from aqueous ammonium acetate (Table 3.1). The charge-state distribution of carbonic anhydrase ions formed from pure water is bimodal (Supplemental Figure 3.1), with a small distribution of higher charge state ions indicative of partially unfolded structure.[3] The conformation of proteins in aqueous solution can be affected by the presence of salts.[61,62] To determine if these differences in charging from pure water versus aqueous ammonium salt solutions are due to salts in solution affecting the conformation of the proteins, the α-helical and β-strand content of cytochrome *c* and carbonic anhydrase was probed using circular dichroism (CD). CD spectra of 10 μM cytochrome *c* and carbonic anhydrase in pure water, 10 mM ammonium acetate, and 10 mM potassium acetate from 200 to 260 nm are shown in Figure 3.1a and 1b. K^+ was chosen because NH_4^+ and K^+ have similar ionic radii,[63] activity coefficients,[64] and Gibbs solvation free energies.[63] The CD spectrum of carbonic anhydrase in pure water has a band at 204 nm that is absent in the CD spectra of carbonic anhydrase with ammonium or potassium acetate (Figure 3.1a). This band corresponds to a molar ellipticity contribution from tryptophan residues that couple with other aromatic residues.[65] This band in the spectrum of carbonic anhydrase in water but not in ammonium or potassium acetate indicates that the conformation is different in water when these two salts are not present. The CD spectra of cytochrome *c* in pure water, ammonium acetate and potassium acetate have unresolved bands at 208 and 222 nm (Figure 3.1b). These bands are characteristic of a predominately α-helical protein.[65] The ellipticity at 222 nm of cytochrome *c* in pure water is slightly more negative than that of cytochrome *c* in aqueous potassium or ammonium acetate solutions. The ellipticity of a partially denatured protein can become more negative at 222 nm as a result of the loss of positive ellipticity contributions of aromatic side chains.[65] The CD spectra of carbonic anhydrase and cytochrome c in aqueous ammonium and potassium acetate solutions are very similar (Figure 3.1a-b), indicating that secondary structure of the protein in these solutions is also similar. These CD measurements indicate that the presence of salts in solution affects the secondary structure of carbonic anhydrase and to a lesser extent, cytochrome *c*, compared to that in pure water, and the secondary structure of these two proteins is similar in ammonium and potassium acetate.

The protein conformation in solution can also affect the resulting conformations of ions produced by ESI from these solutions.[66-68] Ion mobility experiments were performed to investigate if the gas-phase conformations of carbonic anhydrase and cytochrome *c* ions formed from pure water and aqueous ammonium acetate differ. The collision cross sections of carbonic anhydrase and cytochrome *c* ions formed from pure water and aqueous 10 mM ammonium acetate as a function of charge state were obtained using traveling wave ion mobility mass spectrometry and are shown in Figure 3.1c. The collision cross sections for the same charge state ions formed from pure water or ammonium acetate solutions are indistinguishable within experimental error with the exception of 12+ charge state of carbonic anhydrase. For this charge state, the cross section is slightly larger when this ion is formed from water compared to that formed from ammonium acetate (Figure 3.1d). The more extended conformers of the 12+ charge state of carbonic anhydrase ions formed from pure water are more abundant compared to those formed from ammonium acetate (Figure 3.1d).

The collisional cross sections of the 6+ through 8+ charge states of cytochrome *c* ions formed from 10 mM aqueous ammonium acetate and pure water are indistinguishable, except for the relative abundances of the the two conformers of the 8+ charge state (Figure 3.1d). The compact conformer of 8+ cytochrome *c* is slightly more abundant from 10 mM ammonium acetate than from pure water (Figure 3.1d). Higher charge states of cytochrome *c* and carbonic anhydrase ions that are formed from pure water have larger collision cross sections than the lower charge states that are formed from both ammonium acetate and pure water (Figure 3.1c). These ion mobility measurements show that the conformations of cytochrome *c* and carbonic anhydrase ions formed from pure water can be different than the conformation of these ions formed from 10 mM ammonium acetate. The CD measurements show that cytochrome *c* and carbonic anhydrase have different secondary structure in pure water and ammonium acetate, and this produces a difference in the gas-phase conformations. These results show that the difference in charging of cytochrome *c* and carbonic anhydrase ions formed from pure water and 10 mM ammonium acetate is likely due to differences in conformations of the proteins in these solutions.

3.4.2 Gas-phase proton-transfer reactions between protein ions and volatile bases

In order to determine if proton transfer reactivity between NH_3 and proteins affects the charge of protein ions formed from aqueous ammonium acetate solutions,[23,46,47] proton-transfer experiments for five proteins ranging in molecular weight from 12.3 to 79.7 kDa and pI values of 5.4 to 9.6 were performed with volatile bases with gas-phase basicities (GB) that are higher than that of NH_3 (196 kcal/mol). The charge-state distribution of each protein (cytochrome *c*, myoglobin, carbonic anhydrase, concanavalin A dimer, holo-transferrin) did not change when these ions were reacted with 2-fluoropyridine (2-FP) (GB = 204 kcal/mol) for 120 s at 1.0×10^{-8} Torr. Lower charge states of these five proteins were formed by proton transfer to pyridine, diethylamine (DEA), and dipropylamine (DPA), which have GB values of GB = 215, 221, 225 kcal/mol, respectively.[69] For example, there is no change in the charge-state distribution of concanavalin A dimer ions after reaction with 2-FP for 120 s (Figure 3.2). However, reaction of these ions with pyridine (120 s) results in a decrease in relative abundance of the 16+ charge state and increase in the relative abundances of the 14+ and 13+ (Figure 3.2). The absence of any proton-transfer between the five proteins and 2-FP (204 kcal/mol) indicates that no proton-transfer reaction with NH_3 (196 kcal/mol) would occur under these same conditions. These results show that the apparent GB values for all the protein ions formed directly from aqueous ammonium acetate are more than 8 kcal/mol higher than the GB of NH_3.

The concentration of the bases in these experiments is very low and is substantially lower than the corresponding concentration of ammonium in solution and gaseous ammonia in the ESI interface, although the long reaction times used in these experiment at least partially compensates for this

difference. To evaluate if ammonium or ammonia affect protein charging from aqueous buffered ammonium acetate solutions, cytochrome *c* ions were formed from either 10 mM ammonium acetate or 10 mM potassium acetate. Potassium has a similar ionic radius,[63] activity coefficient,[64] and Gibbs solvation free energy[63] to ammonium but potassium cannot undergo proton transfer reactions with protein ions. In addition, secondary structure of cytochrome *c* in ammonium and potassium acetate solutions is very similar (Figure 3.1a and 3.1b). The charge-state distributions of cytochrome *c* ions from these solutions are the same (Figure 3.3, top). This result provides compelling evidence that the presence of NH_4^+ or NH_3 in solution does not affect the charging of proteins in native mass spectrometry. Moreover, the charge-state distributions of ions formed from either aqueous ammonium acetate or potassium acetate solutions do not change upon reaction with 2-FP (Figure 3.3). This demonstrates that the apparent gas-phase basicity of proteins is greater than the gas-phase basicity of NH_3 whether or not NH_3 or NH_4^+ is present. Acetate and water can potentially proton-transfer with proteins. Different anions can affect protein charging from solutions in which proteins are denatured[70] or solutions in which proteins have native structures.[71] In these experiments, acetate and water are present in both the ammonium and potassium acetate solutions, and therefore should not affect our conclusion about NH_4^+ or NH_3 not affecting protein charge. These results clearly show that proton-transfer between proteins and NH_3 does not affect the charge of ions formed from ammonium acetate solutions and that proton transfer to ammonia does not limit the charging of proteins in native mass spectrometry.

3.4.3 Charging of Protein Ions and the Rayleigh Limit

To determine if the charging of the protein ions under these conditions is close to Z_R,[7,15,31,32] the maximum and average charge of the protein ions, Z_{max} and Z_{av}, respectively, were compared to Z_R for water droplets of comparable sizes to the proteins. Z_R was calculated by approximating protein ions as spheres with a density of 1 g/cm^3.[7,15,31,32] For protein ions formed from aqueous ammonium acetate, Z_{av} is between 73.2 and 86.5 % of Z_R and Z_{max} is between 85.7 and 95.0 % of Z_R, which is within the range of previously reported values.[15,31,32] However, Z_{av} and Z_{max} for protein ions formed from pure water are higher than the values for ions formed from aqueous ammonium acetate. Z_{av} for ions formed from pure water is between 93.6 and 96.1 % of Z_R and Z_{max} is between 137 and 142 % of Z_R.

To determine if the difference in the conformation of the protein in pure water compared to in aqueous ammonium acetate can account for Z_{max} greater than Z_R for protein ions formed from pure water, $Z_{R(CCS)}$ was calculated by approximating the protein ions as spheres with densities obtained from average collision cross sections, CCS_{av}. CCS_{av} values were calculated as an average weighted sum of the collision cross sections for each charge-state distribution from the solution from which the ions were formed. $Z_{R(CCS)}$ takes into account, in part, conformational differences of protein ions formed from pure water and aqueous ammonium acetate because protein ions with larger collision cross sections have lower effective densities. The average effective density of protein ions formed from aqueous ammonium acetate is 0.58 g/cm^3, which is comparable to previously reported values.[60] However, the effective densities of cytochrome *c* and carbonic anhydrase ions formed from pure water are slightly lower than those of ions formed from aqueous ammonium acetate (Table 3.1).

Z_R, $Z_{R(CCS)}$, Z_{max} and Z_{av} for protein ions formed from pure water and aqueous ammonium acetate are shown as a function of molecular weight (Supplemental Figure 3.2) and normalized to Z_R (Figure 3.4). Z_{max} and Z_{av} for protein ions formed from ammonium acetate increase with the square root of molecular weight (Supplemental Figure 3.2), consistent with previously reported results.[15,31,32] $Z_{R(CCS)}$ is greater than Z_R by an average of 41 ± 14 % (Figure 3.4), consistent with protein ions formed from pure water that are partially elongated and not spherical. Z_{max} for protein ions formed from pure

water is between 85 and 110 % of $Z_{R(CCS)}$ and Z_{av} is between 56 and 75 % of $Z_{R(CCS)}$. The results are consistent with the higher charging for the ions formed from pure water being a result of their less compact structures compared to those formed from ammonium acetate.

Recently, Allen et al. investigated the effects of charge carrier emission of buffer ions on the charging of proteins ions formed from buffered aqueous ESI solutions by comparing Z_{av} of protein ions to Z_R.[31] The authors calculated Z_R by approximating the ions as spherical with densities of 0.6, 1.0, and 1.2 g/cm^3. For a density of 1.0 g/cm^3, Z_{av} of protein cations with molecular weights between 5.8 and 468 kDa was 60-90 % of Z_R.[31] Z_{av} of protein cations with molecular weights less than 130 kDa were only up to 83 % of Z_R, but Z_{av} of ions greater than 130 kDa were closer to Z_R.[31] The authors suggest that this shows a molecular weight dependence of protein ions charging to Z_R that is consistent with charge-carrier emissions of buffer ions at critical field strengths limiting the charge of protein ions.[31] Here, the molecular weight range of proteins investigated is much smaller, only 12.3 to 79.7 kDa, but there is no trend between protein molecular weight and charging of protein ions to Z_R within this molecular weight range. (Figure 3.4). Z_{max} of the protein ions formed from aqueous ammonium acetate is close to Z_R, ranging from 86 to 95 % Z_R. The extent of charging is very close to that expected from the charged residue mechanism, given that factors, such as conformation, can affect charging in this simplistic assumption in determining Z_R. Our results suggest that if charge-carrier emission from aqueous ammonium acetate solutions occurs, it does not significantly affect the charge of the protein ions in native mass spectrometry.

3.4.4 Factors that affect the relative proton-transfer reactivities of protein ions

The relative proton-transfer reactivities of the five proteins with basic molecules was investigated by comparing the change in charge-state distributions when the ions are reacted with DPA (Table 3.1). The relative extent of proton-transfer between the five proteins investigated and DPA does not trend with the protein pI, number of basic residues, or the fraction of basic residues in the protein (Table 3.1, Figure 3.5b-e). The extent of proton-transfer between protein ions and DPA is greater for ions formed from pure water than from aqueous ammonium acetate (Table 3.1). The proton-transfer reactivity of a protein ion is affected by both the number of charges and the ion conformation.[56,72] The ions from pure water are more highly charged than those formed from aqueous ammonium acetate, which can increase proton-transfer reactivity but are also less compact, which can decrease proton-transfer reactivity. Some partial collapse of the more highly charged, less compact ions may also occur in the gas phase[73] which would result in higher proton transfer reactivity. The time scale of the ion mobility measurements and the proton transfer reactivity experiments differ significantly, and any change in conformation in the latter may not be reflected in the ion mobility measurements.

The extent of proton-transfer of protein ions with DPA trends with how closely the ions are charged to Z_R. Figure 3.5a shows the absolute decrease in protein ion charge, ΔZ_{max} and ΔZ_{av}, upon reaction with DPA (120 s) as a function of percent Z_{max} and Z_{av} of Z_R for the protein ions before reaction. Protein ions with the greatest Z/Z_R value undergo the most proton-transfer with DPA (Figure 3.5a). This suggests that how closely protein ions are charged to Z_R affects the proton-transfer reactivities of the ions.

3.5 Conclusions

Factors that limit the charge of protein ions formed by ESI from aqueous solutions by ESI were investigated. The charge-state distributions of cytochrome *c* ions formed from aqueous

potassium acetate or ammonium acetate are the same. Potassium has a similar Gibbs solvation free energy, activity coefficient, and ionic radius to ammonium, so any ion evaporation that occurs should be similar for both ions. However, potassium cannot undergo proton transfer reactions with proteins. The similar charging of cytochrome *c* ions formed from potassium or ammonium acetate solutions shows that the presence of NH_4^+ or NH_3 does not affect charging in native mass spectrometry. Protein ions from these two solutions do not proton-transfer with 2-fluoropyridine, which has a gas-phase basicity that is 8 kcal/mol higher than that of ammonia, demonstrating that the apparent gas-phase basicity of protein ions formed in native mass spectrometry is greater than that of ammonia.

Protein ions formed from aqueous ammonium acetate solutions are charged closely to the values predicted by the Rayleigh limit for spherical water droplets similar in size to the proteins. The average charge of protein ions formed from aqueous ammonium acetate is between 73 and 87 % of Z_R, which is within the range of previously reported values. The maximum charge of protein ions formed from aqueous ammonium acetate is between 86 to 95 % of Z_R. The maximum charge of the protein ions is close to Z_R, suggesting the charge-carrier emission process in the combined charged residue-field emission model does not significantly limit the charging of these protein ions.

The extent of proton-transfer between protein ions formed from aqueous solutions and molecules with much higher gas-phase basicities depends on several factors. Protein ions formed from pure water are more highly charged with less compact conformations than those formed from aqueous ammonium acetate and undergo more proton transfer with basic molecules. The extent of proton-transfer between protein ions with more basic molecules is related to how closely the protein ions are charged to Z_R for spherical water droplets of comparable size to the proteins. These results are consistent with the charged residue mechanism in which ESI droplet charge limits the charge of protein ions formed from buffered aqueous solutions, when the proteins have compact folded conformations. This knowledge of the factors limiting the charging of protein ions formed from buffered aqueous solutions forms a foundation for efforts to join mass spectrometry with other solution techniques, such as high-throughput X-ray scattering, to reduce gaps between cloning library technologies and the throughput capacity of analytical platforms to characterize proteins.[74]

3.6 Acknowledgements

The authors thank the National Institutes of Health (Grant no. R01GM097357) for financial support and the Sandler-Moore Mass Spectrometry Core Facility at UCSF for use of the Synapt G2. John A. Tainer is partly supported by a Robert A. Welch Chemistry Chair, the Cancer Prevention and Research Institute of Texas, and the University of Texas System Science and Technology Acquisition and Retention. The authors also thank Department of Energy, Office of Basic Energy Sciences, Integrated Diffraction Analysis Technologies (IDAT) program at Lawrence Berkeley National Lab for use of the Jasco 815 spectropolarimeter and Dr. Catherine Going for helpful discussions.

3.7 References

(1) Fenn, J. B.; Mann, M.; Meng, C. K.; Wong, S. F.; Whitehouse, C. M. Electrospray ionization–principles and practice. *Mass Spectrom. Rev.* **1990**, *9* (1), 37–70.

(2) Kebarle, P.; Verkerk, U. H. Electrospray: from ions in solution to ions in the gas phase, what we know now. *Mass Spectrom. Rev.* **2009**, *28* (6), 898–917.

(3) Chowdhury, S. K.; Katta, V.; Chait, B. T. Probing conformational changes in proteins by mass spectrometry. *J. Am. Chem. Soc.* **1990**, *112* (24), 9012–9013.

(4) Dobo, A.; Kaltashov, I. A. Detection of multiple protein conformational ensembles in solution via deconvolution of charge-state distributions in ESI MS. *Anal. Chem.* **2001**, *73* (20), 4763–4773.

(5) Loo, J. A.; Loo, R. R. O.; Udseth, H. R.; Edmonds, C. G.; Smith, R. D. Solvent-induced conformational changes of polypeptides probed by electrospray-ionization mass spectrometry. *Rapid Commun. Mass Spectrom.* **1991**, *5* (3), 101–105.

(6) Iavarone, A. T.; Jurchen, J. C.; Williams, E. R. Effects of solvent on the maximum charge state and charge state distribution of protein ions produced by electrospray ionization. *J. Am. Soc. Mass Spectrom.* **2000**, *11* (11), 976–985.

(7) Iavarone, A. T.; Williams, E. R. Mechanism of Charging and Supercharging Molecules in Electrospray Ionization. *J. Am. Chem. Soc.* **2003**, *125* (8), 2319–2327.

(8) Thomson, B. A. Declustering and fragmentation of protein ions from an electrospray ion source. *J. Am. Soc. Mass Spectrom.* **1997**, *8* (10), 1053–1058.

(9) Iavarone, A. T.; Jurchen, J. C.; Williams, E. R. Supercharged protein and peptide ions formed by electrospray ionization. *Anal. Chem.* **2001**, *73* (7), 1455–1460.

(10) Sterling, H. J.; Cassou, C. A.; Susa, A. C.; Williams, E. R. Electrothermal supercharging of proteins in native electrospray ionization. *Anal. Chem.* **2012**, *84* (8), 3795–3801.

(11) Cassou, C. A.; Sterling, H. J.; Susa, A. C.; Williams, E. R. Electrothermal supercharging in mass spectrometry and tandem mass spectrometry of native proteins. *Anal. Chem.* **2013**, *85* (1), 138–146.

(12) Teo, C. A.; Donald, W. A. Solution additives for supercharging proteins beyond the theoretical maximum proton-transfer limit in electrospray ionization mass spectrometry. *Anal. Chem.* **2014**, *86* (9), 4455–4462.

(13) Lomeli, S. H.; Peng, I. X.; Yin, S.; Loo, R. R. O.; Loo, J. A. New reagents for increasing ESI multiple charging of proteins and protein complexes. *J. Am. Soc. Mass Spectrom.* **2010**, *21* (1), 127–131.

(14) Schnier, P. D.; Gross, D. S.; Williams, E. R. Electrostatic forces and dielectric polarizability of multiply protonated gas-phase cytochrome c ions probed by ion/molecule chemistry. *J. Am. Chem. Soc.* **1995**, *117* (25), 6747–6757.

(15) de la Mora, J. F. Electrospray ionization of large multiply charged species proceeds via Dole's charged residue mechanism. *Anal. Chim. Acta* **2000**, *406* (1), 93–104.

(16) Kharlamova, A.; Prentice, B. M.; Huang, T.-Y.; McLuckey, S. A. Electrospray droplet exposure to gaseous acids for the manipulation of protein charge state distributions. *Anal. Chem.* **2010**, *82* (17), 7422–7429.

(17) Kharlamova, A.; McLuckey, S. A. Negative Electrospray Droplet Exposure to Gaseous Bases for the Manipulation of Protein Charge State Distributions. *Anal. Chem.* **2011**, *83* (1), 431–437.

(18) Williams, E. R. Proton transfer reactivity of large multiply charged ions. *J. Mass. Spectrom.* **1996**, *31* (8), 831–842.

(19) Schnier, P. D.; Gross, D. S.; Williams, E. R. On the maximum charge state and proton transfer reactivity of peptide and protein ions formed by electrospray ionization. *J. Am. Soc. Mass Spectrom.* **1995**, *6* (11), 1086–1097.

(20) Ahadi, E.; Konermann, L. Modeling the behavior of coarse-grained polymer chains in charged water droplets: implications for the mechanism of electrospray ionization. *J. Phys. Chem. B* **2012**, *116* (1), 104–112.

(21) Wang, G.; Cole, R. B. Charged residue versus ion evaporation for formation of alkali metal halide cluster ions in ESI. *Anal. Chim. Acta* **2000**, *406* (1), 53–65.

(22) Wang, G.; Cole, R. B. Effect of solution ionic strength on analyte charge state distributions in positive and negative ion electrospray mass spectrometry. *Anal. Chem.* **1994**, *66* (21), 3702–3708.

(23) Felitsyn, N.; Peschke, M.; Kebarle, P. Origin and number of charges observed on multiply-protonated native proteins produced by ESI. *Int. J. Mass Spectrom.* **2002**, *219* (1), 39–62.

(24) Samalikova, M.; Grandori, R. Protein Charge-State Distributions in Electrospray-Ionization Mass Spectrometry Do Not Appear To Be Limited by the Surface Tension of the Solvent. *J. Am. Chem. Soc.* **2003**, *125* (44), 13352–13353.

(25) Samalikova, M.; Grandori, R. Testing the role of solvent surface tension in protein ionization by electrospray. *J. Mass. Spectrom.* **2005**, *40* (4), 503–510.

(26) Marchese, R.; Grandori, R.; Carloni, P.; Raugei, S. A computational model for protein ionization by electrospray based on gas-phase basicity. *J. Am. Soc. Mass Spectrom.* **2012**, *23* (11), 1903–1910.

(27) Spencer, E. A. C.; Ly, T.; Julian, R. R. Formation of the serine octamer: Ion evaporation or charge residue? *Int. J. Mass Spectrom.* **2008**, *270* (3), 166–172.

(28) Dole, M.; Mack, L. L.; Hines, R. L.; Mobley, R. C. Molecular Beams of Macroions. *J. Chem. Phys.* **1968**, *49* (5), 2240–2449.

(29) Hogan, C. J., Jr.; Carroll, J. A.; Rohrs, H. W.; Biswas, P.; Gross, M. L. Combined Charged Residue-Field Emission Model of macromolecular electrospray ionization. *Anal. Chem.* **2009**, *81* (1), 369–377.

(30) Metwally, H.; McAllister, R. G.; Konermann, L. Exploring the Mechanism of Salt-Induced

Signal Suppression in Protein Electrospray Mass Spectrometry Using Experiments and Molecular Dynamics Simulations. *Anal. Chem.* **2015**, *87* (4), 2434–2442.

(31) Allen, S. J.; Schwartz, A. M.; Bush, M. F. Effects of polarity on the structures and charge States of native-like proteins and protein complexes in the gas phase. *Anal. Chem.* **2013**, *85* (24), 12055–12061.

(32) Heck, A. J. R.; Van Den Heuvel, R. H. H. Investigation of intact protein complexes by mass spectrometry. *Mass Spectrom. Rev.* **2004**, *23* (5), 368–389.

(33) Konermann, L.; Ahadi, E.; Rodriguez, A. D.; Vahidi, S. Unraveling the mechanism of electrospray ionization. *Anal. Chem.* **2013**, *85* (1), 2–9.

(34) Konermann, L.; Rodriguez, A. D.; Liu, J. On the formation of highly charged gaseous ions from unfolded proteins by electrospray ionization. *Anal. Chem.* **2012**, *84* (15), 6798–6804.

(35) Yue, X.; Vahidi, S.; Konermann, L. Insights into the mechanism of protein electrospray ionization from salt adduction measurements. *J. Am. Soc. Mass Spectrom.* **2014**, *25* (8), 1322–1331.

(36) Vahidi, S.; Stocks, B. B.; Konermann, L. Partially disordered proteins studied by ion mobility-mass spectrometry: implications for the preservation of solution phase structure in the gas phase. *Anal. Chem.* **2013**, *85* (21), 10471–10478.

(37) Flick, T. G.; Williams, E. R. Supercharging with trivalent metal ions in native mass spectrometry. *J. Am. Soc. Mass Spectrom.* **2012**, *23* (11), 1885–1895.

(38) Zhu, M. M.; Rempel, D. L.; Zhao, J.; Giblin, D. E.; Gross, M. L. Probing Ca^{2+}-induced conformational changes in porcine calmodulin by H/D exchange and ESI-MS: Effect of cations and ionic strength. *Biochemistry* **2003**, *42* (51), 15388–15397.

(39) Liu, H.; Håkansson, K. Divalent metal ion-peptide interactions probed by electron capture dissociation of trications. *J. Am. Soc. Mass Spectrom.* **2006**, *17* (12), 1731–1741.

(40) Ly, T.; Julian, R. R. Protein-metal interactions of calmodulin and α-synuclein monitored by selective noncovalent adduct protein probing mass spectrometry. *J. Am. Soc. Mass Spectrom.* **2008**, *19* (11), 1663–1672.

(41) Verkerk, U. H.; Peschke, M.; Kebarle, P. Effect of buffer cations and of H_3O^+ on the charge states of native proteins. Significance to determinations of stability constants of protein complexes. *J. Mass. Spectrom.* **2003**, *38* (6), 618–631.

(42) Prakash, H.; Kansara, B. T.; Mazumdar, S. Effects of salts on the charge-state distribution and the structural basis of the most-intense charge-state of the gaseous protein ions produced by electrospray ionization. *Int. J. Mass Spectrom.* **2010**, *289* (2-3), 84–91.

(43) Grandori, R. Origin of the conformation dependence of protein charge-state distributions in

electrospray ionization mass spectrometry. *J. Mass. Spectrom.* **2003**, *38* (1), 11–15.

(44) Watt, S. J.; Sheil, M.; Beck, J. L.; Prosselkov, P.; Otting, G.; Dixon, N. E. Effect of protein stabilization on charge state distribution in positive and negative ion electrospray ionization mass spectra. *J. Am. Soc. Mass Spectrom.* **2007**, *18* (9), 1605–1611.

(45) Kebarle, P. A brief overview of the present status of the mechanisms involved in electrospray mass spectrometry. *J. Mass. Spectrom.* **2000**, *35* (7), 804–817.

(46) Peschke, M.; Verkerk, U. H.; Kebarle, P. Features of the ESI mechanism that affect the observation of multiply charged noncovalent protein complexes and the determination of the association constant by the titration method. *J. Am. Soc. Mass Spectrom.* **2004**, *15* (10), 1424–1434.

(47) Peschke, M.; Blades, A.; Kebarle, P. Charged states of proteins. Reactions of doubly protonated alkyldiamines with NH_3: Solvation or deprotonation. Extension of two proton cases to multiply protonated globular proteins observed in the gas phase. *J. Am. Chem. Soc.* **2002**, *124* (38), 11519–11530.

(48) Hiraoka, K.; Asakawa, Y.; Kawashima, Y.; Okazaki, S.; Nakamura, M.; Yamamoto, Y.; Takamizawa, A. The effect of the presence of foreign salts on the formation of gaseous ions for electrospray and laser spray. *Rapid Commun. Mass Spectrom.* **2004**, *18* (20), 2437–2442.

(49) Catalina, M. I.; Van Den Heuvel, R. H. H.; van Duijn, E.; Heck, A. J. R. Decharging of globular proteins and protein complexes in electrospray. *Chem. Eur. J.* **2005**, *11* (3), 960–968.

(50) Le Blanc, J. C. Y.; Wang, J.; Guevremont, R.; Siu, K. W. M. Electrospray mass spectra of protein cations formed in basic solutions. *Org. Mass Spectrom.* **1994**, *29* (11), 587–593.

(51) Loo, R. R. O.; Smith, R. D. Proton transfer reactions of multiply charged peptide and protein cations and anions. *J. Mass. Spectrom.* **1995**, *30*, 339–347.

(52) Cassady, C. J.; Wronka, J.; Kruppa, G. H.; Laukien, F. H.; Hettich, R. Deprotonation reactions of multiply protonated ubiquitin ions. *Rapid Commun. Mass Spectrom.* **1994**, *8* (5), 394–400.

(53) Winger, B. E.; Light-Wahl, K. J.; Smith, R. D. Gas-phase proton transfer reactions involving multiply charged cytochrome c ions and water under thermal conditions. *J. Am. Soc. Mass Spectrom.* **1992**, *3* (6), 624–630.

(54) Valentine, S. J.; Counterman, A. E.; Clemmer, D. E. Conformer-dependent proton-transfer reactions of ubiquitin ions. *J. Am. Soc. Mass Spectrom.* **1997**, *8*, 954–961.

(55) McLuckey, S. A.; Van Berkel, G. J.; Glish, G. L. Reactions of dimethylamine with multiply charged ions of cytochrome c. *J. Am. Chem. Soc.* **1990**, *112* (14), 5668–5670.

(56) Gross, D. S.; Schnier, P. D.; Rodriguez-Cruz, S. E.; Fagerquist, C. K.; Williams, E. R. Conformations and folding of lysozyme ions in vacuo. *Proc. Natl. Acad. Sci. U.S.A.* **1996**, *93*

(7), 3143–3148.

(57) Ogorzalek Loo, R. R.; Smith, R. D. Investigation of the Gas-Phase Structure of Electrosprayed Proteins Using Ion-Molecule Reactions. *J. Am. Soc. Mass Spectrom.* **1994**, *5* (4), 207–220.

(58) Ogorzalek Loo, R. R.; Udseth, H. R.; Smith, R. D. A new approach for the study of gas-phase ion-ion reactions using electrospray ionization. *J. Am. Soc. Mass Spectrom.* **1992**, *3* (7), 695–705.

(59) Jurchen, J. C.; Williams, E. R. Origin of asymmetric charge partitioning in the dissociation of gas-phase protein homodimers. *J. Am. Chem. Soc.* **2003**, *125* (9), 2817–2826.

(60) Bush, M. F.; Hall, Z.; Giles, K.; Hoyes, J.; Robinson, C. V.; Ruotolo, B. T. Collision cross sections of proteins and their complexes: a calibration framework and database for gas-phase structural biology. *Anal. Chem.* **2010**, *82* (22), 9557–9565.

(61) Baldwin, R. L. How Hofmeister ion interactions affect protein stability. *Biophys. J.* **1996**, *71* (4), 2056–2063.

(62) Goto, Y.; Fink, A. L. Conformational states of beta-lactamase: molten-globule states at acidic and alkaline pH with high salt. *Biochemistry* **1989**, *28* (3), 945–952.

(63) Marcus, Y. Thermodynamics of solvation of ions. Part 5. Gibbs free energy of hydration at 298.15 K. *Faraday Trans.* **1991**, *87* (18), 2995–2999.

(64) Kielland, J. Individual Activity Coefficients of Ions in Aqueous Solutions. *J. Am. Chem. Soc.* **1937**, *59* (9), 1675–1678.

(65) *Circular Dichroism and the Conformational Analysis of Biomolecules*; Fasman, G. D., Ed.; Springer Science and Business Media: Boston, MA, 2013.

(66) Shi, L.; Holliday, A. E.; Khanal, N.; Russell, D. H.; Clemmer, D. E. Configurationally-Coupled Protonation of Polyproline-7. *J. Am. Chem. Soc.* **2015**, *137* (27), 8680–8683.

(67) Hernández, H.; Robinson, C. V. Determining the stoichiometry and interactions of macromolecular assemblies from mass spectrometry. *Nat. Protoc.* **2007**, *2* (3), 715–726.

(68) Han, L.; Hyung, S.-J.; Mayers, J. J. S.; Ruotolo, B. T. Bound anions differentially stabilize multiprotein complexes in the absence of bulk solvent. *J. Am. Chem. Soc.* **2011**, *133* (29), 11358–11367.

(69) Hunter, E. P. L.; Lias, S. G. Evaluated gas phase basicities and proton affinities of molecules: an update. *J. Phys. Chem. Ref. Data* **1998**, *27* (3), 413–656.

(70) Mirza, U. A.; Chait, B. T. Effects of Anions on the Positive Ion Electrospray Ionization Mass Spectra of Peptides and Proteins. *Anal. Chem.* **1994**, *66* (18), 2898–2904.

(71) Flick, T. G.; Cassou, C. A.; Chang, T. M.; Williams, E. R. Solution additives that desalt protein

ions in native mass spectrometry. *Anal. Chem.* **2012**, *84* (17), 7511–7517.

(72) Loo, R. R. O.; Loo, J. A.; Udseth, H. R.; Fulton, J. L.; Smith, R. D. Protein structural effects in gas phase ion/molecule reactions with diethylamine. *Rapid Commun. Mass Spectrom.* **1992**, *6* (3), 159–165.

(73) Bornschein, R. E.; Hyung, S.-J.; Ruotolo, B. T. Ion mobility-mass spectrometry reveals conformational changes in charge reduced multiprotein complexes. *J. Am. Soc. Mass Spectrom.* **2011**, *22* (10), 1690–1698.

(74) Brunette, T. J.; Parmeggiani, F.; Huang, P.-S.; Bhabha, G.; Ekiert, D. C.; Tsutakawa, S. E.; Hura, G. L.; Tainer, J. A.; Baker, D. Exploring the repeat protein universe through computational protein design. *Nature* **2015**, *528* (7583), 580–584.

(75) UniProt Consortium. UniProt: a hub for protein information. *Nucleic Acids Res.* **2015**, *43* (Database issue), D204–D212.

3.8 Tables and Figures

Table 3.1. Molecular weight, pI,[75] number of basic residues, maximum charge (Z_{max}), average charge (Z_{av}), extent of proton-transfer with DPA, and effective density values for each protein. Ions formed from 10 mM aqueous ammonium acetate solution unless otherwise noted

	molecular weight (kDa)	pI	number of basic residues	Z_{max}	Z_{av}	reaction with DPA (120 s)		Effective Density (g/cm^3)
						$-\Delta Z_{max}$	$-\Delta Z_{av}$	
cytochrome *c*	12.3	9.6	24	8	7.1	1.0 ± 0.0	1.1 ± 0.1	0.50
cytochrome *c* (water)	12.3	9.6	24	12	8.1	3.0 ± 0.0	1.8 ± 0.1	0.44
myoglobin	17.6	7.4	32	9	8.0	0.3 ± 0.5	0.6 ± 0.3	0.52
carbonic anhydrase	29.1	6.8	43	12	9.8	0.7 ± 0.5	0.4 ± 0.1	0.74
carbonic anhydrase (water)	29.1	6.8	43	19	12.9	4.3 ± 2.0	2.8 ± 0.1	0.69
concanavalin A dimer	51.7	6.0	48	17	15.1	1.3 ± 0.5	1.5 ± 0.5	0.58
holo-transferrin (200 mM ammonium acetate)	79.7	5.4	64	21	19.2	1.7 ± 0.5	1.4 ± 0.3	0.60

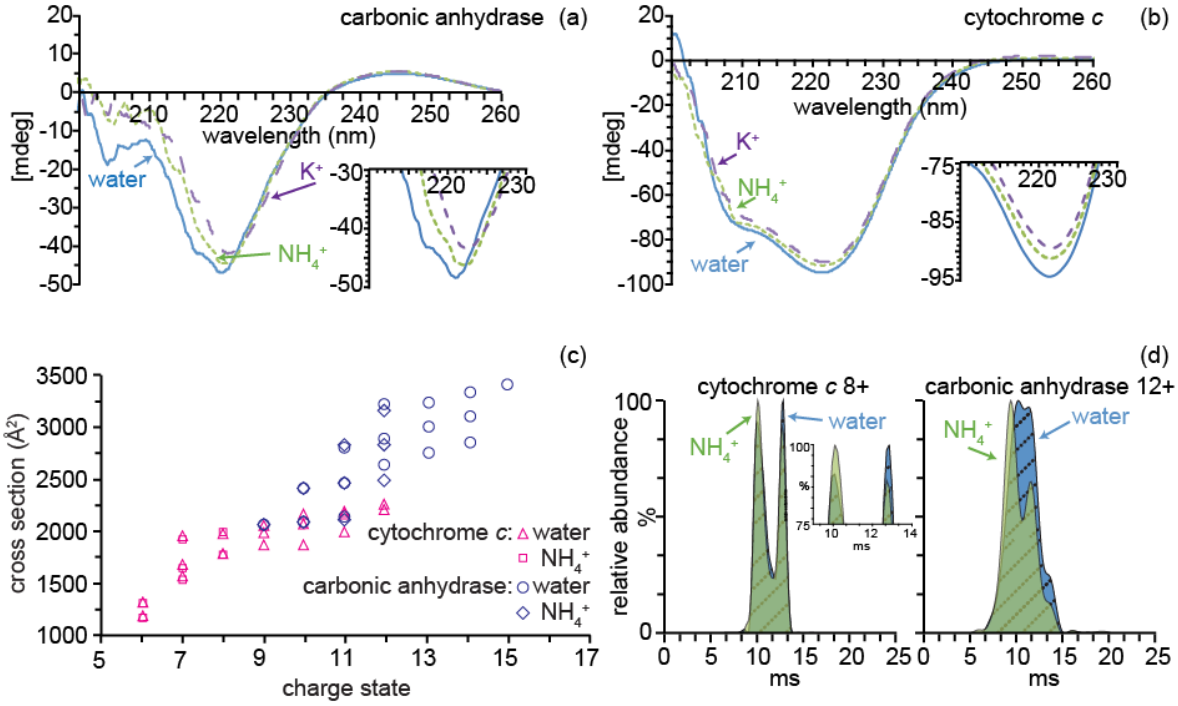

Figure 3.1. (a) CD spectra of 10 μM carbonic anhydrase and (b) 10 μM cytochrome *c* in pure water (solid blue line), 10 mM ammonium acetate (green dotted line), and 10 mM potassium acetate (purple dashed line). (c) Collision cross sections of 10 μM cytochrome *c* ions (pink) and carbonic anhydrase ions (blue) and formed from 10 mM ammonium acetate (square, diamond, respectively) or pure water (triangle, circle, respectively) as a function of charge state. (d) Arrival time distributions of cytochrome *c* 8+ ions and carbonic anhydrase 12+ ions formed from water (blue) or 10 mM ammonium acetate (green)

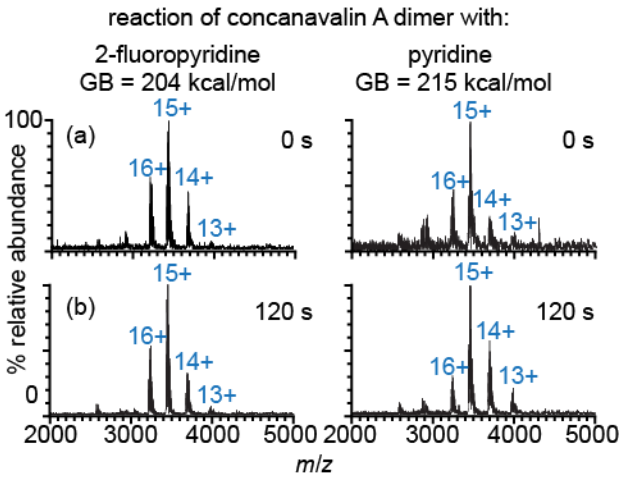

Figure 3.2. Mass spectra of concanavalin A dimer ions formed from 10 mM ammonium acetate after reaction with either 2-fluoropyridine or pyridine for (a) 0 and (b) 120 s

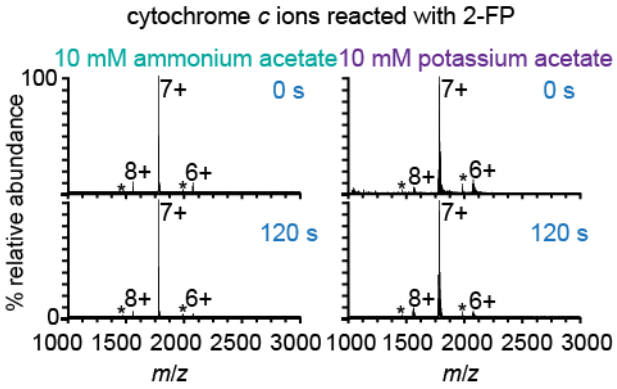

Figure 3.3. Mass spectra of 10 μM cytochrome *c* ions formed from 10 mM ammonium acetate and 10 mM potassium acetate reacted with 2-fluoropyrine for 0 and 120 s

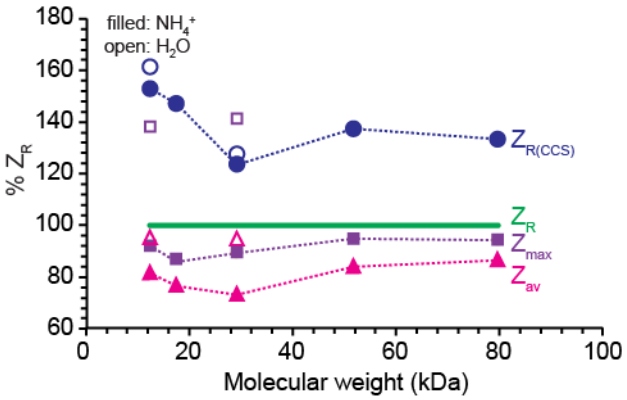

Figure 3.4. Z_{max} (purple square), Z_{av} (pink triangles), $Z_{R(CCS)}$ (blue circles) for protein ions formed from aqueous ammonium acetate (filled) or pure water (open) relative to Z_R (green line) as a function of molecular weight. Z_R represents the maximum number of charges on a protein predicted using the Rayleigh limit for a droplet the same size as a spherical protein with a density of 1.0 g/cm^3. $Z_{R(CCS)}$ represents the maximum number of charges predicted using the Rayleigh limit for a spherical droplet with the same radius as the CCS_{av} for the protein ions.

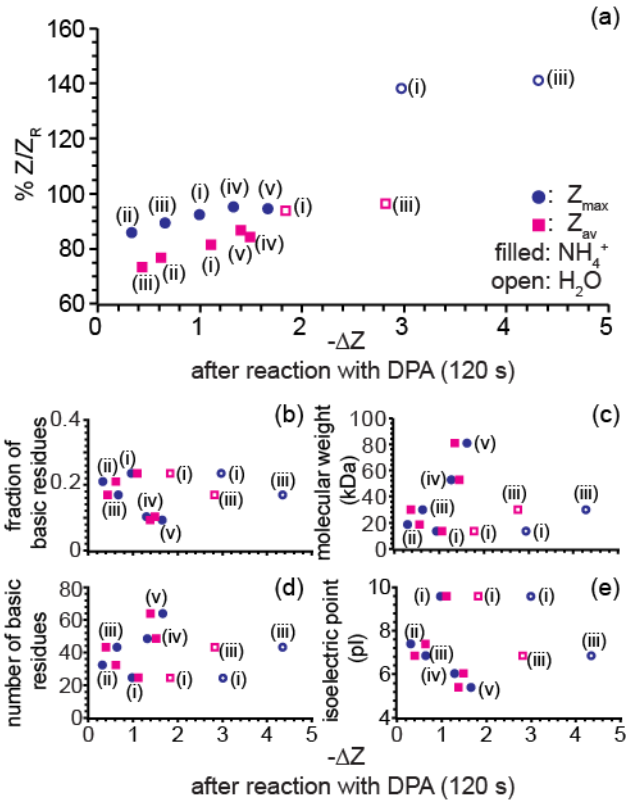

Figure 3.5. (a) The percent Z_{max} (circle) and Z_{av} (square) of Z_R, for protein ions formed from aqueous ammonium acetate (filled markers) or pure water (open markers) prior to reaction with a base v. the decrease in Z_{max} (circle) and Z_{av} (square) after 120 s reaction with DPA. (b) fraction of basic residues, (c) molecular weight (d) number of basic residues (e) isoelectric point (pI) for each protein as a function of the decrease in Z_{max} (circle) and Z_{av} (square) after 120 s reaction with DPA. (i) corresponds to cytochrome *c*, (ii) myoglobin, (iii) carbonic anhydrase, (iv) concanavalin A dimer and (v) holo-transferrin ions, respectively.

3.9 Supplemental Information

Supplemental Table 3.1. Collisional cross sections (CCS) of cytochrome *c* and carbonic anhydrase ions formed from pure water or 10 mM aqueous ammonium acetate.

	10 mM ammonium acetate CCS (Å^2)	**Water CCS (Å^2)**
Cytochrome *c*		
6+	1150, 1250	1150, 1250
7+	1510, 1640, 1970	1520, 1650, 1980
8+	1750, 1990	1750, 1980
9+	-	1800, 1960, 2040
10+	-	1880, 2030, 2100
11+	-	1940, 2100, 2160
12+	-	2180, 2230
Carbonic anhydrase		
9+	2060	2060
10+	2070, 2390	2060, 2390
11+	2100, 2430, 2760	2080, 2430, 2750
12+	2460, 2810, 3160	2600, 2830, 3140
13+	-	2710, 2900, 3230
14+	-	2800, 3120, 3290
15+	-	3380

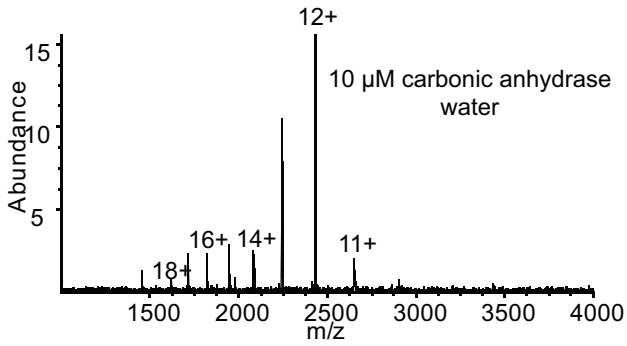

Supplemental Figure 3.1. Mass spectrum of 10 μM carbonic anhydrase formed from pure water (FT-ICR).

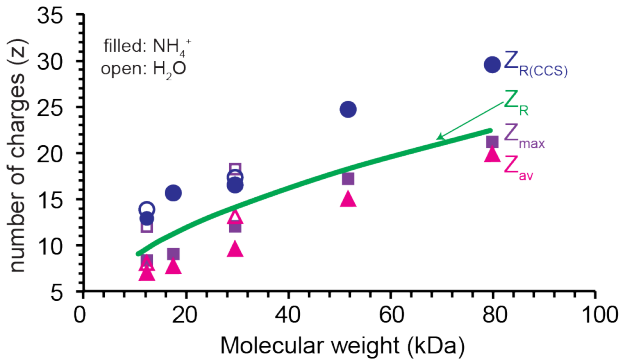

Supplemental Figure 3.2. Z_{max} (purple square), Z_{av} (pink triangles) for protein ions formed from aqueous ammonium acetate (filled) or pure water (open) as a function of molecular weight. Green line represents Z_R, the maximum number of charges on a protein predicted using the Rayleigh limit for a droplet the same size as a spherical protein with a density of 1.0 g/cm^3. $Z_{R(CCS)}$ (blue circles) represents the maximum number of charges predicted using the Rayleigh limit for a spherical droplet with the same radius as the CCS_{av} for the protein ions.

Chapter 4

Small Emitter Tips for Native Mass Spectrometry of Proteins and Protein Complexes from Nonvolatile Buffers that Mimic the Intracellular Environment

This chapter is reproduced with permission from:

Anna C. Susa, Zijie Xia, Evan R. Williams
"Small Emitter Tips for Native Mass Spectrometry of Proteins and Protein Complexes from Nonvolatile Buffers that Mimic the Intracellular Environment"
Analytical Chemistry, **2017**

4.1 Abstract

Salts are often necessary to maintain the native structures and functions of many proteins and protein complexes, but many buffers adversely affect protein analysis by native mass spectrometry (MS). Here, protein and protein complex ions are formed directly from a 150 mM KCl and 25 mM Tris-HCl buffer at pH 7 that is widely used in protein chemistry to mimic the intracellular environment. The protein charge-state distributions are not resolved from electrospray ionization MS using 1.6 μm diameter emitter tips resulting in no mass information. In contrast, the charge-state distributions are well-resolved using 0.5 μm tips, from which the masses of proteins and protein complexes can be obtained. Salt adduction to protein ions decreases with decreasing tip size below ~1.6 μm but not above this size. This suggests that the mechanism for reducing salt adduction is the formation of small initial droplets with on average fewer than one protein molecule per droplet which lowers the salt-to-protein ratio in droplets that contain a protein molecule. This is the first demonstration of native mass spectrometry of protein and protein complex ions formed from a buffer containing physiological ionic strengths of nonvolatile salts that mimics the intracellular environment, and this method does not require sample preparation or addition of reagents to the protein solution before or during mass analysis.

4.2 Introduction

Interactions of ions with proteins, whether specific or nonspecific, can significantly influence protein structure and function.[1-6] Tris and phosphate buffers as well as potassium and sodium chloride are often used to stabilize the native structures and functions of proteins and protein complexes by mimicking the intracellular environment, which has an ionic strength of 100-200 mM.[7] Salts provide the high ionic strength necessary for some protein complexes to assemble, and specific salts can be essential for some protein-protein, protein-ligand, and enzyme-cofactor interactions.[8-10] For example, casein kinase 2 (CK2), a serine/threonine selective protein kinase, forms spherical structures at an

ionic strength of 500 mM but forms ring-like structures at 200 mM that are stabilized by the cofactor $MgCl_2$.[10]

In native mass spectrometry (MS), electrospray ionization (ESI) is used to produce intact gaseous ions of proteins and noncovalent complexes directly from aqueous solutions. Native MS is widely used to measure the masses of large biomolecules such as intact protein complexes, DNA, ribosomes and virus capsids.[11-15] The stoichiometries of intact protein and protein complexes can be obtained from molecular weight measurements and noncovalent (specific-ion or ligand) binding information can be obtained from tandem MS experiments.[16-20] However, some salts commonly used in protein sample preparation, such as sodium, potassium, Tris and phosphate buffers adversely affect the ionization process. Salts can significantly lower sensitivity by increasing baseline noise and can cause ion suppression.[21-24] Many salts can also adduct to protein ions which distributes the protein signal over multiple ions, reducing the detection limit for large proteins and protein complexes. For large molecules or complexes for which adduct ions are not resolved, salt adduction broadens the mass spectral peaks, reducing the mass measuring accuracy and the ability to detect and identify post-translational modifications or proteins with similar masses in complexes. Robinson and coworkers showed that the increase in mass due to adduction to noncovalent complexes can be estimated based on the peak widths for charge states of the complex.[11] Individual charge states of large protein complex ions, such as alcohol dehydrogenase, are difficult to resolve if Tris or HEPES is present in concentrations even as low as 10 mM.[21]

To circumvent the adverse effects of some salts on protein signal in native mass spectrometry, salts are typically removed from solutions prior to ESI using methods such as dialysis,[25] diafiltration,[26,27] or ion chromatography.[21,28] Because high ionic strengths are often necessary to maintain protein structure, solutions are often buffer exchanged into volatile ammonium salt solutions, such as ammonium acetate or ammonium bicarbonate, because these ammonium salts do not adduct to proteins. Desalting ESI solutions and buffer exchanging into ammonium salt solutions can significantly alter the structure and function of some proteins that require specific salts to assemble. For example, an activator protein, NtrC4 from *Aquifex aeolicus*, requires millimolar concentrations of specific salts to form a 270 kDa homohexamer.[29,30] Removing salts that are necessary for complexes to assembly makes analyzing these complexes by native mass spectrometry challenging.

Several alternatives to desalting protein samples before ESI make it possible to retain specific salts necessary for protein structure and function. These methods include buffer loading using high concentrations, e.g., 1 M, of ammonium acetate,[21,24] adding low concentrations of reagents that desalt protein ions in the ESI process,[31-34] or reacting ions with organic vapors.[35] These methods of reducing sodium adduction to protein ions are effective for proteins in pure water or water with volatile ammonium salts that contain between 1 and 20 mM NaCl.[21,24,31-35] Schmidt et al. also reported fewer sodium ions adducted to insulin ions formed from water/methanol/acid solution with ESI emitters with ~1 μm diameter tips than with ~12 μm tips.[36] The authors proposed that the lower sodium adduction with the smaller tip was due either to less solvent evaporation and thus lower concentration of contaminants prior to ion release or higher extent of solvent oxidation and formation of H_3O^+.[36] Although these methods are effective for solutions with relatively low concentrations of salts and for volatile buffers, native MS has not been reported from typical buffers used in protein chemistry that mimic the intracellular environment.

Here, a simple and fast method for desalting protein and protein complex ions formed by ESI of solutions containing a buffer that mimics the intracellular environment is demonstrated. The signal-to-noise ratios (S/N) and resolution of protein and protein complex ions formed with nano-electrospray emitters with tip diameters less than 1 μm are higher than those of ions formed with tip diameters greater than 1 μm. We show that this ion desalting method is more effective than adding

reagents that desalt protein ions. This is the first demonstration of desalting protein ions during ESI directly from a biologically relevant buffer that is commonly used in many different laboratories to investigate protein chemistry.

4.3 Experimental

Mass spectral data were acquired using a Waters Quadrupole-Time-of-Flight (Q-TOF) Premier mass spectrometer (Waters, Milford, MA, USA). Protein ions were formed by nano-electrospray ionization using borosilicate capillaries (1.0 mm o.d./0.78 mm i.d., Sutter Instruments, Novato, CA, USA) that were pulled with a Flaming/Brown micropipette puller (Model P-87, Sutter Instruments, Novato, CA, USA) to form tips with inner diameters that range from 0.2 μm to 38 μm. Tip diameters and taper lengths were measured with a scanning electron microscope (Hitachi TM-1000 SEM, Schaumburg, IL, USA) at the Electron Microscope Laboratory at UC Berkeley. Tips were measured in triplicate, and the standard deviation of the tip diameter for each tip size is ± 10 %. The borosilicate capillaries were filled with 5 μM protein solution, and nano-electrospray was initiated by applying a potential of about +0.6 to 2.0 kV to a 0.127 mm diameter platinum wire that is inserted into the capillary and is in contact with the sample solution. The electrospray voltage (0.6 – 2.0 kV) and the sampling cone voltage (100-200 V) were optimized for each emitter tip. The extraction cone voltage, voltage in the collision cell, and source temperature were 5.0 V, 5.0 V and 80 °C, respectively. The backing pressure in the source region was maintained at ~6 mbar. Ions formed from aqueous solutions with 25 mM ammonium bromide were collisionally activated as previously described.[33] Mass spectral replicates were acquired with at least three different tips, and one spectrum from each set of replicates is shown.

The width, centroid and area of each protein or protein complex ion charge state was determined by fitting these data to Gaussian functions in OriginPro. The masses of salt-adducted protein ions were determined from the centroid of the unresolved adducts for each charge state in the distribution. The masses of unadducted ions were calculated from the elemental composition using average masses. The extent of adduction was obtained from the difference between these two masses for each charge state. The average number of adducts for each charge state was determined from the difference in mass between the mass of the salt-adducted protein ion and the theoretical mass and dividing by the mass of the primary adducting species, Na^+ from 10 mM Na^+ acetate or K^+ from 25 mM Tris-HCl 150 mM KCl (Supplemental Figure 4.6). Average charge was determined from a weighted abundance corresponding to the area of each charge state. Signal-to-noise (S/N) ratios were determined from the signal of the most abundant protein ion charge state to the noise in a baseline region that is m/z 100 lower than that of the protein charge state. The ratio of oligomeric species was determined as a ratio of the corresponding area of each oligomeric species. The reported error for each measurement is the standard deviation of replicate measurements with at least three different emitters.

Lyophilized protein powders of yeast alcohol dehydrogenase (ADH), bovine serum albumin (BSA), jack bean concanavalin A, egg white avidin, ammonium acetate, ammonium sulfate, ammonium phosphate dibasic, ammonium bromide, tris hydrochloride and *m*-nitrobenzyl alcohol (*m*-NBA) are from Sigma (St. Louis, MO) and were used without further purification.

4.4 Results and Discussion

4.4.1 Effects of Tip Diameter on Salt Adduction to Protein Ions

In order to evaluate the effects of emitter tip diameter on the extent of salt adduction on protein ions, BSA ions were formed from aqueous 10 mM sodium acetate solutions using nano-ESI emitters with tips ranging in inner diameter from 0.2 μm to 38 μm. The most abundant charge states of BSA ions are 14+ and 13+, and the average charge of BSA ions is similar for all tip sizes investigated. The average charge of BSA ions is 13.53 ± 0.14 and 13.41 ± 0.21 with the 0.2 μm to 38 μm tips, respectively. Higher protein charging occurs from smaller tip diameters when ions are formed from solutions containing organic solvents and acid,[37,38] or from aqueous buffered solutions in which the protein has a net positive charge which can result in protein surface interactions at small tip sizes.[39] The net charge of BSA in this solution is negative (pI = 5.6),[40] consistent with no change in charging with tip size.[39]

Representative mass spectra of BSA ions formed from 0.7 μm and 2.9 μm diameter tips, and the average number of sodium ions adducted to the 14+ and 13+ charge states of BSA ions as a function of emitter tip diameter are shown in Figure 4.1. Because individual adducts to BSA ions were not resolved, the increase in mass from adduction was determined from the centroid of the adducted protein ion charge states and the theoretical mass of the unadducted ion. Individual adducts to cytochrome *c*, a lower molecular weight protein, formed from 10 mM sodium acetate are well-resolved, and these results show that the adducts from this solution are primarily Na^+ (Supplemental Figure 4.6). Therefore, we estimate the number of adducts to BSA by assuming all adducts are Na^+, recognizing that there may be a small contribution from other adducts as well. The number of sodium ions adducted to BSA decreases with decreasing tip diameter from 1.6 to 0.2 μm. The 14+ charge state of BSA formed with 1.6 μm diameter tips has 108 ± 15 Na^+ adducted (2,362 ± 300 Da greater than the calculated mass of BSA), but the same charge state from 0.2 μm tips only has 22 ± 3 Na^+ adducted (470 ± 66 Da greater than the calculated mass of BSA). More ions adduct to the 14+ charge state than to the 13+ charge state for all tip sizes investigated. Sodium adduction to BSA does not change significantly with tip diameters greater than ~1 μm. The number of Na^+ adducts on the 14+ charge state of BSA ions formed from tip diameters from 1.6 to 38 μm is between 103 and 123 Na^+ (2,266 to 2,706 Da greater than the calculated mass of BSA). This number of adducts is slightly higher than the 99 acidic residues of BSA, indicating that sodium ions are adducted to mostly the carboxylate form of nearly all acidic residues as well as coordinating to polarizable functional groups, such as the amide oxygen atoms.[41,42] These results demonstrate that using emitters with submicrometer diameter tips is beneficial for desalting protein ions formed by nano-ESI from aqueous solutions.

4.4.2 Desalting protein ions from a buffer that mimics the intracellular environment

To determine the effectiveness of submicrometer tips at desalting protein ions directly from buffers that are commonly used in biochemical laboratories, protein and protein complex ions were formed from 150 mM KCl and 25 mM Tris-HCl at pH 7 (Figure 4.2). This buffer is commonly used to prepare protein samples because it mimics the intracellular environment.[7,43] Bovine serum albumin, concanavalin A, and alcohol dehydrogenase (ADH) ions were formed using both 1.6 μm tips, on the lower end of commonly used tip sizes in native mass spectrometry, and 0.5 μm tips. The spectra shown in Figure 4.2 are representative of at least three replicate measurements with different tips for each measurement.

With the 1.6 μm tips, there are ions corresponding to discrete salt clusters below m/z 4000, and a broad, unresolved multimodal peak is between m/z 4000 and 8000 in the mass spectrum of BSA (Figure 4.2a). Individual protein ion charge states are not resolved, and it is not possible to obtain the molecular weight of the protein from these spectra (Figure 4.2a). In contrast, the protein charge-state distribution of the BSA is well resolved with the 0.5 μm tips (Figure 4.2b). The protein ions are salt adducted, but the individual adducts are not resolved. The molecular mass of these salt adducted BSA ions is 1955 ± 41 Da greater than the calculated mass. The adducts to carbonic anhydrase ions formed from these solutions are well-resolved and demonstrate that the adduction is nearly exclusively due to K^+ (Supplemental Figure 4.6). Thus, the 1955 ± 41 Da greater mass observed for BSA corresponds to ~50 K^+ adducts on each charge state (Figure 4.2b). The much higher m/z of the broad multimodal peak observed with the 1.6 μm tips (Figure 4.2a) indicates a significantly higher number of adducts to the BSA ions.

Similar results are obtained for concanavalin A and for alcohol dehydrogenase, both of which form tetramers in solution. There is a broad bimodal peak between m/z 3500 and 6500 in the spectra of both proteins with the 1.6 μm tips. In striking contrast, the charge-state distributions of the tetramers of both proteins are well resolved with the 0.5 μm tips. The relative abundance ratio of the concanavalin A dimer to tetramer is 0.75, which is close to that reported previously for concanavalin A formed from ammonium acetate solutions of similar ionic strength.[44] The molecular masses of concanavalin A tetramer and alcohol dehydrogenase ions with the 0.5 μm tips are 2890 and 4680 Da (~75 and ~120 K^+ adducted), respectively, greater than the theoretical masses of the adduct-free protein complex ions. The ratio of adducts to ion charge is about 4-5 for BSA and the two tetramer complexes.

The centroids of the bimodal peaks in the broad, high m/z peaks for both concanavalin A (Figure 4.2c) and for alcohol dehydrogenase (Figure 4.2e) obtained with the 1.6 μm tips are not the same for both protein complexes and appear at lower m/z values than the corresponding charge- state distributions of tetramer of concanavalin A (Figure 4.2d) and the tetramer of alcohol dehydrogenase (Figure 4.2f) obtained with the 0.5 μm tips. Moreover, the tetramer is the only protein species observed for alcohol dehydrogenase with the 0.5 μm tips, yet the broad peak with the 1.6 μm tips is bimodal. These results indicates that the broad, high m/z peaks for both proteins obtained with the 1.6 μm tips is not due to salt adduction on the protein tetramer ions but rather from clustering of salts and sample impurities. Commercially purchased yeast ADH contains significant impurities, and 2 % of the sample is citrate buffer. It is possible that citrate buffer ions form large ionic clusters with KCl and Tris-HCl and also some ADH monomer ions.

Protein ions formed directly from buffers with KCl or NaCl concentrations of 100-200 mM and Tris that mimics the intracellular environment have not been reported previously. This is the first demonstration of directly measuring resolved charge-state distributions of protein and protein complex ions formed by nano-ESI from a biologically relevant buffer with high concentrations of nonvolatile salts, and this method eliminates any sample preparation needed to desalt protein solutions prior to ion formation and mass analysis.

4.4.3 Desalting ions from aqueous ammonium salt solutions

In order to determine the effectiveness of nano-ESI emitters with submicrometer tip sizes at desalting protein ions formed from aqueous ammonium acetate solutions that are commonly used in native mass spectrometry, protein and protein complex ions were formed from 175 mM ammonium acetate solution with 1.6 μm and 0.5 μm tips (Figure 4.3). With the 1.6 μm tips, charge states of ADH

tetramer ions are resolved, but the widths of the individual charge states are broad (Figure 4.3a). The 3652 ± 88 Da higher mass with the 1.6 μm tips for the 23+ charge state corresponds to 166 ± 4 Na^+ adducted. The baseline is elevated due to impurities in the sample (Figure 4.3a). When ADH ions are formed from this same solution using 0.5 μm tips, the peaks are much narrower. The number of Na^+ adducts on the 23+ charge state is 42 ± 10 (924 ± 220 Da), and the baseline chemical noise is significantly lower (Figure 4.3b). The S/N ratio of the most abundant charge state formed with the 0.5 μm tips is 105 times larger than with the 1.6 μm tips (Supplemental Table 4.1). The average number of Na^+ adducts on charge states of the avidin tetramer ions formed from aqueous ammonium acetate with both sizes of tips is similar, but the baseline noise is significantly reduced with the small tip size (Supplemental Figure 4.1). The number of Na^+ adducts on the individual charge states of BSA and concanavalin A ions formed from ammonium acetate is similar from both tip sizes (Supplemental Figure 4.1). These results demonstrate that submicrometer tips are useful for desalting protein ions from solutions that contain salt impurities, such as buffer salts, in the lyophilized solid sample, but are less effective when there are minimal salts present in the sample.

Solutions containing sulfate or phosphate are typically challenging in native mass spectrometry because sulfate and phosphate adduct to protein ions.[45] In order to determine if submicrometer tips are also useful for desalting protein ions from solutions containing phosphate and sulfate, BSA ions were formed from 10 mM aqueous ammonium phosphate or ammonium sulfate with both 1.6 μm and 0.5 μm tips (Figure 4.3). With the 1.6 μm tips, the individual charge states of BSA ions are resolved but very broad from adduction, the baseline is elevated, and cluster ions are are abundant compared to the protein signal, especially for ammonium phosphate. Sulfate appears to adduct to the protein to a significantly higher extent, and the broad peaks in the multimodal distribution at high m/z correspond to salt adducted charge states of BSA. With the submicrometer tips, the baseline chemical noise is essentially eliminated and individual charge states of BSA are well resolved for both solutions. The abundance of low m/z cluster ions is also significantly reduced (Figure 4.3). The spectra of BSA from these solutions with the 0.5 μm tips are nearly identical to that obtained from ammonium acetate (Supplemental Figure 4.1). These results demonstrate that the adverse effects of anions, such as phosphate and sulfate, can be significantly reduced using submicrometer emitter tips.

4.4.4 Combining Ion Desalting Methods: ESI Solution Additives and Small Tips

Reagents that are added to the solution prior to ion formation, such as high concentrations of ammonium acetate,[21,24] supercharging reagents,[32] e.g., *m*-nitrobenzyl alcohol, or select anions,[33] e.g., ammonium bromide, can also be used to desalt protein ions formed in native mass spectrometry. In order to determine the effectiveness of these reagents at desalting protein ions formed from a buffer that mimics the intracellular environment, the effectiveness of these reagents at desalting protein ions was evaluated with ADH in aqueous 150 mM KCl 25 mM Tris-HCl buffer with 1.6 μm tips. The concentrations of these additives were chosen based on previously reported conditions where these additives were found to be effective in pure water or aqueous ammonium salt solutions containing up to 20 mM NaCl. There is ion signal between m/z 3000 and 7000 in the spectra with each of these additives (Figure S-2). However, there are no resolved charge-state distributions, and it is not possible to obtain the mass of the protein from these data. Thus, these previously reported methods are ineffective with this biologically relevant buffer.

In order to determine if these reagents could further improve the ion desalting that is achieved using the emitters with the submicrometer tips, results were obtained for the same solutions using 0.5 μm tips (Supplemental Figure 4.3 and Supplemental Table 4.1). The charge-state distribution is clearly

resolved for ADH ions formed with the small tips without additives. Because the number of individual adducts could not be resolved, the number of K^+ ions adducted to the protein and protein ions formed from the small tips with and without solution additives was estimated by assuming all adduction was K^+ (Supplemental Figure 4.6). The average number of K^+ adducted to the 23+ charge state formed without any additional solution additives is 123 ± 30 (4,651 ± 1,140 Da). The number of K^+ adducts is 97 ± 32 (3,640 ± 1,216 Da), 121 ± 15 (4,575 ± 570 Da), and 163 ± 23 (6,156 ± 874 Da) K^+ with the addition of *m*-NBA, ammonium bromide and ammonium acetate, respectively. These results show that addition of these ion desalting additives to the ESI solution does not significantly remove salt adduction to the protein ions when submicrometer emitter tips are used. Addition of *m*-NBA does decrease the abundance of low mass salt clusters (Supplemental Figure 4.3), as shown previously,[32] which could be beneficial if the protein ion signal is in the m/z range of the cluster ions. Solution additives that desalt protein ions have been shown to reduce salt adduction for ions formed from aqueous solutions with 1 to 20 mM NaCl,[24,31-33] but these additives are not effective for 150 mM KCl 25 mM Tris-HCl at pH 7 with either size tips. Nano-ESI emitters with small tip diameters are much more effective for desalting protein ions formed from solutions with salt concentrations higher than 20 mM compared to adding reagents that desalt protein ions to the ESI solution, but combining both methods does not further improve the desalting of protein ions under these conditions.

4.4.5 Time Dependence of Ion Signal

The time evolution of the total ion signal and total protein ion signal of ADH, BSA and concanavalin A formed from 150 mM KCl 25 mM Tris-HCl with 0.5 μm tips as a function of time was investigated (Figure 4.4 and Supplemental Figure 4.4). Initially, the total ion signal is high but there are no distinguishable protein ions. The total ion signal is composed of primarily $(nKCl+K)^+$ clusters, but much less abundant $(nKCl+H)^+$, $(nKCl+2H)^{2+}$, $(nKCl+2K)^{2+}$ clusters are also observed. Multiply charged KCl cluster ions have been previously reported.[46] After ~30 seconds to several minutes (Supplemental Figure 4.4), the total ion signal sharply decreases, and the high m/z salt clusters decrease in abundance. With the sharp decrease in total ion signal, there is a concomitant increase in protein ion signal and resolved protein ion charge states are observed. For some of the tips, a shift back to high total ion signal and low protein signal occurred for several seconds, only to shift back to the desalted protein ions (Supplemental Figure 4.4). The trend of increasing protein ion signal as the salt cluster ion signal deceases was reproduced at least 20 times, although the fluctuations in total ion count and time dependence of the onset of protein ion signal is highly tip dependent (Supplemental Figure 4.4). It is possible that this time dependence of ion desalting with small tips is due to a shift in spraying modes[47,48] where larger droplets are formed upon initiation of electrospray, and smaller droplets are formed when the spray stabilizes.

4.4.6 Mechanism for desalting protein and protein complex ions with submicrometer tips

The effect of tip size on the extent of sodium adduction to BSA ions (Figure 4.1) suggests a plausible mechanism for the ion desalting observed with the smaller tips. There is essentially no effect for tip sizes above 1.6 μm and a steady decrease in salt adduction with decreasing tip diameters below 1.6 μm. If the initial droplet that is formed by ESI contains one or more protein molecules, then the ratio of salt to protein will remain essentially constant when solvent evaporation from the droplet occurs. If, on the other hand, the ESI droplets contain on average fewer than one protein molecule, then each droplet that contains a protein molecule will have a lower salt-to-protein ratio. This ratio will continue to decrease as the initial droplet size decreases, and the majority of salt will be contained

in droplets that do not contain a protein molecule. Solvent evaporation from droplets that do contain a protein molecule will result in fewer salt molecules that can associate with the protein molecule.

For the 5 μM protein solutions used here, an initial droplet that is 85 nm in diameter would, on average, contain just one protein molecule. With 150 mM KCl, this droplet would contain on average 30,000 K^+ with a K^+-to-protein ratio of 30,000. Droplets above this size would have this same ratio. However, an initial droplet that is 30 nm in diameter would have a K^+-to-protein ratio of 1,400 and only one in ~22 droplets would contain a protein molecule. Based on the observed trend in sodium adduction with tip size (Figure 4.1), the transition from droplets containing on average fewer than one protein molecule per droplet occurs at a tip size of between 1.2 and 1.6 μm. This result would suggest that the initial ESI droplet diameter is about 1/14 to 1/20 of the inner diameter of the electrospray emitters.

The size of initial droplets formed in ESI depends on many factors including ionization current,[49-51] flow rate,[52,53] ESI emitter diameter,[36] and solution composition.[54-56] Recently, Bush and coworkers reported that droplets formed by ESI using similar tips (~1-3 μm) and conditions common for native mass spectrometry are ~60 nm in diameter.[49] Thus, under similar conditions, their measurements of initial droplet diameter correspond to ~$1/17^{th}$ or less of the tip size, consistent with the range of values we infer from our measurements. With the submicrometer tips, potassium chloride salt clusters are still observed in the mass spectra. However, the very large salt clusters, such as observed for concanavalin A and alcohol dehydrogenase (Figure 4.2c,e) with the large tip size are absent with the small tip size (Figure 4.2d, f). This is likely due to the smaller initial droplet containing fewer salt molecules that can form the large clusters.

Even with the smallest tips, there are many more potassium ions in the initial droplet than ultimately adduct to the protein. Some potassium ions may be lost by ion evaporation as solvent evaporation occurs.[57] It is also possible that a Rayleigh fission event occurs which would further reduce the K^+-to-protein ratio if one of the fission product droplets contains the protein molecule. Huber and coworkers used high-speed microscopic images to observe fission of large 48 μm diameter droplets charged close to the Rayleigh limit and found that ~100 progeny droplets were produced, and these droplets carry away 0.3 % of the mass of the original droplet.[58] If similar fission events occurred for the much smaller initial droplet sizes reported here, then the diameter of the progeny droplets formed by the 0.5 μm tips and 1.6 μm tips would be ~1 nm and 3 nm in diameter, respectively. However, these droplet sizes are much smaller than the largest protein complex investigated here, concanavalin A tetramer, which is ~8 nm in diameter.[59,60] This suggests that the protein and protein complex ions are formed directly from the initial droplets produced from the electrospray process for the submicrometer tip sizes.

4.5 Conclusions

A simple method for desalting protein and protein complex ions formed by electrospray ionization from 150 mM KCl 25 mM Tris-HCl buffer pH 7 buffer without any sample preparation or change to solution composition is demonstrated. This buffer is commonly used in protein chemistry to mimic the intracellular environment but adversely affects protein analysis by native mass spectrometry. Solutions containing nonvolatile salts are typically cleaned up to remove these ions or buffer exchanged into ammonium acetate which is the typical volatile buffer used in native MS. The use of submicrometer electrospray ionization emitter tips leads to a reduction of salt adduction onto protein ions and clearly resolved charge-state distributions of proteins and protein complexes can be obtained. This method is equally applicable to other aqueous solution compositions that are often used in native mass spectrometry. The reduction in sodium adduction obtained with the small tips is

similar to or better than that achieved with other methods for desalting ions during ESI, including buffer loading,[21,24] addition of reagents,[31-34] or reaction with organic vapors.[35]

The reduction of salt adduction and salt cluster formation appears to be attributable to the small initial droplet size produced by submicrometer electrospray emitter tips. Formation of droplets that contain on average, fewer than one protein molecule per droplet, limits the exposure of an individual protein molecule to salts, and is consistent with reduction of salt adduction with emitter tip size below ~1.4 μm. Although the results presented here are only for one biologically relevant buffer and several protein and protein complex ions, extending the capabilities of native mass spectrometry to large macromolecules and macromolecular complexes in such buffers should eliminate to the need to reinvestigate properties of these molecules in ammonium buffers that are ubiquitously used in native MS but not typically used in protein chemistry laboratories. Future studies will include investigating this method with a wider range of biologically relevant buffers, such as phosphate buffers, in addition to reagents that are commonly added to buffers such as glycerol or reducing agents.

4.6 Acknowledgements

The authors thank the National Institutes of Health (Grant no. R01GM097357) for financial support. The authors also thank Dr. Catherine Going and Dr. Anthony Iavarone for helpful discussions.

4.7 References

(1) Nostro, Lo, P.; Ninham, B. W. Hofmeister phenomena: an update on ion specificity in biology. *Chem. Rev.* **2012**, *112* (4), 2286–2322.

(2) Baldwin, R. L. How Hofmeister ion interactions affect protein stability. *Biophys. J.* **1996**, *71* (4), 2056–2063.

(3) van den Bremer, E. T. J.; Jiskoot, W.; James, R.; Moore, G. R.; Kleanthous, C.; Heck, A. J. R.; Maier, C. S. Probing metal ion binding and conformational properties of the colicin E9 endonuclease by electrospray ionization time-of-flight mass spectrometry. *Protein Sci.* **2002**, *11* (7), 1738–1752.

(4) Zhu, M. M.; Rempel, D. L.; Zhao, J.; Giblin, D. E.; Gross, M. L. Probing Ca2+-induced conformational changes in porcine calmodulin by H/D exchange and ESI-MS: effect of cations and ionic strength. *Biochemistry* **2003**, *42* (51), 15388–15397.

(5) Maret, W. New perspectives of zinc coordination environments in proteins. *J. Inorg. Biochem.* **2012**, *111*, 110–116.

(6) Zhang, Y.; Cremer, P. S. Chemistry of Hofmeister anions and osmolytes. *Annu. Rev. Phys. Chem.* **2010**, *61* (1), 63–83.

(7) Lodish, H.; Berk, A.; Zipursky, S. L.; Matsudaira, P.; Baltimore, D.; Darnell, J. *Molecular Cell Biology*, 4 ed.; W.H. Freeman: New York, 2000.

(8) Gamba, G. Molecular physiology and pathophysiology of electroneutral cation-chloride cotransporters. *Physiol. Rev.* **2005**, *85* (2), 423–493.

(9) Toyoshima, C.; Nomura, H. Structural changes in the calcium pump accompanying the dissociation of calcium. *Nature* **2002**, *418* (6898), 605–611.

(10) Valero, E.; De Bonis, S.; Filhol, O.; Wade, R. H.; Langowski, J.; Chambaz, E. M.; Cochet, C. Quaternary structure of casein kinase 2. Characterization of multiple oligomeric states and relation with its catalytic activity. *J. Biol. Chem.* **1995**, *270* (14), 8345–8352.

(11) McKay, A. R. C.; Ruotolo, B. T.; Ilag, L. L.; Robinson, C. V. Mass measurements of increased accuracy resolve heterogeneous populations of intact ribosomes. *J. Am. Chem. Soc.* **2006**, *128* (35), 11433–11442.

(12) Uetrecht, C.; Barbu, I. M.; Shoemaker, G. K.; van Duijn, E.; Heck, A. J. R. Interrogating viral capsid assembly with ion mobility-mass spectrometry. *Nat. Chem.* **2011**, *3* (2), 126–132.

(13) Heck, A. J. R.; Van Den Heuvel, R. H. H. Investigation of intact protein complexes by mass spectrometry. *Mass Spectrom. Rev.* **2004**, *23* (5), 368–389.

(14) Videler, H.; Ilag, L. L.; McKay, A. R. C.; Hanson, C. L.; Robinson, C. V. Mass spectrometry of intact ribosomes. *FEBS Lett.* **2005**, *579* (4), 943–947.

(15) Loo, J. A. Electrospray ionization mass spectrometry: a technology for studying noncovalent macromolecular complexes. *Int. J. Mass Spectrom.* **2000**, *200* (1-3), 175–186.

(16) Han, L.; Hyung, S.-J.; Mayers, J. J. S.; Ruotolo, B. T. Bound anions differentially stabilize multiprotein complexes in the absence of bulk solvent. *J. Am. Chem. Soc.* **2011**, *133* (29), 11358–11367.

(17) Zhang, H.; Cui, W.; Gross, M. L. Native electrospray ionization and electron-capture dissociation for comparison of protein structure in solution and the gas phase. *Int. J. Mass Spectrom.* **2013**, *354-355*, 288–291.

(18) Zhou, M.; Huang, C.; Wysocki, V. H. Surface-induced dissociation of ion mobility-separated noncovalent complexes in a quadrupole/time-of-flight mass spectrometer. *Anal. Chem.* **2012**, *84* (14), 6016–6023.

(19) Pacholarz, K. J.; Garlish, R. A.; Taylor, R. J.; Barran, P. E. Mass spectrometry based tools to investigate protein–ligand interactions for drug discovery. *Chem. Soc. Rev.* **2012**, *41* (11), 4335–4355.

(20) Zinnel, N. F.; Pai, P.-J.; Russell, D. H. Ion mobility-mass spectrometry (IM-MS) for top-down proteomics: increased dynamic range affords increased sequence coverage. *Anal. Chem.* **2012**, *84* (7), 3390–3397.

(21) Hernández, H.; Robinson, C. V. Determining the stoichiometry and interactions of macromolecular assemblies from mass spectrometry. *Nat. Protoc.* **2007**, *2* (3), 715–726.

(22) Wang, G.; Cole, R. B. Effect of solution ionic strength on analyte charge state distributions

in positive and negative ion electrospray mass spectrometry. *Anal. Chem.* **1994**, *66* (21), 3702–3708.

(23) Pan, P.; McLuckey, S. A. The effect of small cations on the positive electrospray responses of proteins at low pH. *Anal. Chem.* **2003**, *75* (20), 5468–5474.

(24) Iavarone, A. T.; Udekwu, O. A.; Williams, E. R. Buffer loading for counteracting metal salt-induced signal suppression in electrospray ionization. *Anal. Chem.* **2004**, *76* (14), 3944–3950.

(25) Xiang, F.; Lin, Y.; Wen, J.; Matson, D. W. An integrated microfabricated device for dual microdialysis and on-line ESI-ion trap mass spectrometry for analysis of complex biological samples. *Anal. Chem.* **1999**, *71* (8), 1485–1490.

(26) Prodanov, M.; Garrido, I.; Vacas, V.; Lebrón-Aguilar, R.; Dueñas, M.; Gómez-Cordovés, C.; Bartolomé, B. Ultrafiltration as alternative purification procedure for the characterization of low and high molecular-mass phenolics from almond skins. *Anal. Chim. Acta* **2008**, *609* (2), 241–251.

(27) DeMarco, M. L.; Burnham, C.-A. D. Diafiltration MALDI-TOF mass spectrometry method for culture-independent detection and identification of pathogens directly from urine specimens. *Am. J. Clin. Pathol.* **2014**, *141* (2), 204–212.

(28) Jiang, Y.; Hofstadler, S. A. A highly efficient and automated method of purifying and desalting PCR products for analysis by electrospray ionization mass spectrometry. *Anal. Biochem.* **2003**, *316* (1), 50–57.

(29) Batchelor, J. D.; Sterling, H. J.; Hong, E.; Williams, E. R.; Wemmer, D. E. Receiver Domains Control the Active-State Stoichiometry of Aquifex aeolicus σ54 Activator NtrC4, as Revealed by Electrospray Ionization Mass Spectrometry. *J. Mol. Biol.* **2009**, *393* (3), 634–643.

(30) Batchelor, J. D.; Doucleff, M.; Lee, C.-J.; Matsubara, K.; De Carlo, S.; Heideker, J.; Lamers, M. H.; Pelton, J. G.; Wemmer, D. E. Structure and Regulatory Mechanism of Aquifex aeolicus NtrC4: Variability and Evolution in Bacterial Transcriptional Regulation. *J. Mol. Biol.* **2008**, *384* (5), 1058–1075.

(31) Clarke, D. J.; Campopiano, D. J. Desalting large protein complexes during native electrospray mass spectrometry by addition of amino acids to the working solution. *Analyst* **2015**, *140* (8), 2679–2686.

(32) Cassou, C. A.; Williams, E. R. Desalting protein ions in native mass spectrometry using supercharging reagents. *Analyst* **2014**, *139* (19), 4810–4819.

(33) Flick, T. G.; Cassou, C. A.; Chang, T. M.; Williams, E. R. Solution additives that desalt protein ions in native mass spectrometry. *Anal. Chem.* **2012**, *84* (17), 7511–7517.

(34) Pan, J.; Xu, K.; Yang, X.; Choy, W.-Y.; Konermann, L. Solution-phase chelators for suppressing nonspecific protein-metal interactions in electrospray mass spectrometry. *Anal. Chem.* **2009**, *81* (12), 5008–5015.

(35) DeMuth, J. C.; McLuckey, S. A. Electrospray droplet exposure to organic vapors: metal ion removal from proteins and protein complexes. *Anal. Chem.* **2015**, *87* (2), 1210–1218.

(36) Schmidt, A.; Karas, M.; Dülcks, T. Effect of different solution flow rates on analyte ion signals in nano-ESI MS, or: when does ESI turn into nano-ESI? *J. Am. Soc. Mass Spectrom.* **2003**, *14* (5), 492–500.

(37) Yuill, E. M.; Sa, N.; Ray, S. J.; Hieftje, G. M.; Baker, L. A. Electrospray Ionization from Nanopipette Emitters with Tip Diameters of Less than 100 nm. *Anal. Chem.* **2013**, *85* (18), 8498–8502.

(38) Li, Y.; Cole, R. B. Shifts in peptide and protein charge state distributions with varying spray tip orifice diameter in nanoelectrospray Fourier transform ion cyclotron resonance mass spectrometry. *Anal. Chem.* **2003**, *75* (21), 5739–5746.

(39) Mortensen, D. N.; Williams, E. R. Electrothermal supercharging of proteins in native MS: effects of protein isoelectric point, buffer, and nanoESI-emitter tip size. *Analyst* **2016**, *141* (19), 5598–5606.

(40) UniProt Consortium. UniProt: a hub for protein information. *Nucleic Acids Res.* **2015**, *43* (Database issue), D204–D212.

(41) Flick, T. G.; Merenbloom, S. I.; Williams, E. R. Effects of Metal Ion Adduction on the Gas-Phase Conformations of Protein Ions. *J. Am. Soc. Mass Spectrom.* **2013**, *24* (11), 1654–1662.

(42) Hu, P.; Gross, M. L. Strong interactions of anionic peptides and alkaline earth metal ions: metal-ion-bound peptides in the gas phase. *J. Am. Chem. Soc.* **1992**, *114*, 9153–9160.

(43) Ferguson, W. J.; Braunschweiger, K. I.; Braunschweiger, W. R.; Smith, J. R.; McCormick, J. J.; Wasmann, C. C.; Jarvis, N. P.; Bell, D. H.; Good, N. E. Hydrogen ion buffers for biological research. *Anal. Biochem.* **1980**, *104* (2), 300–310.

(44) Sterling, H. J.; Kintzer, A. F.; Feld, G. K.; Cassou, C. A.; Krantz, B. A.; Williams, E. R. Supercharging protein complexes from aqueous solution disrupts their native conformations. *J. Am. Soc. Mass Spectrom.* **2012**, *23* (2), 191–200.

(45) Chowdhury, S. K.; Katta, V.; Beavis, R. C.; Chait, B. T. Origin and Removal of Adducts (Molecular Mass = 98 u) Attached to Peptide and Protein Ions in Electrospray Ionization Mass Spectra. *J. Am. Soc. Mass Spectrom.* **1990**, *1* (5), 382–388.

(46) Hao, C.; March, R. E.; Croley, T. R.; Smith, J. C.; Rafferty, S. P. Electrospray ionization tandem mass spectrometric study of salt cluster ions. Part 1--investigations of alkali metal chloride and sodium salt cluster ions. *J. Mass. Spectrom.* **2001**, *36* (1), 79–96.

(47) Nemes, P.; Marginean, I.; Vertes, A. Spraying mode effect on droplet formation and ion chemistry in electrosprays. *Anal. Chem.* **2007**, *79* (8), 3105–3116.

(48) Juraschek, R.; Röllgen, F. W. Pulsation phenomena during electrospray ionization. *Int. J. Mass Spectrom.* **1998**, *177* (1), 1–15.

(49) Davidson, K. L.; Oberreit, D. R.; Hogan, C. J., Jr.; Bush, M. F. Nonspecific aggregation in native electrokinetic nanoelectrospray ionization. *Int. J. Mass Spectrom.* **2016**.

(50) Gañán-Calvo, A. M.; Dávila, J.; Barrero, A. Current and droplet size in the electrospraying of liquids. Scaling laws. *J. Aerosol Sci.* **1997**, *28* (2), 249–275.

(51) Srikanth, A.; Karnawat, J.; Kushari, A. The effect of charge density on electro-sprayed droplets. *Open Appl. Phys. J.* **2009**, No. 2, 53–57.

(52) Chen, D.-R.; Pui, D. Y. H.; Kaufman, S. L. Electrospraying of conducting liquids for monodisperse aerosol generation in the 4 nm to 1.8 μm diameter range. *J. Aerosol Sci.* **1995**, *26* (6), 963–977.

(53) Gomez, A.; Tang, K. Charge and fission of droplets in electrostatic sprays. *Phys. Fluids* **1994**, *6* (1), 404–414.

(54) Grimm, R. L.; Beauchamp, J. L. Evaporation and discharge dynamics of highly charged multicomponent droplets generated by electrospray ionization. *J. Phys. Chem. A* **2010**, *114* (3), 1411–1419.

(55) Smith, J. N.; Flagan, R. C.; Beauchamp, J. L. Droplet evaporation and discharge dynamics in electrospray ionization. *J. Phys. Chem. A* **2002**, *106*, 9957–9967.

(56) Taflin, D. C.; Ward, T. L.; Davis, E. J. Electrified droplet fission and the Rayleigh limit. *Langmuir* **1989**, *5* (2), 376–384.

(57) Iribarne, J. V.; Thomson, B. A. On the evaporation of small ions from charged droplets. *J. Chem. Phys.* **1976**, *64* (6), 2287–2294.

(58) Duft, D.; Achtzehn, T.; Müller, R.; Huber, B. A.; Leisner, T. Coulomb fission: Rayleigh jets from levitated microdroplets. *Nature* **2003**, *421* (6919), 128.

(59) Bush, M. F.; Hall, Z.; Giles, K.; Hoyes, J.; Robinson, C. V.; Ruotolo, B. T. Collision cross sections of proteins and their complexes: a calibration framework and database for gas-phase structural biology. *Anal. Chem.* **2010**, *82* (22), 9557–9565.

(60) Hardman, K. D.; Ainsworth, C. F. Structure of concanavalin A at 2.4-Ang resolution. *Biochemistry* **1972**, *11* (26), 4910–4919.

4.8 Tables and Figures

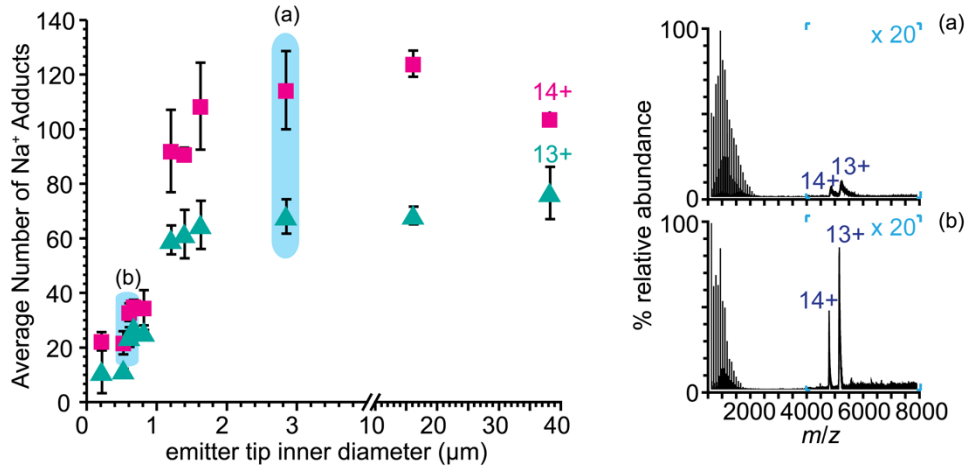

Figure 4.1. Average number of Na^+ adducted to 14+ and 13+ charge states of BSA ions obtained from 10 mM aqueous sodium acetate as a function of emitter tip inner diameter. Electrospray ionization mass spectra of BSA ions from 10 mM aqueous sodium acetate with (a) 2.9 μm or (b) 0.7 μm emitter tips

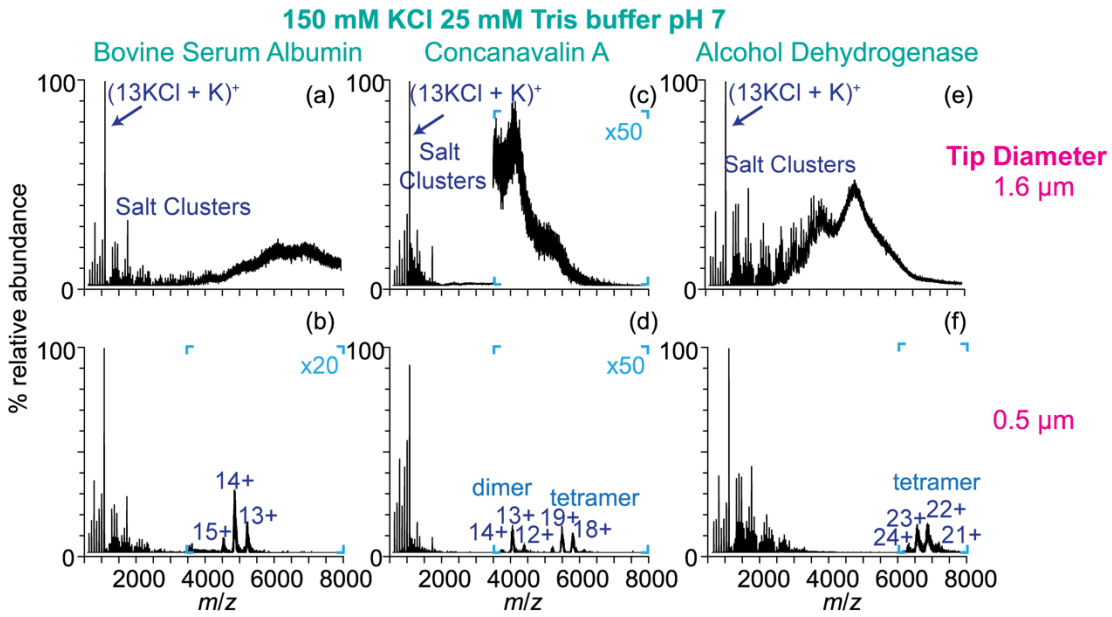

Figure 4.2. Electrospray ionization mass spectra of protein and protein complex ions obtained from 150 mM KCl 25 mM Tris-HCl buffer pH 7 with 1.6 µm (a,c,e) and 0.5 µm (b,d,f) diameter emitter tips.

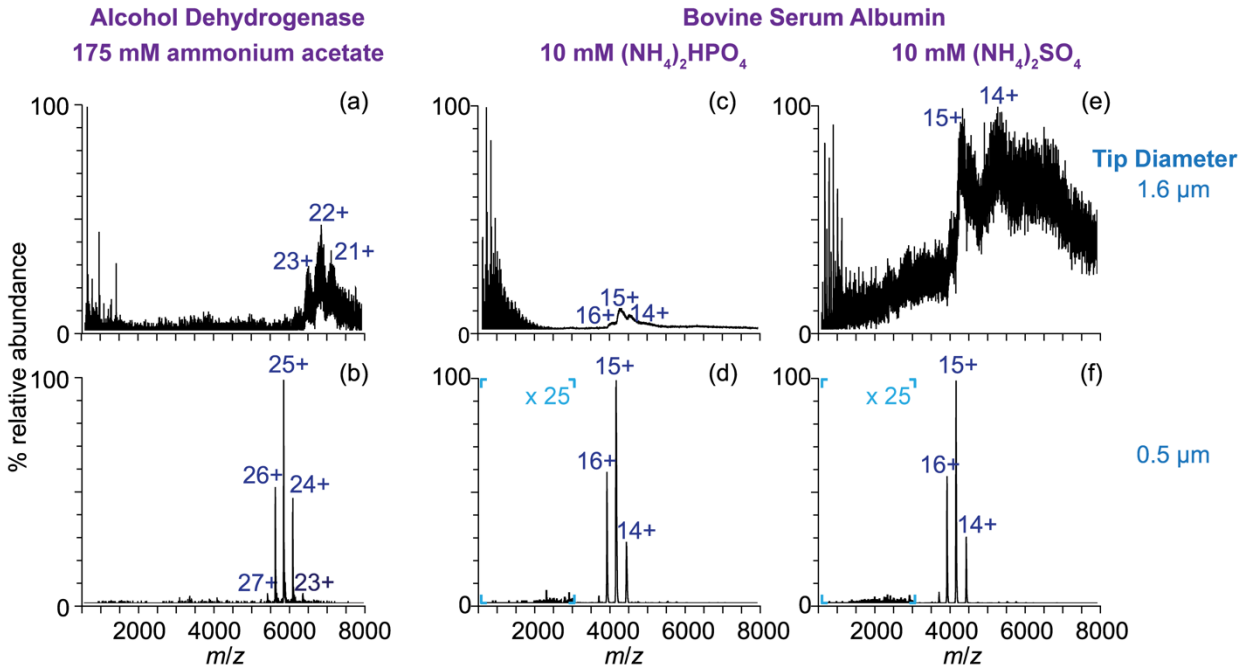

Figure 4.3. Electrospray ionization mass spectra of alcohol dehydrogenase ions obtained from 175 mM ammonium acetate with 1.6 μm (a) and 0.5 μm (b) diameter emitter tips. Electrospray ionization mass spectra of bovine serum albumin ions obtained from 10 mM ammonium phosphate (c-d) or 10 mM ammonium sulfate (e-f) with 1.6 μm (c,e) and 0.5 μm (d,f) diameter emitter tips.

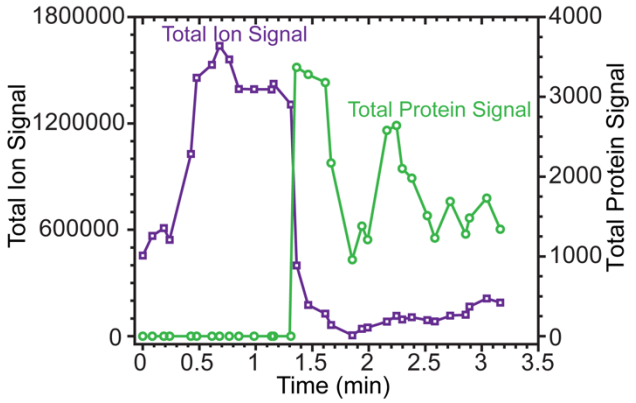

Figure 4.4. Total ion signal (purple squares) and total bovine serum albumin signal (green circles) obtained from electrospray ionization of 5 μM bovine serum albumin in 150 mM KCl 25 mM Tris-HCl buffer at pH 7 with a 0.5 μm diameter emitter tip. Each time point corresponds to six signal averaged spectra.

4.9 Supplemental Information

Supplemental Table 4.1. Signal to noise ratio and number of adducts to ADH tetramer (with and without solution additives that desalt proteins), BSA, and concanavalin A tetramer, avidin ions obtained from ammonium acetate or 150 mM KCl 25 mM Tris-HCl buffer at pH 7 with 0.5 μm and 1.6 μm diameter emitter tips.

	Tip Diameter	S/N of most abundant charge state	Number of Adducts per charge state
ammonium acetate ADH tetramer (175 mM)	1.6 μm	6	24+ 129 ± 14 (Na^+) 23+ 166 ± 4 22+ 173 ± 22 21+ 184 ± 14
	0.5 μm	630	26+ 39 ± 7 25+ 40 ± 8 24+ 41 ± 9 23+ 42 ± 10
BSA (175 mM)	1.6 μm	5550	16+ 6 ± 0.2 15+ 8 ± 0.5 14+ 9 ± 1.6
	0.5 μm	218000	16+ 6 ± 0.1 15+ 7 ± 0.3 14+ 9 ± 0.3
Concanavalin A tetramer (175 mM)	1.6 μm	90000	21+ 49 ± 1 20+ 52 ± 2 19+ 58 ± 8
	0.5 μm	134200	21+ 46 ± 2 20+ 48 ± 3 19+ 53 ± 2
Avidin (10 mM)	1.6 μm	200	17+ 2 ± 2 16+ 7 ± 2 15+ 36 ± 22
	0.5 μm	1260	17+ 14 ± 6 16+ 21 ± 11 15+ 21 ± 13
150 mM KCl 25 mM Tris BSA	1.6 μm	-	-
	0.5 μm	251	15+ 50 ± 2 (K^+) 14+ 52 ± 2 13+ 52 ± 2
Concanavalin A tetramer	1.6 μm	-	-
	0.5 μm	750	20+ 75 ± 24 19+ 70 ± 12 18+ 84 ± 26
ADH tetramer	1.6 μm	-	-
	0.5 μm	570	24+ 124 ± 30 23+ 123 ± 30 22+ 123 ± 27
+ 1.5 % *m*-NBA	1.6 μm	-	-
	0.5 μm	330	24+ 118 ± 16 23+ 97 ± 32 22+ 97 ± 30
+ 25 mM NH_4Br (Collision Voltage 20 V)	1.6 μm	-	-
	0.5 μm	90	24+ 115 ± 4 23+ 121 ± 15 22+ 121 ± 13
+ 1 M ammonium acetate	1.6 μm	-	-
	0.5 μm	12	23+ 163 ± 22 22+ 186 ± 48 21+ 185 ± 55

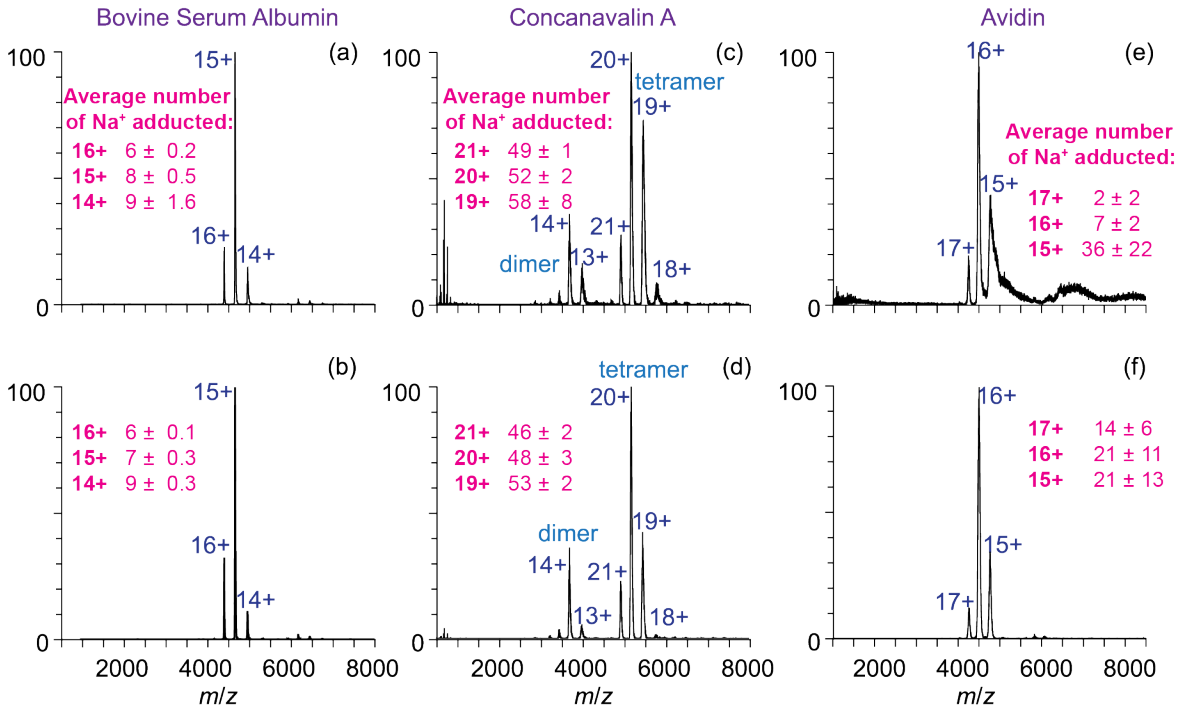

Supplemental Figure 4.1. Electrospray ionization mass spectra of bovine serum albumin and concanavalin A ions obtained from 175 mM ammonium acetate and avidin from 10 mM ammonium acetate with 1.6 μm (a,c,e) and 0.5 μm (b,d,f) diameter emitter tips.

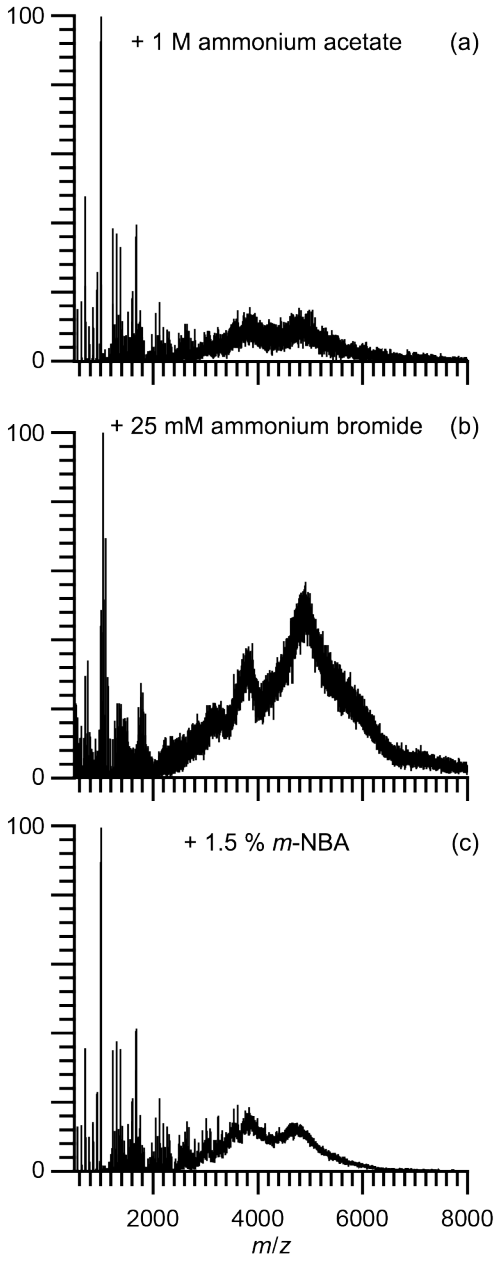

Supplemental Figure 4.2. Electrospray ionization mass spectra of ADH ions obtained from 150 mM KCl 25 mM Tris buffer at pH 7 with 1.6 μm diameter emitter tips with the addition of (a) 1M ammonium acetate (b) 25 mM ammonium bromide (collision voltage 20 V) (c) 1.5 % *m*-NBA

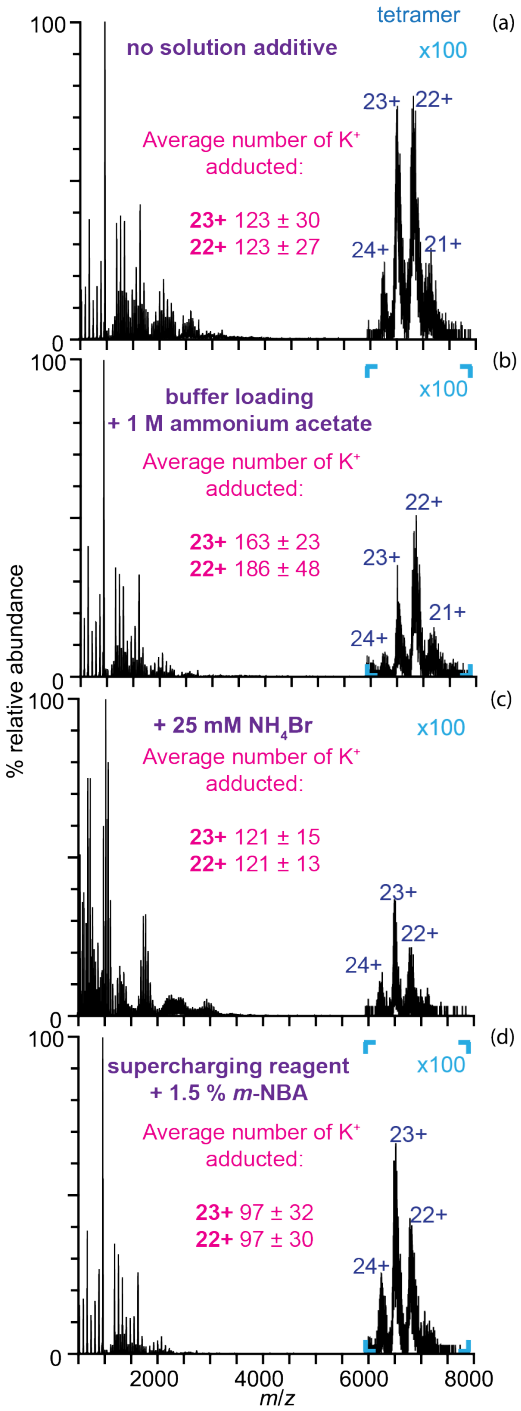

Supplemental Figure 4.3. Electrospray ionization mass spectra of ADH tetramer ions obtained from 150 mM KCl 25 mM Tris-HCl buffer with 0.5 μm diameter emitter tips (a) without any solution additive or with (b) 1 M ammonium acetate, (c) 25 mM ammonium bromide (collision voltage 20 V) or (d) 1.5 % *m*-NBA

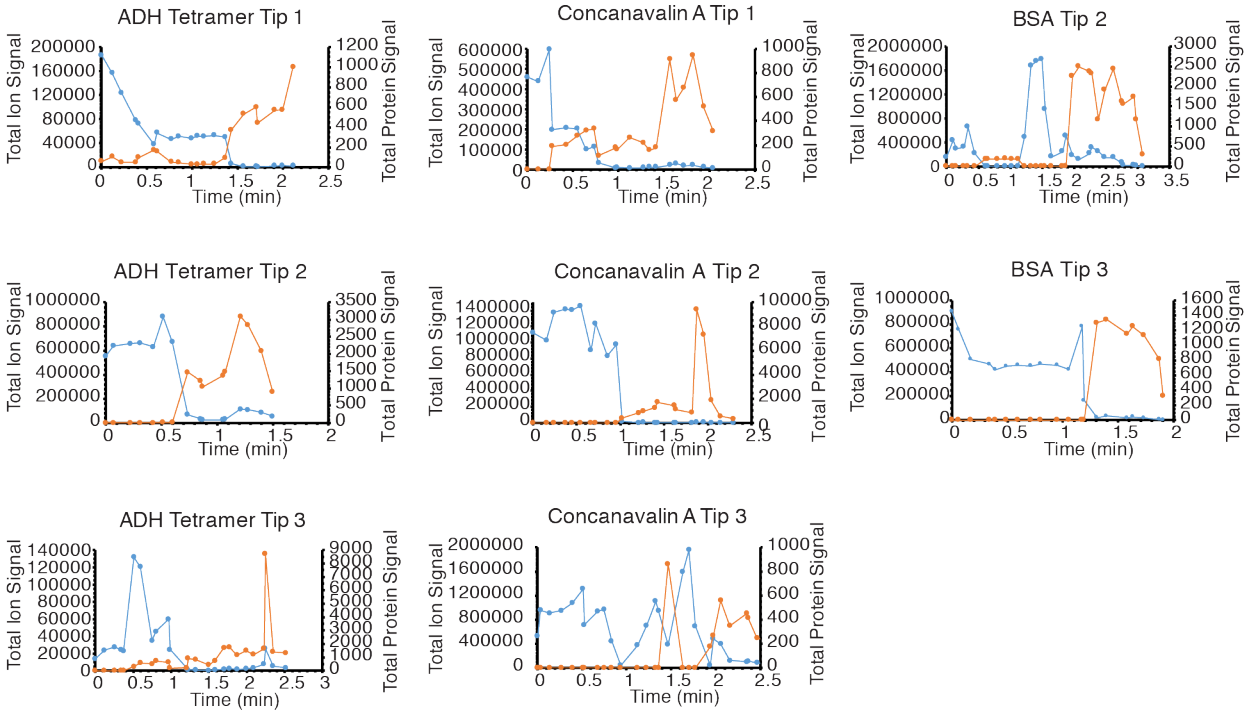

Supplemental Figure 4.4. Total ion signal (blue) and total protein signal (orange) of concanavalin A, BSA, ADH ions obtained from 150 mM KCl 25 mM Tris-HCl at pH 7 with 0.5 μm diameter emitter tips as a function of time. Each time point represents six signal averaged spectra.

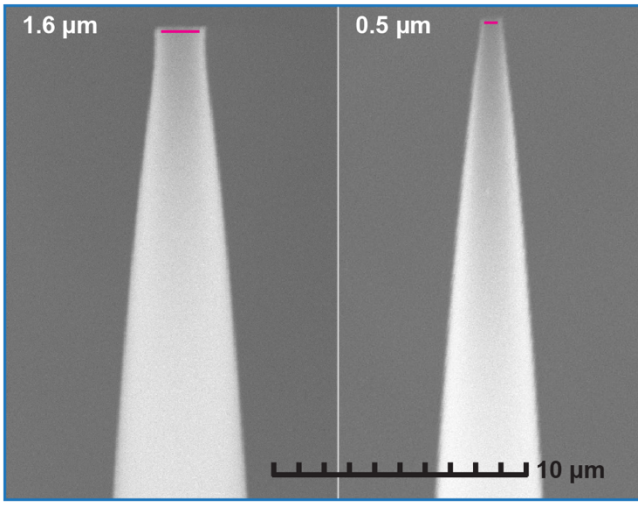

Supplemental Figure 4.5. Scanning electron microscope images of 1.6 µm and 0.5 µm tips.

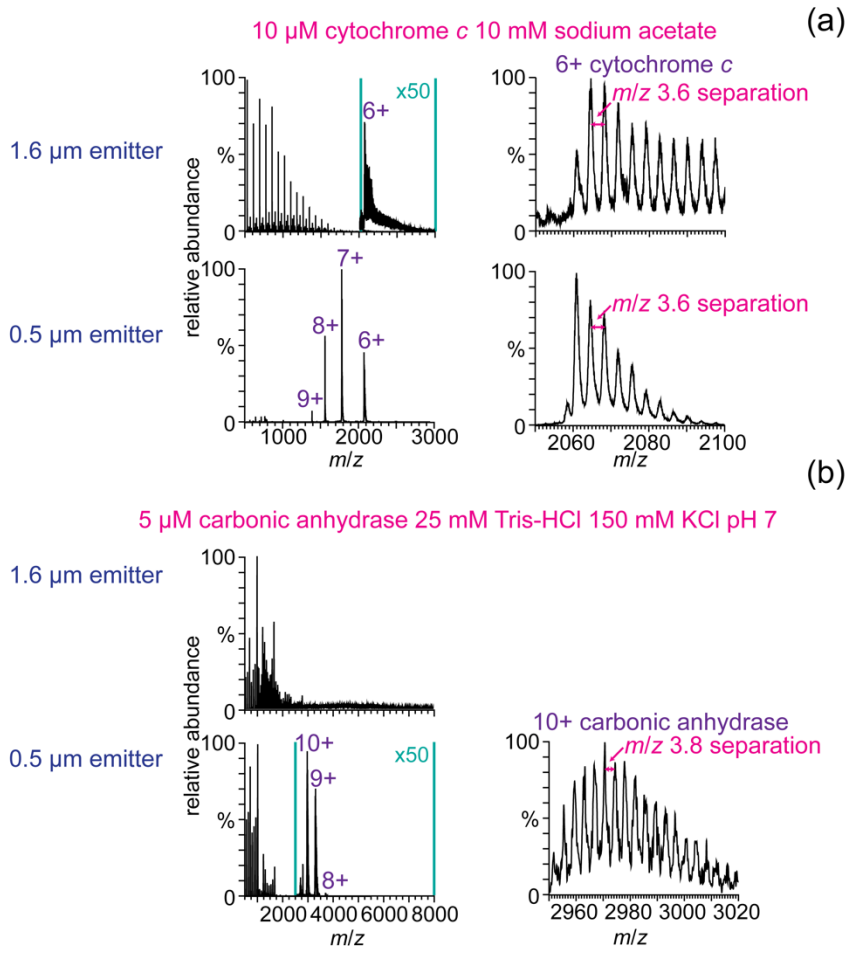

Supplemental Figure 4.6. Electrospray ionization mass spectra of (a) cytochrome *c* ions obtained from 10 mM sodium acetate showing a m/z spacing between adducts to the 6+ charge state which corresponds to Na^+ adduction, and (b) carbonic anhydrase ions obtained from 25 mM Tris-HCl 150 mM KCl showing a m/z spacing between adducts to the 10+ charge state which corresponds to K^+ adduction.

Chapter 5

Native Mass Spectrometry from Buffers that Mimic the Extracellular Environment

This chapter is reproduced with permission from:

Anna C. Susa, Zijie Xia, Evan R. Williams
"Native Mass Spectrometry from Buffers that Mimic the Extracellular Environment"
Submitted to Angewandte Chemie, **2017**

5.1 Abstract

Nonvolatile salts are essential for the structures and functions of many proteins and protein complexes, but nonvolatile salts can severely degrade performance of native mass spectrometry by adducting to protein and protein complex ions thereby reducing sensitivity and mass measuring accuracy. Here, small nanoelectrospray emitters are used to form ions of protein and protein complexes directly from high ionic strength (>150 mM) nonvolatile buffers that mimic the extracellular environment. Charge-state distributions are not obtained for protein and protein complexes from six commonly used nonvolatile buffers with conventional sized nanoelectrospray emitter tips but these distributions are clearly resolved with 0.5 μm tips. This method enables mass measurements of proteins and protein complexes directly from commonly used nonvolatile buffers and eliminates the need to buffer exchange into ammonium acetate or other volatile buffers traditionally used in native mass spectrometry.

5.2 Introduction

Ions can significantly influence protein structure and function with specific salts regulating some interactions between proteins and protein binding with ligands and co-factors.[1,2] Salts also provide high ionic strength required for some protein complexes to assemble.[3] In native mass spectrometry (MS), volatile buffers, such as ammonium acetate and ammonium bicarbonate, are typically used to provide high ionic strength in order to measure masses, stoichiometries, and structures of large protein complexes.[4-6] These volatile buffers also provide the additional advantage of desalting protein ions at high buffer concentrations.[7,8] However, buffers containing nonvolatile salts are often used in biochemistry to mimic the extracellular and intracellular environment, which has an ionic strength of 150-200 mM.[9] Nonvolatile salts degrade mass spectra by adducting to protein and protein complex ions, which distributes the analyte ion signal over many peaks thereby reducing detection limits, resolution, and mass measuring accuracy. Salt cluster ions also increase chemical noise and cause ion suppression which significantly lowers sensitivity.[8,10] Individual charge states of protein complex ions can be difficult to resolve if buffers, such as Tris-HCl or HEPES, are used in concentrations even as low as 10 mM.[8] To avoid these adverse effects of salts on protein ion signal, nonvolatile salts are typically removed from solutions by dialysis,[11] diafiltration,[12] or ion chromatography,[8] and the solutions are buffer exchanged into aqueous ammonium salt solutions prior

to electrospray ionization (ESI). Ammonium salts do not adduct to protein ions significantly during ESI. However, removing nonvolatile salts from solution can change the structures and chemistry of some proteins.

There are alternatives to desalting protein samples before ESI in order to retain specific salts and to reduce the effects of low levels of nonvolatile salts. Reagents that desalt protein ions in the ESI process or in the gaseous phase can be used for solutions containing up to 25 mM NaCl. [7,8,13-17] Nanoelectrospray (nano-ESI) emitters with tip diameters ~1 μm or smaller produce ions that have less sodium ion adduction than do those formed using larger tips.[18-20] This method has been demonstrated for solutions containing organic solvents and acid in which proteins are denatured and from aqueous solutions with up to 25 mM NaCl.[18,19] It has been proposed that the droplets from the smaller emitter tips undergo more solvent acidification and less solvent evaporation and fission events than larger droplets.[18] Recently, submicrometer tips were used to produce resolved charge-state distributions of proteins and protein complexes from a 150 mM KCl 25 mM Tris-HCl pH 7 buffer that mimics the *intra*cellular environment.[20] Here, we demonstrate for the first time that this simple and fast method for producing resolved charge-state distributions of proteins and protein complexes is effective for six common buffers containing nonvolatile salts at high ionic strengths (150 mM and greater with >137 mM NaCl) that mimic the *extra*cellular environment.

5.3 Experimental

Mass spectral data were acquired using a Waters Quadrupole-Time-of-Flight (Q-TOF) Premier mass spectrometer (Waters, Milford, MA, USA). Borosilicate capillary emitters (1.0 mm o.d./0.78 mm i.d., Sutter Instruments, Novato, CA, USA) were pulled with a Flaming/Brown micropipette puller (Model P-87, Sutter Instruments, Novato, CA, USA) and the tip size was varied by changing the velocity and pull parameters. Emitter tip diameters were measured with a scanning electron microscope (Hitachi TM-1000 SEM, Schaumburg, IL, USA), and the tip size has a standard deviation of ± 10 %. Nano-electrospray was initiated by applying a potential of about +0.6 to 2.0 kV to a 0.127 mm diameter platinum wire that is inserted into the capillary and is in contact with the sample solution (~5 μL) and the potential was optimized for each sample. The sampling cone, extraction cone and collision cell were held at 100 V, 5 V and 5 V, respectively, and the source temperature was 80 °C. The backing pressure in the source region was maintained at ~6-7 mbar. Mass spectral replicates were acquired with at least three tips. The centroid of each protein or protein complex ion charge state was determined by fitting the data to Gaussian functions in OriginPro. The percent mass increase from salt adduction to the proteins and protein complexes was determined from difference between mass calculated from the centroid of the unresolved adducted ions and mass of unadducted ions calculated from the elemental composition using average masses. All chemicals were from Sigma (St. Louis, MO) and were used without further purification.

5.4 Results and Discussion

The effects of nano-ESI emitter tip diameter on mass spectra for several protein and protein complexes formed from a phosphate buffered saline (PBS) solution (aqueous 137 mM NaCl, 2.7 mM KCl, 10 mM Na_2HPO_4, 1.8 mM KH_2PO_4) are shown in Figure 5.1e-i and are compared to conventional nano-ESI spectra obtained from aqueous 150 mM ammonium acetate without added nonvolatile salts (Figure 5.1a-d). A 1.6 μm tip was chosen because it is on the small end of commonly used nano-ESI emitters; commercially available emitter tips are typically greater than 2 μm (Supplemental Table 2). Mass spectra of four proteins/protein complexes formed from PBS show

well resolved salt clusters at low m/z and a broad multimodal peak at m/z > 2500 (Figure 5.1e-h). For comparison, results for the same proteins in a 150 mM ammonium acetate solution without added nonvolatile salts show well resolved charge-state distributions for these proteins/protein complexes (Figure 5.1a-d). No molecular mass information can be obtained from any of the spectra obtained from the PBS solution using 1.6 μm tips. In contrast, the charge-state distributions of the protein and protein complexes are well resolved from PBS with the 0.5 μm emitter tips (Figure 5.1i-l). The charge-state distributions of these four proteins and protein complexes from PBS are similar to those from ammonium acetate (Figure 5.1), but the width of these peaks indicate that the ions are adducted with some salt. Adducts to the lowest molecular weight protein, myoglobin, are resolved and show that these ions are adducted with a combination of phosphate, potassium and sodium ions (1-3 phosphate ions in addition to ~1 K^+ and up to 10 Na^+). The salt adduction from PBS to myoglobin (17.6 kDa), carbonic anhydrase (29 kDa), concanavalin A dimer (52 kDa), avidin tetramer (64 kDa), and concanavalin A tetramer (102 kDa) ions increases the masses of these proteins and protein complexes by 1.7 ± 0.2, 1.9 ± 0.2, 3.6 ± 1.0, 8.0 ± 0.6, and 3.4 ± 1.0 %, respectively. For comparison, salt adduction from ammonium acetate without any added nonvolatile salts increases the masses by 0.2 ± 0.1, 0.1 ± 0.1, 2.9 ± 0.6, 0.3 ± 0.2, 1.8 ± 0.1 %, respectively, indicating that the extent of salt adduction does not directly trend with protein molecular weight but must depend on other factors as well. These results demonstrate that submicrometer emitter tips are useful for obtaining resolved protein complex ion and protein ion charge-state distributions from solutions containing high ionic strengths of nonvolatile salts and that this technique is applicable to proteins and protein complexes with a range of pI values, molecular weights and stoichiometries.

The effectiveness of submicrometer emitters for desalting protein and protein complex ions from five additional buffers commonly used in many biochemical laboratories to investigate protein structure and function was investigated. Avidin tetramer ions formed from five buffers containing ~170 mM nonvolatile salts with conventionally sized nano-ESI emitters (1.6 μm inner diameter tips) and smaller emitters (0.5 μm tips) are shown in Figure 5.2. Similar results for myoglobin and concanavalin A are shown in Supplemental Figures 5.1-5.2. Broad, multimodal peaks are observed from m/z ~3000 to 8000 for each of the buffers with the 1.6 μm emitter tips and no individual charge states of the avidin tetramer ions are resolved. In contrast, the charge-state distributions of avidin tetramer ions (+14 to +16) are well resolved with the 0.5 μm emitter tips for all five buffers (Figure 5.2, bottom). The masses of the ions are ~9.6-11.5 % greater than the calculated mass with each of these buffers (Supplemental Table 1) indicating a substantial extent of salt adduction. The adducts to myoglobin ions from each of these buffers are resolved, and each adduct is composed of either multiple Na^+ with or without a buffer ion (PIPES, MOPS, HEPES, TRIS, MES) (Supplemental Figure 5.3). The origin of the broad peaks at high m/z formed with the larger 1.6 μm tips is difficult to ascertain, but these peaks start at lower m/z than the clearly resolved protein charge-state distributions formed with the 0.5 μm tips. This effect is most dramatic for MES where the m/z of the broad peak formed with the 1.6 μm tip is below that of the highest charge state formed with the 0.5 μm tip. These results indicate that the broad peaks formed at high m/z with the 1.6 μm tips are predominantly large salt clusters that may not contain a protein molecule.

We recently proposed that this desalting phenomenon with small emitter tips occurs when initial droplets are small enough to contain on average fewer than one protein molecule, such that small droplets that contain a protein molecule have a lower ratio of salt to protein than larger droplets that contain on average multiple protein molecules.[20] The much larger salt cluster ions observed with the larger tips than with the smaller tips (e.g., Figure 5.2e vs. 5.2j) is consistent with this mechanism. The charge-state distributions of the protein and protein complexes from all six buffers with the submicrometer emitter tips are nearly identical to those from aqueous ammonium acetate with the

larger emitter tips, indicating that any effects of acidification and proton-enrichment of the smaller droplets is negligible.[18]

This is the only method to produce protein and protein complex ions directly from buffer solutions containing nonvolatile salts at concentrations that mimic the extracellular environment that does not require any additional preparation of the sample, such as buffer exchanging into ammonium salt solutions. This technique is useful for proteins and protein complexes that are not stable in conventional native MS buffers that contain ammonium salts or that require high strengths of specific salts in solution to maintain native forms and functions. This method for native MS from buffers that are commonly used in protein chemistry laboratories eliminates concerns that aqueous ammonium salts will alter the native forms and functions of proteins and makes native MS more compatible with other traditional biophysical techniques.

5.5 Conclusions

This is the only method to produce protein and protein complex ions directly from buffer solutions containing nonvolatile salts at concentrations that mimic the extracellular environment that does not require any additional preparation of the sample, such as buffer exchanging into ammonium salt solutions. This technique is useful for proteins and protein complexes that are not stable in conventional native MS buffers that contain ammonium salts or that require high strengths of specific salts in solution to maintain native forms and functions. This method for native MS from buffers that are commonly used in protein chemistry laboratories eliminates concerns that aqueous ammonium salts will alter the native forms and functions of proteins and makes native MS more compatible with other traditional biophysical techniques.

5.6 Acknowledgements

The authors thank the National Institutes of Health (Grant no. R01GM097357) for financial support and thank Henry Y.H. Tang for helpful discussions.

5.7 References

(1) Baldwin, R. L. How Hofmeister ion interactions affect protein stability. *Biophys. J.* **1996**, *71* (4), 2056–2063.

(2) Toyoshima, C.; Nomura, H. Structural changes in the calcium pump accompanying the dissociation of calcium. *Nature* **2002**, *418* (6898), 605–611.

(3) Valero, E.; De Bonis, S.; Filhol, O.; Wade, R. H.; Langowski, J.; Chambaz, E. M.; Cochet, C. Quaternary structure of casein kinase 2. Characterization of multiple oligomeric states and relation with its catalytic activity. *J. Biol. Chem.* **1995**, *270* (14), 8345–8352.

(4) Ruotolo, B. T.; Benesch, J. L. P.; Sandercock, A. M.; Hyung, S.-J.; Robinson, C. V. Ion mobility–mass spectrometry analysis of large protein complexes. *Nat. Protoc.* **2008**, *3* (7), 1139–1152.

(5) Pacholarz, K. J.; Garlish, R. A.; Taylor, R. J.; Barran, P. E. Mass spectrometry based tools to investigate protein–ligand interactions for drug discovery. *Chem. Soc. Rev.* **2012**, *41* (11), 4335–

4355.

(6) Heck, A. J. R.; Van Den Heuvel, R. H. H. Investigation of intact protein complexes by mass spectrometry. *Mass Spectrom. Rev.* **2004**, *23* (5), 368–389.

(7) Iavarone, A. T.; Udekwu, O. A.; Williams, E. R. Buffer loading for counteracting metal salt-induced signal suppression in electrospray ionization. *Anal. Chem.* **2004**, *76* (14), 3944–3950.

(8) Hernández, H.; Robinson, C. V. Determining the stoichiometry and interactions of macromolecular assemblies from mass spectrometry. *Nat. Protoc.* **2007**, *2* (3), 715–726.

(9) Lodish, H.; Berk, A.; Zipursky, S. L.; Matsudaira, P.; Baltimore, D.; Darnell, J. *Molecular Cell Biology*, 4 ed.; W.H. Freeman: New York, 2000.

(10) Wang, G.; Cole, R. B. Effect of solution ionic strength on analyte charge state distributions in positive and negative ion electrospray mass spectrometry. *Anal. Chem.* **1994**, *66* (21), 3702–3708.

(11) Xiang, F.; Lin, Y.; Wen, J.; Matson, D. W. An integrated microfabricated device for dual microdialysis and on-line ESI-ion trap mass spectrometry for analysis of complex biological samples. *Anal. Chem.* **1999**, *71* (8), 1485–1490.

(12) Prodanov, M.; Garrido, I.; Vacas, V.; Lebrón-Aguilar, R.; Dueñas, M.; Gómez-Cordovés, C.; Bartolomé, B. Ultrafiltration as alternative purification procedure for the characterization of low and high molecular-mass phenolics from almond skins. *Anal. Chim. Acta* **2008**, *609* (2), 241–251.

(13) Cassou, C. A.; Williams, E. R. Desalting protein ions in native mass spectrometry using supercharging reagents. *Analyst* **2014**, *139* (19), 4810–4819.

(14) Flick, T. G.; Cassou, C. A.; Chang, T. M.; Williams, E. R. Solution additives that desalt protein ions in native mass spectrometry. *Anal. Chem.* **2012**, *84* (17), 7511–7517.

(15) Clarke, D. J.; Campopiano, D. J. Desalting large protein complexes during native electrospray mass spectrometry by addition of amino acids to the working solution. *Analyst* **2015**, *140* (8), 2679–2686.

(16) DeMuth, J. C.; McLuckey, S. A. Electrospray droplet exposure to organic vapors: metal ion removal from proteins and protein complexes. *Anal. Chem.* **2015**, *87* (2), 1210–1218.

(17) Pan, J.; Xu, K.; Yang, X.; Choy, W.-Y.; Konermann, L. Solution-phase chelators for suppressing nonspecific protein-metal interactions in electrospray mass spectrometry. *Anal. Chem.* **2009**, *81* (12), 5008–5015.

(18) Hu, J.; Guan, Q.-Y.; Wang, J.; Jiang, X.-X.; Wu, Z.-Q.; Xia, X.-H.; Xu, J.-J.; Chen, H.-Y. Nanoemitters Suppress the Formation of Metal Adduct Ions in Electrospray Ionization Mass Spectrometry. *Anal. Chem.* **2017**.

(19) Schmidt, A.; Karas, M.; Dülcks, T. Effect of different solution flow rates on analyte ion signals

in nano-ESI MS, or: when does ESI turn into nano-ESI? *J. Am. Soc. Mass Spectrom.* **2003**, *14* (5), 492–500.

(20) Susa, A. C.; Xia, Z.; Williams, E. R. Small Emitter Tips for Native Mass Spectrometry of Proteins and Protein Complexes from Nonvolatile Buffers That Mimic the Intracellular Environment. *Anal. Chem.* **2017**, acs.analchem.6b04897.

5.8 Tables and Figures

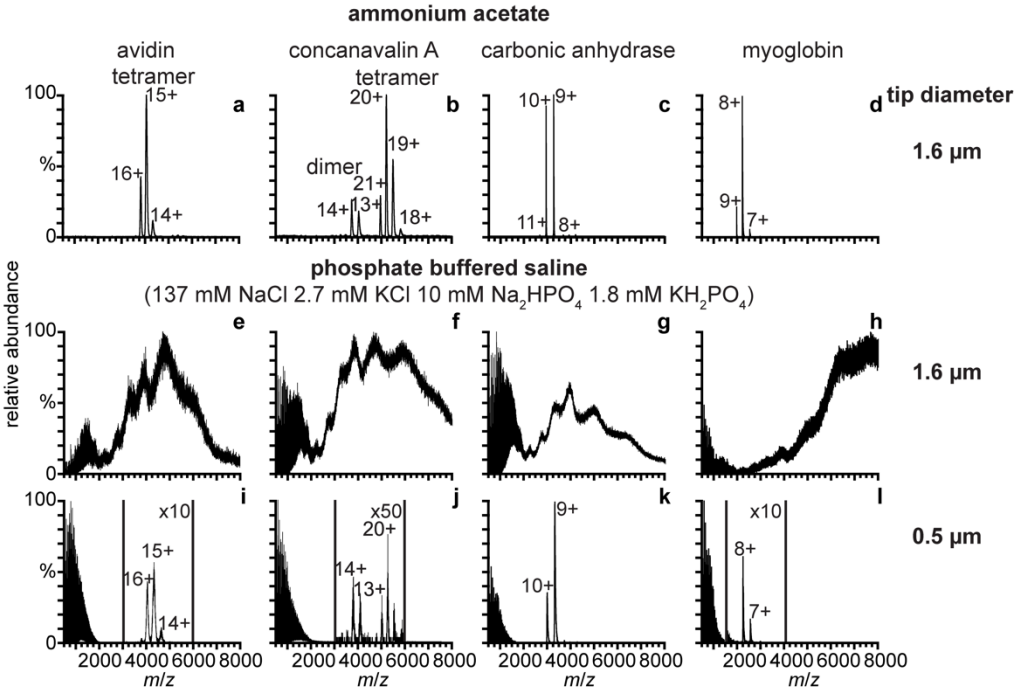

Figure 5.1. Electrospray ionization mass spectra of 5 μM avidin tetramer (a,e,i), concanavalin A (b,f,j), carbonic anhydrase (c,g,k) and myoglobin (d,h,l) ions formed from 150 mM aqueous ammonium acetate with 1.6 μm emitter tips (a-d) or phosphate buffered saline with 1.6 μm emitter tips (e-h) and 0.5 μm emitter tips (i-l).

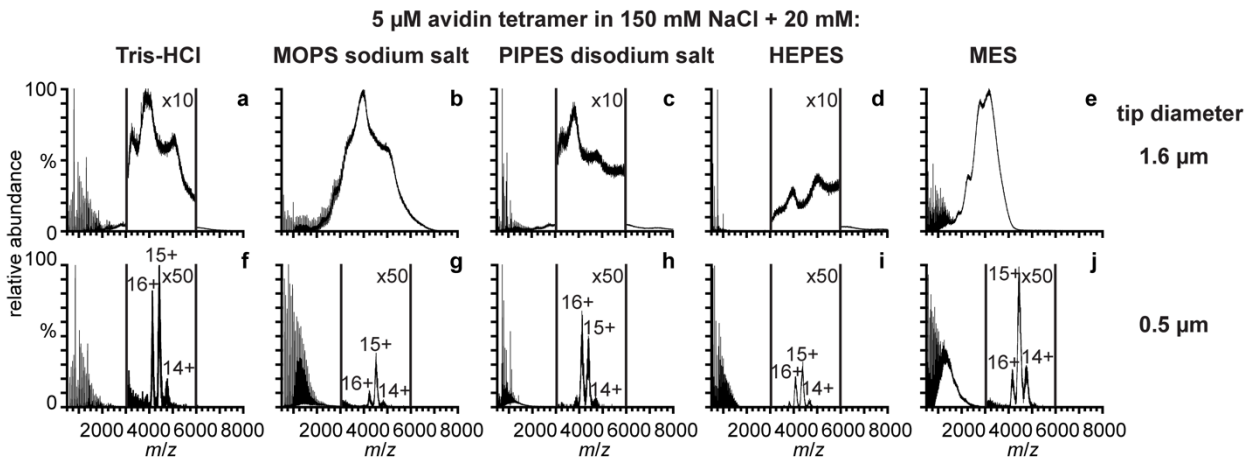

Figure 5.2. Electrospray ionization mass spectra of 5 μM avidin tetramer ions formed from aqueous solutions containing 150 mM NaCl and 20 mM of the following buffers (a,f) Tris-HCl, (b,g) MOPS, (c,h) PIPES, (d,i) HEPES, (e,j) MES with 1.6 μm emitter tips (a-e) or 0.5 μm emitter tips (g-j)

5.9 Supplemental Information

Supplemental Table 5.1. Percent mass increase from salt adduction to avidin tetramer, concanavalin A dimer and tetramer ions obtained from seven buffers with 0.5 μm diameter emitter tips unless otherwise noted. The mass of unadducted ions was calculated from the elemental composition using average masses.

Buffer	**Avidin tetramer**	**Concanavalin A dimer**	**Concanavalin A tetramer**
Ammonium acetate (1.6 μm)	0.3 ± 0.2 %	2.9 ± 0.6 %	1.8 ± 0.1 %
Ammonium acetate (0.5 μm)	0.06 ± 0.2 %	1.6 ± 0.6 %	1.6 ± 0.1 %
150 mM NaCl 20 mM Tris-HCl	9.6 ± 0.4 %	3.6 ± 0.8 %	3.0 ± 0.4 %
150 mM NaCl 20 mM HEPES	9.8 ± 1.6 %	3.4 ± 0.4 %	-
150 mM NaCl 20 mM PIPES	10.7 ± 1.3 %	6.0 ± 0.8 %	4.6 ± 0.3 %
150 mM NaCl 20 mM MES	10.9 ± 0.4 %	8.3 ± 1.9 %	-
150 mM NaCl 20 mM MOPS	11.5 ± 0.3 %	5.5 ± 0.9 %	4.6 ± 0.8 %
137 mM NaCl 2.7 mM KCl 10 mM Na_2HPO_4 1.8 mM KH_2PO_4	8.0 ± 0.7 %	3.6 ± 1.0 %	3.4 ± 1.0 %
Tris-HCl: tris(hydroxymethyl)aminomethane hydrochloride HEPES: 4-(2-hydroxyethyl)-1-piperazineethanesulfonic acid PIPES: piperazine-N,N'-bis-2-ethanesulfonic acid MES: 2-(N-morpholino)ethanesulfonic acid MOPS: (3-(N-morpholino)propanesulfonic acid			

Supplemental Table 5.2. Diameters of commercially available nano-ESI emitter tips

Supplier	**Product**	**Tip size (μm)**
Thermo Scientific	ES791, ES792	7, 20
New Objective	-	2-100

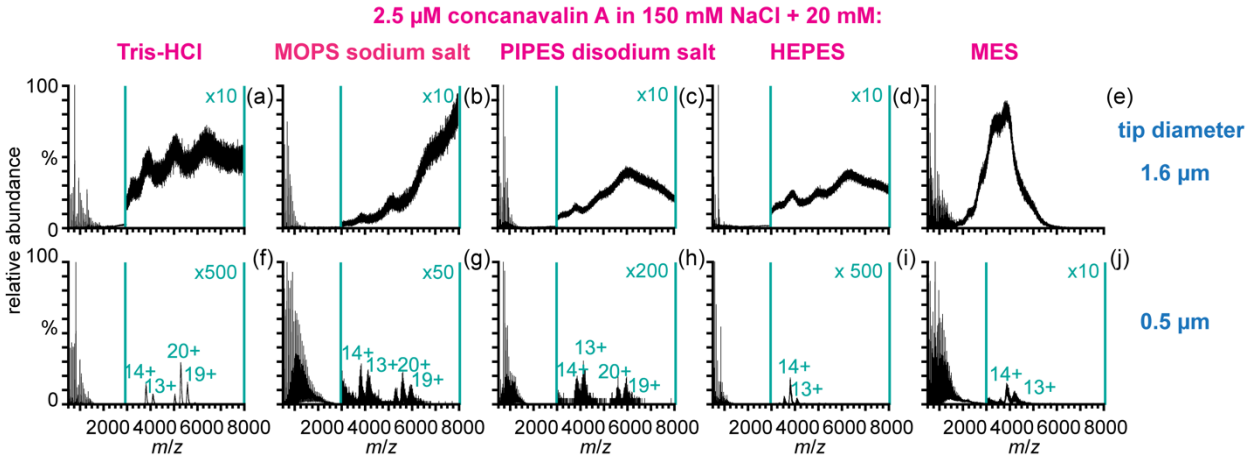

Supplemental Figure 5.1. Electrospray ionization mass spectra of concanavalin A obtained from aqueous solutions containing 150 mM NaCl and 20 mM of the following buffers (a,f) Tris-HCl (b,g) MOPS (c,h) PIPES (d,i) HEPES (e,j) MES with 1.6 µm (a-e) and 0.5 µm (f-j) diameter emitter tips.

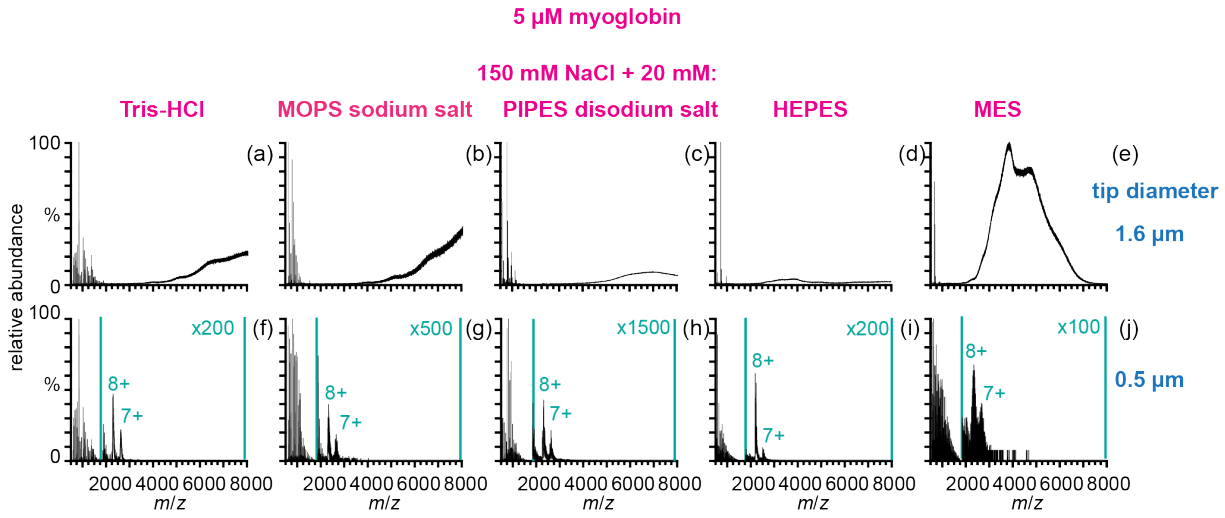

Supplemental Figure 5.2. Electrospray ionization mass spectra of myoglobin obtained from aqueous solutions containing 150 mM NaCl and 20 mM of the following buffers (a,f) Tris-HCl (b,g) MOPS (c,h) PIPES (d,i) HEPES (e,j) MES with 1.6 µm (a-e) and 0.5 µm (f-j) diameter emitter tips.

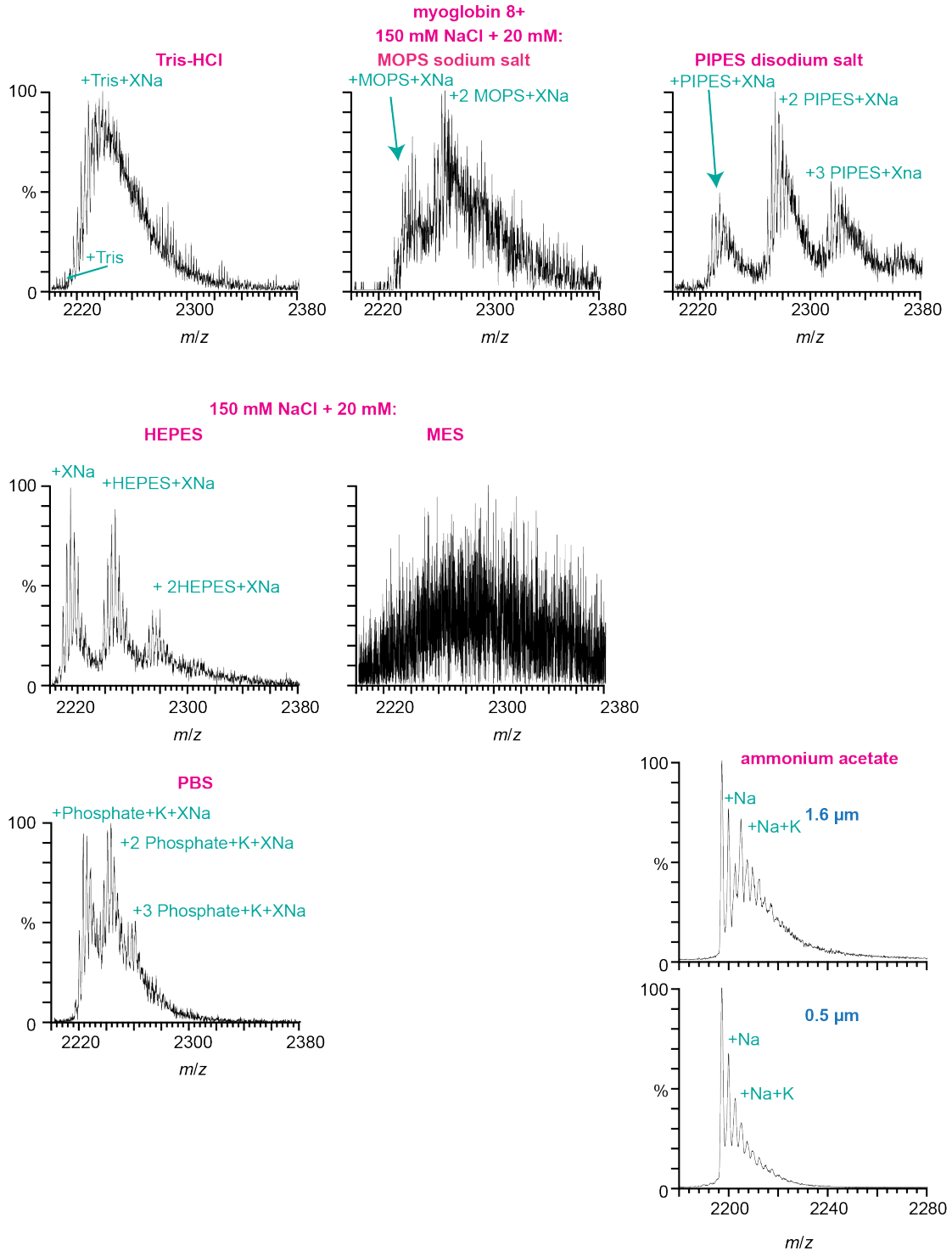

Supplemental Figure 5.3. Adducts to myoglobin 8+ charge state obtained from 150 mM NaCl and 20 mM Tris-HCl, MOPS, PIPES, HEPES, MES and PBS with 0.5 µm diameter emitter tips and ammonium acetate with 1.6 µm and 0.5 µm diameter emitter tips.

Chapter 6

Summary and Future Directions

The work in this dissertation provides insight into the factors that control charging of macromolecules in native mass spectrometry (Chapters 2 and 3) and presents a novel method for native mass spectrometry of proteins and protein complexes from buffers that mimic the cellular environment (Chapters 4 and 5). Understanding of the factors that control protein ion charging in ESI is beneficial to the field of native mass spectrometry because it facilitates interpretation of mass spectral data and aids in developing methods to manipulate protein ion charge, which is useful for tandem mass spectrometry experiments. The method for desalting protein and protein complex ions from solutions containing high ionic strengths of nonvolatile salts can significantly alter the way native mass spectrometry experiments are performed because it eliminates the need to adapt protein solutions so that they are compatible with mass spectral analysis.

Several applications of desalting ions with submicrometer nano-ESI emitter tips could be investigated in the future. Many protein complexes require specific buffer conditions with nonvolatile salts. The work presented here in this dissertation demonstrates the use of submicrometer nano-ESI emitters to desalt protein and protein complex ions from samples that are relatively stable in conventional mass spectrometry solutions such as aqueous ammonium acetate. It would be remarkable to use submicrometer emitter tips to desalt protein complex ions for a complex that is only stable in a very specific buffer. It would also be interesting to investigate a protein or protein complex that undergoes conformational change with high ionic strengths of specific salts. The technique of desalting ions with submicrometer emitter tips could also be a tool to enable the study of salt-loving (halophilic) proteins in the gas phase. Halophilic proteins are distinguished from non-halophilic proteins by their inability to maintain native conformations and activities in low salt solutions (typically less than 1 M salt). This would demonstrate that proteins or protein complexes that require very specific salt solution conditions to maintain their native structures and functions can be studied in the gas phase without disrupting their native forms and functions by buffer exchanging into aqueous ammonium acetate.

The work described in this dissertation focuses on protein ions and protein complex ions formed from native solutions, but it would be interesting to determine if the submicrometer emitter tips can desalt protein ions formed from denaturing solutions containing guanidinium or urea. High concentrations of compounds such as guanidinium or urea are commonly used to denature proteins, however these compounds are not compatible with ESI. This would be beneficial for investigating the folding/unfolding of proteins with different concentrations of denaturants in combination with mass spectrometry. The capability of forming ions directly from denaturing solutions with guanidinium or urea would also be useful for checking protein purity by mass spectral analysis directly after protein purification without needing to exchange the protein solution into a denaturing solution compatible for mass spectral analysis, such as water/methanol/acid solutions.

Another avenue for the use of small emitter tips is for the formation of very small droplets that contain only one analyte of interest. This could be useful for investigating analyte systems for which concentration effects interfere with data acquisition or analysis or for mixing droplets that each contain a single analyte to determine bimolecular reaction rates.

The factors that affect the extent of protein ion charging from aqueous solutions were thoroughly investigated (Chapters 2 and 3), but there are some aspects that could still be explored.

The experiments in this dissertation are focused on positively charged protein and protein complex ions and cations (alkali metal ions, alkylammonium, and ammonium), but effects of anions on negatively charged protein and protein complex ions would also provide insight into factors that control charging of protein ions in ESI. Experimental evidence for two of the more recent ion formation mechanisms for macromolecules in ESI, the chain ejection model (CEM) and combined charged-residue model (CCRFEM), is limited; therefore, more experiments to conclusively determine the ESI ion formation mechanism for macromolecules would be of interest. These experiments are challenging, because in order to investigate these ion formation mechanisms, often more than one experimental condition is changed at once. For example, changing the identity of buffer ion in the ESI solution can also affect the conformation of the protein or a solution additive can change the surface tension of the ESI droplet.

This dissertation provides insight into the factors that control the charging of macromolecules in ESI and demonstrates the first technique for ESI of proteins and protein complexes directly from buffers containing ionic strengths of nonvolatile salts that mimic the cellular environment. This changes the way native mass spectrometry is performed by making it more compatible for solutions commonly used in biochemical laboratories.